geodiversitas

2022 • 44 • 32

Dental ontogeny in the early Paleocene placental mammal *Alcidedorbignya inopinata* (Pantodonta) from Tiupampa (Bolivia)

Christian de MUIZON & Guillaume BILLET

art. 44 (32) — Published on 1 December 2022
www.geodiversitas.com

PUBLICATIONS SCIENTIFIQUES

MUSÉUM NAL HIST NATURELLE

Geodiversitas est indexé dans / Geodiversitas *is indexed in:*
– Science Citation Index Expanded (SciSearch®)
– ISI Alerting Services®
– Current Contents® / Physical, Chemical, and Earth Sciences®
– Scopus®

Geodiversitas est distribué en version électronique par / Geodiversitas *is distributed electronically by:*
– BioOne® (http://www.bioone.org)

Les articles ainsi que les nouveautés nomenclaturales publiés dans *Geodiversitas* sont référencés par / *Articles and nomenclatural novelties published in* Geodiversitas *are referenced by:*
– ZooBank® (http://zoobank.org)

Geodiversitas est une revue en flux continu publiée par les Publications scientifiques du Muséum, Paris
Geodiversitas *is a fast track journal published by the Museum Science Press, Paris*

Les Publications scientifiques du Muséum publient aussi / *The Museum Science Press also publish:* ***Adansonia***, ***Zoosystema***, ***Anthropozoologica***, ***European Journal of Taxonomy***, ***Naturae***, ***Cryptogamie*** **sous-sections** ***Algologie***, ***Bryologie***, ***Mycologie, Comptes Rendus Palevol***

Diffusion – Publications scientifiques Muséum national d'Histoire naturelle
CP 41 – 57 rue Cuvier F-75231 Paris cedex 05 (France)
Tél. : 33 (0)1 40 79 48 05 / Fax : 33 (0)1 40 79 38 40
diff.pub@mnhn.fr / http://sciencepress.mnhn.fr

ISSN (imprimé / *print*) : 1280-9659/ ISSN (électronique / *electronic*) : 1638-9395

Dental ontogeny in the early Paleocene placental mammal *Alcidedorbignya inopinata* (Pantodonta) from Tiupampa (Bolivia)

Christian de MUIZON
Guillaume BILLET
Muséum national d'Histoire naturelle,
Centre de Recherche en Paléontologie – Paris (CR2P),
CNRS/MNHN/Sorbonne Université,
case postale 38, 57 rue Cuvier, F-75231 Paris cedex 05 (France)

Submitted on 25 January 2022 | accepted on 20 April 2022 | published on 1 December 2022

urn:lsid:zoobank.org:pub:3E4FC5D6-A030-47B1-802B-39A21819AE73

Muizon C. de & Billet G. 2022. — Dental ontogeny in the early Paleocene placental mammal *Alcidedorbignya inopinata* (Pantodonta) from Tiupampa (Bolivia). *Geodiversitas* 44 (32): 989-1050. https://doi.org/10.5252/geodiversitas2022v44a32. http://geodiversitas.com/44/32

ABSTRACT
Within the abundant mammal fauna of Tiupampa (Early Paleocene, Bolivia), the pantodont *Alcidedorbignya inopinata* Muizon & Marshall, 1987 is the eutherian represented by the largest number of specimens. The sample recovered in this locality includes numerous isolated teeth and jaws as well as six skulls, most of them being associated with complete or partial skeletons. It is composed of a similar number (excluding isolated teeth) of adults (71) and juveniles (75), which likely belong to the same population. The present study focusses on the dental eruption sequence of juveniles, which spans ontogenetically from perinatal individuals to sub-adults. Eight ontogenetic stages have been defined for juveniles (1, 2, 2+, 3, 3+, 4, 5, 6) and criteria for their definition are proposed. Two more stages (7 & 8) are defined for adults. Stage 7 includes specimens with fully erupted and little worn dentition, and Stage 8 is composed of a small number of specimens with worn dentition but not totally erasing the inner profile of the tooth, even on M1/m1. Our stages have been correlated to the six "Individual Dental Age Stages" (IDAS) proposed by others for fossil and extant placental mammals. Description of the dental ontogenetic stages of *Alcidedorbignya* establishes the dental eruption sequence for this taxon. Excluding incisors (for which we have almost no data), the upper eruption sequence is as follows: dC-dP2-4 (probably erupted at birth, order unknown), M1, dP1, M2, I3, C, P4, P3, P2-3, M3. The lower eruption sequence (excluding i1-2 for which we have no data) is as follows: di1-3-dc-dp3-4 (probably erupted at birth, order unknown), dp2, m1, dp1, m2, i3, c, p2, p4, p3, m3. This sequence is identical to that of *Coryphodon*, the most derived pantodont genus. In *Alcidedorbignya,* as in *Coryphodon* Owen, 1845, the M3/m3 erupt last, which may constitute a derived, although very convergent, character within placentals. The use of computed tomography provided further information regarding tooth mineralisation. It indicates that on lower cheek teeth the trigonid mineralises before the talonid and on the former the order of mineralisation is protoconid, metaconid and paraconid. On the upper cheek teeth the paracone mineralises first. This mineralisation sequence for cusps fits well with the general pattern described for placentals. The scrutiny of wear facets and eruption sequence of cheek teeth then

enabled us to propose hypotheses regarding the timing of life history events such as weaning and sexual maturity, using comparisons with extant placentals. Several measurements of the skull and dentary also indicate that the juveniles of *Alcidedorbignya* with no more than 20% of erupted permanent cheek teeth (p3 to m3, P3 to M3) are rather small compared to adults, which may represent a plesiomorphic pattern. Finally, the study of the mortality profile of this pantodont assemblage shows that the number of juveniles remains is similar to that of adults. Among juveniles, the greater abundance of specimens is observed for unweaned individuals. *Alcidedorbignya inopinata* is, by far, the Paleocene taxon represented by the greatest number of juvenile individuals, which suggests that Tiupampa may have been a breeding locality for this gregarious Paleocene placental. The remarkably well-documented collection of juvenile and adult fossils of *Alcidedorbignya* offers an unprecedented glimpse into the craniodental ontogeny of an early diverging placental mammal.

KEY WORDS
Placentalia,
Pantodonta,
Alcidedorbignya,
Paleocene,
Tiupampa,
Bolivia,
dental ontogeny,
eruption stages,
mortality profile.

RÉSUMÉ

Ontogénie dentaire chez le mammifère placentaire du Paléocène inférieur Alcidedorbignya inopinata *(Pantodonta) de Tiupampa (Bolivie).*

Au sein de la faune de mammifères de Tiupampa (Paléocène inférieur, Bolivie), le pantodonte, *Alcidedorbignya inopinata* Muizon & Marshall, 1987 est l'euthérien représenté par le plus grand nombre de spécimens. L'échantillon récolté, comprend de nombreuses dents isolées et mâchoires ainsi que six crânes pour la plupart, associés à des squelettes complets ou partiels. Il se compose d'un nombre à peu près similaire (en excluant les dents isolées) de spécimens adultes (71) et juvéniles (75) qui appartiennent très probablement à la même population. La présente étude se concentre sur l'éruption dentaire des juvéniles qui s'étend ontogénétiquement depuis des individus à un stade périnatal jusqu'à des sub-adultes. Huit stades ontogénétiques ont été définis (1, 2, 2+, 3, 3+, 4, 5, 6) et des critères ont été proposés pour les définir. Deux autres stades (7 et 8) ont été définis pour les adultes. Le stade 7 comprend des spécimens avec une dentition permanente totalement fonctionnelle et peu usée. Le stade 8 se compose d'un petit nombre d'individus dont la dentition définitive est usée mais sans atteindre une abrasion totale des structures des molaires, même sur les M1/m1. Nos stades ont été corrélés aux six « Individual Dental Age Stages » (IDAS) proposés par d'autres auteurs pour les mammifères actuels et fossiles. La description des huit stades d'ontogénie dentaire chez *Alcidedorbignya* a permis d'établir la séquence d'éruption dentaire pour ce taxon. À l'exclusion des incisives (pour lesquelles nous n'avons que très peu de données), la séquence d'éruption des dents supérieures est comme suit : dC-dP2-4 (probablement fonctionnelles à la naissance, ordre inconnu), M1, dP1, M2, I3, C, P4, P2-3, M3. La séquence d'éruption dentaire des dents inférieures (à l'exclusion des i1 et i2 pour lesquelles nous n'avons pas de données) est comme suit : di1-3-dc-dp3-4 (probablement fonctionnelles à la naissance, ordre inconnu), dp2, m1, dp1, m2, i3, c, p2, p4, p3, m3. Cette séquence est semblable à celle de *Coryphodon* Owen, 1845 le genre de pantodonte le plus dérivé. En particulier, chez *Alcidedorbignya*, comme chez *Coryphodon*, les M3/m3 sortent les dernières, ce qui constitue probablement un caractère dérivé bien que très convergeant parmi les placentaires. L'utilisation de la tomographie informatisée a fourni des données supplémentaires concernant la séquence de minéralisation dentaire et a permis l'étude des germes dentaires. Celle-ci montre que, sur les dents inférieures le trigonide se minéralise avant le talonide et, sur le premier, l'ordre de minéralisation des cuspides est le suivant : protoconide, métaconide, paraconide. Aux molaires supérieures, le paracone est le premier minéralisé. Cette séquence de minéralisation des cuspides correspond au patron général décrit pour les placentaires. L'analyse des facettes d'usure et de la séquence d'éruption dentaire a permis de proposer des hypothèses sur l'apparition d'événement d'histoire de vie tels que le sevrage et la maturité sexuelle par comparaison avec des données connues pour des placentaires actuels. La comparaison de plusieurs mesures crâniennes et mandibulaires indique que les individus périnataux et juvéniles d'*Alcidedorbignya* avec 20% de dents jugales définitives fonctionnelles (p3 à m3 ; P3 à M3) sont relativement petit en comparaison aux adultes, ce qui pourrait représenter un caractère plésiomorphe. Enfin, l'étude du profil de mortalité de cet ensemble de fossiles *d'Alcidedorbignya* montre que le nombre de restes de juvéniles était semblable à celui des adultes. Parmi les juvéniles, le plus grand nombre de spécimens est observé pour des individus non sevrés. *Alcidedorbignya inopinata* est de loin le taxon de la faune représenté par le plus grand nombre d'individus juvéniles, ce qui suggère que Tiupampa constituait probablement un lieu de rassemblement de reproduction pour ce placentaire grégaire au Paléocène. La collection de fossiles de juvéniles et d'adultes d'*Alcidedorbignya inopinata*, remarquablement bien documentée (pour le Paléocène inférieur), procure une information unique et sans précédent pour comprendre l'ontogénie cranio-dentaire d'un mammifère placentaire basal.

MOTS CLÉS
Placentalia,
Pantodonta,
Alcidedorbignya,
Paléocène,
Tiupampa,
Bolivie,
ontogénie dentaire,
stades d'éruption,
profil de mortalité.

INTRODUCTION

Dental eruption sequence is generally poorly known in stem and early mammals because of the scarcity and the incompleteness of fossils jaws of juvenile individuals, although valuable exceptions exist (e.g., Martin 1997; Luo *et al.* 2004; O'Meara & Asher 2016; Mao *et al.* 2019; Schultz *et al.* 2019; Jäger *et al.* 2021). This scarce record and preservation are, in part, the consequence of the poor ossification of juvenile bones and of the extreme weakness of the cranial sutures, which, in very early stages are still partly cartilaginous. As a consequence, juvenile jaws preserving most of the teeth or, even, only most of the cheek teeth, are uncommon in the Late Cretaceous or Paleocene mammal faunas. While the discovery of a complete juvenile jaw is already remarkable, it is insufficient, alone, to elucidate the dental eruption sequence in a given fossil mammal and is not comparable to what can be done with extant mammals, for which all the stages can be available for upper and lower dental series of the same species.

However, among early members of Placentalia, some exceptions are to be mentioned in the Paleocene and Eocene of North America. West (1971) revised the deciduous dentition of phenacodontids and studied 164 specimens referred to *Tetraclaenodon* Scott, 1892*, Phenacodus*, and *Ectocion* Cope, 1882. Many of these specimens are partial jaws, which only preserved (at best) dP3 and dP4. None of the more anterior deciduous teeth of these genera are known. Furthermore, the age of these specimens ranges through the middle Paleocene (Torrejonian) to the late middle Eocene (late Bridgerian) and are from a vast number of localities or regions (e.g., San Juan Basin, New Mexico; Crazy Mountain field, Montana; Bighorn Basin, Buckman hollow, Wind River Basin, and Fossil Basin, Wyoming). Some isolated juvenile specimens (a crushed skull and a partial mandible) of *Hyopsodus paulus* Leidy, 1870 from Green River Basin (middle Eocene) have also been described by West (1979). These specimens only preserve dP3-dP4 and dp2-dp4 and, as mentioned by West (1979: 27-28), "the paucity of juvenile jaws retaining both deciduous and permanent teeth in various stages of eruption makes the actual sequence of eruption difficult to reconstruct". More recently, a paleopopulation of the late diverging pantodont *Coryphodon lobatus* Cope, 1877 including many specimens of juvenile individuals, has been described from Piceance Creek basin (earliest Eocene, Colorado) by McGee & Turnbull (2010). An assemblage of at least 12 individuals of *C. lobatus* ranging from subadult to senescent individuals are regarded by the authors as resulting from a catastrophic or mass death accumulation, therefore likely belonging to the same population. Among five juvenile specimens none bears all deciduous teeth and the youngest specimens have a fully erupted M1. Although highly informative in term of eruption sequence, this sample lacks very young, potentially pre-weaned individuals. Because of the full eruption of their M1s, all the juvenile specimens of this assemblage were probably weaned (Anders *et al.* 2011) and lack information on other, early stages of the deciduous dentition of *C. lobatus*.

So far, only one fossil Paleocene mammal species, the pantodont *Alcidedorbignya inopinata* Muizon & Marshall, 1987 (early Paleocene of Tiupampa, Bolivia; see just below in section Material and Methods for comments on recent statements on the age of the Tiupampa mammal fauna) is represented by a rich collection of juvenile specimens including very early stages of deciduous dentition from what are likely perinatal (i.e., near term foetuses or new born) to subadult individuals with erupted M1s and M2s. This species is also documented by many partial or sub-complete remains of adults (Muizon & Marshall 1992; Muizon *et al.* 2015). The sample includes skulls and jaws from the same locality and probably from the same population, with the fossilisation of the most complete specimens likely resulting from a catastrophic event (Marshall *et al.* 1995; Ladevèze *et al.* 2011; Muizon & Ladevèze 2020; Muizon *et al.* in press). The juvenile sample for this species includes 75 specimens and is composed of three partial skulls with associated mandibles and partial skeletons, 43 isolated sub-complete or partial mandibles and 29 sub-complete or partial maxillae. This collection of non-adult individuals is doubtlessly the oldest, most abundant, and most exhaustive in terms of ontogenetic age documented to date for an early placental. This exceptional sample provides an unprecedented opportunity not only to securely establish the dental eruption sequence but also to compare it to cranial growth, and to suggest hypotheses on the timing of weaning and acquisition of sexual maturity and therefore of the palaeobiology of an early eutherian. The mortality profile of the sample for this placental species at Tiupampa is also briefly addressed.

MATERIAL AND METHODS

In the present paper, we identify and describe dental ontogenetic stages documented by juvenile and adult specimens of the species *Alcidedorbignya inopinata*, from the Paleocene of Tiupampa, Bolivia (Muizon *et al.* 2015). In order to get a view as complete as possible on the formation of teeth within crypts and on eruption stages, CT scanning of the specimens MHNC 8279, 8298, 8373, 8416, 13859, was performed using a GE Sensing and Inspection Technologies phoenix|x-ray v|tome|x L240-180 CT scanner at the AST-RX platform, Muséum national d'Histoire naturelle, Paris, France. CT scanning of the specimens MHNC 1213, 8417, 8423, 13857, 13858, 13861, 13948, 13949 was performed using an EasyTom 150 scanner at the MRI-platform, University of Montpellier, France. Isotropic voxel size of scans is given in figure captions. The Mimics Innovation Suite software (21.0 Research Edition, Materialise) was used to perform the 3D reconstruction (segmentation and 3D rendering). Specimens available for study are from the collections of the Cochabamba Museum of Natural History (MHNC, Bolivia).

Quantification of cranial and mandibular growth was tentatively characterized based on a few selected linear measurements taken directly on the specimens using a calliper, since the sample included non-scanned specimens. Selected

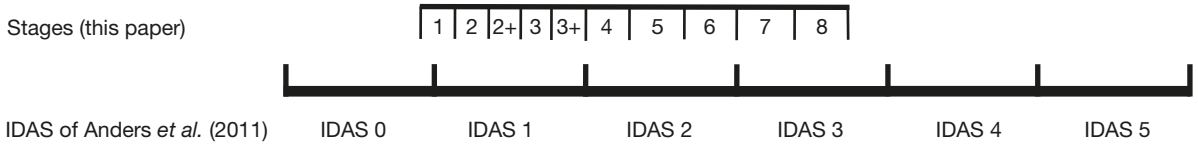

Fig. 1. — Correlation between the dental stage (1 to 8) defined here and the IDAS (Individual Dental Age Stages) of Anders *et al.* (2011).

measurements were those that could be measured on a larger number of specimens preserving most or parts of the cranium or mandible.

The photographs of Fig. 34 have been obtained using an RTI (Reflectance Transforming Imaging) setting as indicated by Decombeix *et al.* (2021) with some specifications, as follows: we used a Canon EOS 5DS digital camera equipped with a Canon MP-E 65 mm macro lens (both Tokyo, Japan); and LEDs of the two lower rings of the light dome were used (i.e., 42 LEDs). Snapshots were extracted using the default' mode (for A and B, light source coordinates X = –0.34, Y = –0.34); for C and D, light source coordinates X = –0.31, Y = 0.44,). On Fig. 34A and B, the wear facet on the paraconule and paracingulum, with the posterior edge of protocristid is best observed with this light orientation, although the latter darkens the distal cusps of the tooth (metacone, metaconule and distal face of protocone). However, observation of these cusps is not the purpose of this figure, which focusses on visualizing the incipient wear facets on M1/m1.

Concerning the tooth wear terminology, we use the term "wear facet" independently of the reason of the wear, without distinguishing attrition (tooth against tooth) from abrasion (tooth against food). In the following description and discussion, we interpret the first premolar as dP1/dp1 following Luckett (1993: 186) who sates that "a successor for dP1 is normally absent in most genera" of placentals (e.g., see condition in macroscelidids, Kindahl [1957]; McKay *et al.* [2022]). However, variation exists since the first premolar of *Canis* is regarded as a permanent tooth with no precursor i.e., P1/p1 (Williams & Evans 1978; McKay *et al.* 2022). Therefore, although the condition of the first premolars (permanent P1/p1 with no precursor or retained dP1/dp1 with no successor) is not identical in all placentals and although the condition of *Alcidedorbignya* cannot be securely resolved (but see discussion below), we designated these teeth as dP1/dp1, because this condition seems to be the most common in placentals.

Note on the age of the Tiupampa mammal fauna

Recently, Beck *et al.* (2022: 310) have stated that "while an early Paleocene age for Tiupampa is plausible, we do not find the evidence for correlating this fauna with chron 28r rather than chron 26r, to be overwhelming." These authors took a compromise position, and assign the Tiupampa mammal fauna to an age range corresponding to the maximum age of chron 28r (65.118 Ma; Sprain *et al.* 2015) and the minimum age of chron 26r, which corresponds to the Selandian-Thanethian boundary (59.2 Ma; Coccioni *et al.* 2012; Cohen *et al.* 2013). This compromise may be a wise solution to the debate on the age of the Tiupampa mammal fauna between Zimicz *et al.* (2020), who supported a correlation with chron 26r and Muizon & Ladevèze (2020) who supported a correlation with chron 28r.

The correlation of the Tiupampa mammal bearing beds with chron 26r by Zimicz *et al.* (2020: 8) has been supported mainly on the basis of what they consider to be a "large amount of recent geological evidence". However, Muizon & Ladevèze (2020: 600-609) have carefully discussed and rejected all the recent geological assumed evidences of Zimicz *et al.* (2020) and presented numerous paleontological arguments and some geological references, which, in our point of view, rather favour a correlation of the Tiupampa beds with chron 28r. Unfortunately, none of these arguments have been discussed in detail by Beck *et al.* (2022), who only provided general comments especially on the fact that comparisons are made between fossil sites at very different paleolatitude (but see Muizon & Ladevèze [2020: 604] for comments on this point). In this context and on the basis of the arguments provided by Muizon & Ladevèze (2020), we consider that correlation of the Tiupampa beds to chron 28r is more defensible than to chron 26r and favour an early Danian age for the Tiupampa mammal fauna.

However, as stated by Muizon & Ladevèze (2020: 609), "it is clear that only radiometric dating at Tiupampa would provide a definitive answer to the question of the age of the Tiupampa mammal-bearing beds. Unfortunately, so far, numerous field seasons at Tiupampa seem to indicate that no tuff or volcanic ashes are present in the Santa Lucía beds on this site".

DESCRIPTION

In the following description, the term juvenile applies to all individuals that do not bear a complete, fully erupted, permanent dentition. In the case of *Alcidedorbignya inopinata,* the latter corresponds to adults that bear the following dental formula: I1-3/i1-3; C/c dP1/dp1; P2-4/p2-4; M1-3/m1-3 (Muizon & Marshall 1992; Muizon *et al.* 2015). We have divided our juvenile sample into six stages identified according to their dental eruption. For each stage, an interpretation of the life history condition (e.g., suckling, weaned, sexually mature...) has been suggested in the discussion. We have correlated our stages of dental eruption with the IDAS (Individual Dental Age Stages) defined by Anders *et al.* (2011), although our large sample of juvenile individuals of a single species allows a clearly more precise subdivision than the IDAS, which consider juvenile as well as adult individuals in all placentals. In order to facilitate

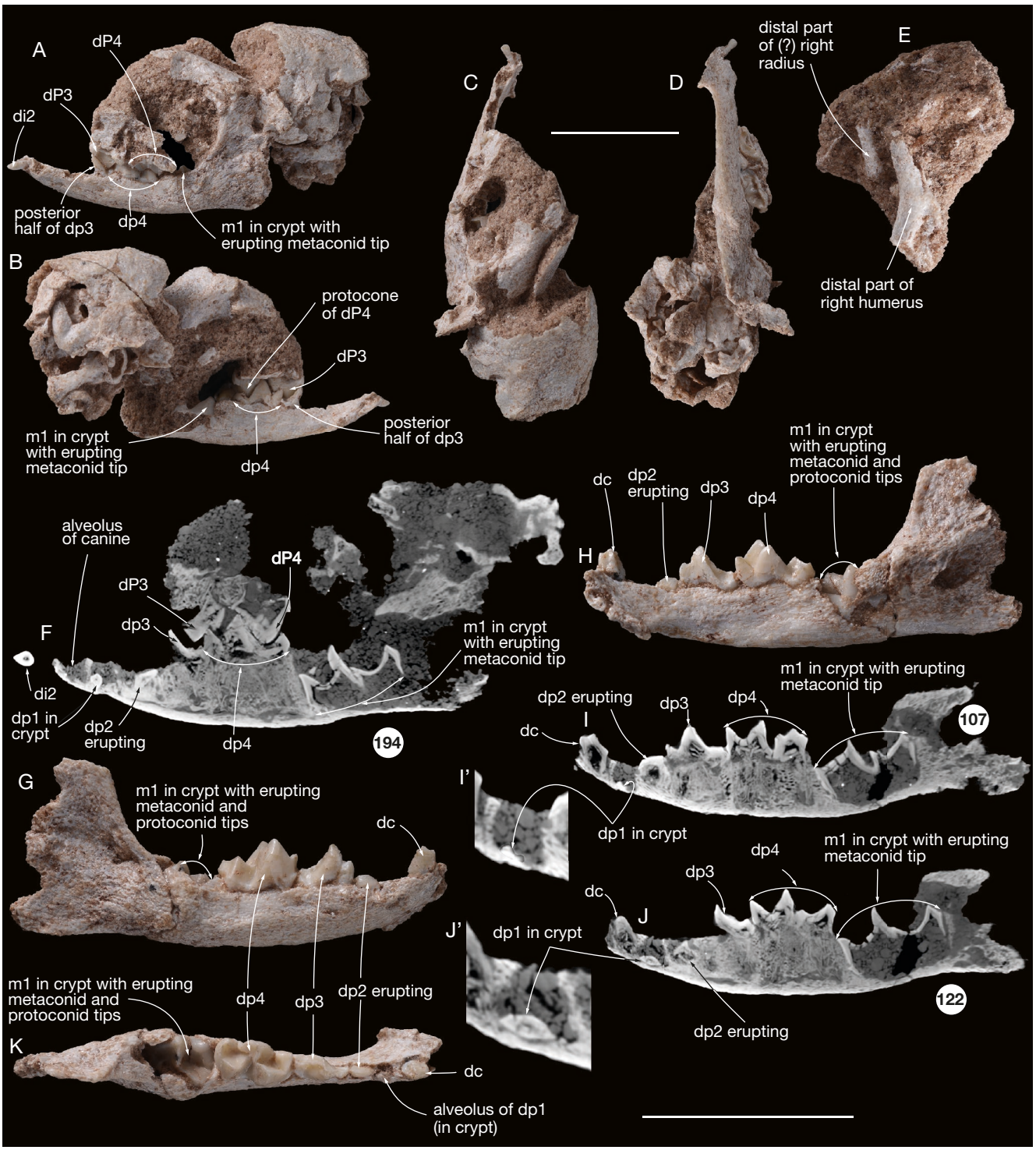

Fig. 2. — Perinatal partial skull and mandibles (MHNC 8373) of *Alcidedorbignya inopinata* (stage 1): **A**, left lateral view of the skull and left mandible; **B**, right lateral view of the skull and left mandible; **C**, dorsal view of the skull and left mandible; **D**, ventral view of the skull and left mandible; **E**, postcranial elements of the same individual; **F**, slice no. 194 of the scan of the skull and left mandible; **G**, Lateral view of the right mandible; **H**, medial view of the right mandible (lateral view); **I**, slice no. 107 of the CT-scan of the right mandible; **I'**, enlargement showing the germ of p1 developing in the bottom of the crypt; **J**, slice no. 122 of the CT-scan of the right mandible (slice 122 is medial to slice 107); **J'**, enlargement showing the germ of p1 developing in the bottom of the crypt; **K**, occlusal view of the right mandible. The number for each illustrated slice refers to the position within the sequence of 771images (resolution binned images voxel size = 0.01857481 mm) for F and 246 images for I and J. Scale bars: 10 mm.

the understanding of the correlation of our stages to the IDAS in the description below, a comparative diagram is presented on Fig. 1. In some cases, we have identified a "stage X +" in addition to two of the six stages we recognize in the series available for *Alcidedorbignya inopinata*. This designation indicates that the condition of dental

TABLE 1. — List of juvenile specimens (jaws, partial jaws, and skulls only) of *Alcidedorbignya inopinata*. Color code: pink, photographs available for study and original specimen in MHNC; green, original specimen on loan at the MNHN; orange, cast at the MNHN but original specimen not available for this study; Abbreviations: **alv**, alveolus; **ctip**, cusp tip; **cry**, crypt (most of tooth in crypt, apex of cusps may be just emerging); **er**, erupting (at least one third of tooth emerged); **l**, left; **r**, right; **rt**, root; **tal**, talonid; **trig**, trigonid. Acronyms: **MHNC**, Museo de Historia Natural de Cochabamba (Bolivia); **YPFB**, Yacimientos petrolíferos fiscales de Bolivia.

Specimen	Stage	Bone	Teeth
Stage undetermined			
YPFB Pal 6375	?	r-maxillary	dP3-4
YPFB Pal 6415	?	r-mandible	dp3
YPFB Pal 6416	?	r-mandible	dp4
YPFB Pal 6417	?	r-mandible	dp4
YPFB Pal 6418	?	r-mandible	dp4
YPFB Pal 6419	?	l-mandible	dp4
YPFB Pal 6450	?	r-maxillary	dp4
YPFB Pal 6451	?	l-maxillary	dp4
Stage 1			
YPFB Pal 6358	1	l-mandible	dp4, m1 in cry
MHNC 8373	1	l-mandible	di2, alvs of di3-c, ctip of dp1 in cry, dp2er, dp3-4, m1 in cry, ctips of m2 in cry
id	1	r-mandible	alvs di1-3, dc, ctip of dp1 in cry, dp2er, dp3-4, m1 in cry, ctips of m2 in cry
id	1	l-maxillary	dP3-4
MHNC 13859	1	r-mandible	di1-c, ctip of dp1 in cry, dp2er, dp3-4, m1 in cry, ctips of m2 in cry
MHNC 13959	1	l-mandible	alv of dp3-4, m1 in cry
MHNC 13966	1	l-mandible	dp4
MHNC 1214	1?	r-mandible	dp3-4
Stage 2			
YPFB Pal 6374	2	l-maxillary	alv of dP2, dP3-4 (unworn)
YPFB Pal 6387	2	r-mandible	(alv of dp1, dp2-3), m1er
YPFB Pal 6399	2	l-mandible	tal of dp4, m1er
YPFB Pal 6449	2	l-maxillary	dP4, cry of M1
MHNC 8423	2	l-mandible	alv of di1, di2, alv of di3, dc, dp1 in cry, dp2-4, m1er, m2 in cry
id	2	r-mandible	alv of di1, di2-3, c, dp1 in cry, dp2-4, m1er, m2 in cry
id	2	l-maxillary	alv of dC, ctip of C in cry, dP1er, dP2-4, M1er, M2 in cry
id	2	r-maxillary	C, dP1er, dP2-4, M1er, M2 in cry
MHNC 13863	2	r-mandible	dp3-4, cry of m1
MHNC 13865	2	r-mandible	alv of dp4, m1er, m2 in cry
MHNC 13866	2	l-mandible	alv of di1, di2-3, rt of dc, dp1 in cry, rt of dp2, dp3, alv of dp4
MHNC 13948	2	r-maxillary	dC, dP1 in cry, alv of dP2, dP3-4, M1er
MHNC 13949	2	l-maxillary	dC, dP1 in cry, dP2-4, cry of M1
MHNC 13950	2	r-maxillary	rt of dP3, dP4, M1er
MHNC 13955	2	r-maxillary	rt of dp3, dP4, cry of M1
MHNC 13961	2	l-mandible	alv of dp4, m1er
MHNC 13967	2	l-mandible	dp3
MHNC 13968	2?	l-mandible	dp3
YPFB Pal 6380	2?	r-maxillary	cry of dP1, dP2-4,
Stage 2+			
YPFB Pal 6352	2+	l-mandible	rt of di1-3, dc, dp1 in cry, dp2-4, m1er, m2?
MHNC 1213	2+	l-mandible	alv of di1-2, di3, dc, dp1in cry, alv of dp2, rt of dp3, dp4, m1er, m2 in cry
MHNC 13969	2+	r-maxillary	Rt of dP4, M1er
Stage 3			
YPFB Pal 6367	3	l-maxillary	dP4-M1, cry of M2
YPFB Pal 6370	3	r-maxillary	dP4-M1
YPFB Pal 6379	3	l-mandible	rt of dc, dp1er, dp2-3
YPFB Pal 6457	3	l-maxillary	dP3 (wear facet on metacrista)
MHNC 1216	3	l-maxillary	dP3-4, alv of M1
MHNC 1212	3	r-mandible	rt of di1, alv of di2, di3, dp1er, dp2-4, alv of m1
MHNC 8416	3	l-mandible	di1-3, i3 in cry, dc, c in cry, dp1er, dp2-4, m1, m2 in cry
id	3	r-mandible	di1-3, cry of i3, dc, dp1er, alv of dp2, dp3-4, m1, m2 in cry
id	3	l-maxillary	dI1-2, alv of dI3, I3 in cry, dC, C in cry, dP1 in cry, dp2-4, M1, M2 in cry
id	3	r-maxillary	dC, C in cry, dP1 in cry, dP2-4, M1, cry of M2
MHNC 8418	3	l-mandible	dp4, m1
MHNC 13864	2+	r-mandible	cry of dp1, rt of dp2, dp3-4, cry of m1
MHNC 13952	3	l-maxillary	cry of dP1, alv of dP2, dP3-4, alv of M1
MHNC 13953	3	r-maxillary	rt of dP2, dP3-4, alv of M1
MHNC 13957	3?	l-mandible	m2 in cry
MHNC 13962	3	r-mandible	alv of m1, m2 in cry
Stage 3+			
YPFB Pal 6353	3+	r-mandible	tal of dp4, m1, m2 in cry
YPFB Pal 6385	3+	l-maxillary	dc, dp1er, dp2
YPFB Pal 6430	3+	r-mandible	dp1er, alv of dp2, dp3-4
MHNC 8279	3+	l-mandible	rt di1, di2-3, dc, c in cry, dp1er, dp2-4, ctip p4 in cry, m1, m2 in cry
MHNC 8298	3+	r-mandible	di1-3, dc, c in cry, dp1er, dp2-4, ctips p4 in cry, m1, m2 in cry
MHNC 13954	3+	r-maxillary	alv of dC, dP1er, dP2-3,

Table 1. — Continuation

Specimen	Stage	Bone	Teeth
Stage 3+ (continuation)			
MHNC 13956	3+	r-mandible	alv of m1, m2 in cry
MHNC 13958	3+	l-mandible	m2 in cry
MHNC 13965	3+	r-mandible	alv of m1, m2 in cry
Stage 4			
YPFB Pal 6369	4	r-maxillary	dP1, dP2-4, P4?
YPFB Pal 6378	4	r-maxillary	dP3-4, P4?, alv of M1
YPFB Pal 6373	4	r-maxillary	dp1, dp2-4
YPFB Pal 6381	4	l-mandible	dp1, dp2-3
YPFB Pal 6448	4	l-maxillary	P4 in cry, dP4
MHNC 8417	4	r-mandible	rt of dp2, dp3-4, m1
MHNC 8286	4	l-mandible	dp4, p4 in cry, m1, m2er, ctip of m3 in cry
MHNC 13857	4	r-maxillary	dC, C in cry, dP1, dP2-3, ctip of P3 in cry, dP4, P4 in cry, M1, M2er
MHNC 13960	4	l-maxillary	rt of dP4, cry of P4, M1, cry of M2
MHNC 13964	4	l-mandible	tal of dp4, m1, cry of m2
MHNC 13861	4	r-maxillary	alv of dC, C in cry, alv of dP1, alv of dP2, P2 in cry, dP3-4, P4 in cry, alv of M1, cry of M2
Stage 5			
YPFB Pal 6351	5	l-mandible	i3er, dc, c in cry, dp1, dp2-4, m1, trig of m2
YPFB Pal 6363	5	l-maxillary	Cer, dP1, P2-3 in cry, dp4, P4 in cry, M1, alv of M2, cry of M3
YPFB Pal 6376	5	r-mandible	rt of dp1, p2er, dp3, rt of dp4
YPFB Pal 6384	5	l-mandible	alv of di1, rt of di2, alv of di3, alv of dc, c in cry, dp1, alv of dp2, rt of dp3
YPFB Pal 6386	5	r-mandible	rt of dp1-p2, p3er, alv of p4
MHNC 13858	5	r-mandible	dc, cer, dp1, p2 in cry, dp3-4, m1, alv of m2, m3 in cry
MHNC 13860	5	r-maxillary	Cer, dP1, alv of P2, P3er, P4-M2, cry of M3
MHNC 13963	5	l-mandible	dp4, p4 in cry
Stage 6			
MHNC 13853	6	l-maxillary	rt of P3, P4-M2, cry of M3

eruption is slightly more advanced than "stage X", but not enough to justify inclusion in a different stage. Among the 75 juvenile jaws, four are referred with doubt to a possible stage and eight are too incomplete (or photographs did not provide enough information) to be securely classified in a specific stage (see Table 1).

Stage 1

Dental ontogenetic criteria for this stage are 1) all deciduous teeth are erupted (except dp2, which is only partly erupted in the youngest individuals), 2) germ of m1 complete but still in crypt, and 3) crypt of m2 in the process of formation with at least one cusp tip partly mineralised (Figs 2-6).

Six specimens are referred to this stage: MHNC 8373, a partial skull missing the right maxilla, with the left maxilla bearing dP3-4, posterior part of the frontals and most of the braincase are preserved but distorted, left mandible with di2 erupting (apex at the edge of the alveolar border), posterior part of dp3, dp4 and m1 as a germ in crypt and right mandible with dc, dp2 erupting, dp3-4 and m1still in crypt; MHNC 1214, right mandible with dp3-4; MHNC 13859, a left mandible with di1-3, dc, dp2-4, m1 in crypt, MHNC 13959, partial left mandible with alveoli of dp3-4 and trigonid of m1 in crypt (talonid missing); MHNC 13966, left mandible fragment with dp4, YPFB Pal 6358; left mandible with dp4 and m1 in crypt. These specimens correspond to a minimum of four different individuals based on the presence of four specimens with a left dp4.

The upper dentition of this stage is known from unworn left dP3 and dP4 in the only preserved maxillary of skull (MHNC 8373). No trace of P3 and P4 are visible above dP3 and dP4 and no crypt is observed in the maxilla (Fig. 2). Furthermore, an isolated left dC and a left dP2 were found during preparation very close to the left maxilla of the skull. As preserved the root of the deciduous canine is as long as the crown and, since its apex is broken, it was longer than the crown. Therefore, it is likely that the upper deciduous canines were erupted at birth. The root of dP2 is approximately as long as the crown and it is also probable that this tooth was erupted or, at least, erupting at birth.

The lower dentition is more complete than the upper. The anterior teeth are better preserved on MHNC 13859, in which the three deciduous incisors and canine are preserved. Their roots are open. There is no indication of a permanent canine in crypt. On MHNC 8373, the dp1 is present as a small germ, with a widely open crown, at the bottom of the alveolus (Fig. 2I, J) (see Material and Method section for the interpretation of the first premolars as non-replaced deciduous teeth). The dp2 is not fully erupted and only the apex of the crown is emerging from the dentary (Fig. 2K, H). The root is short, open, and extends ventrally as far as mid-height of the dentary. The dp3 and dp4 are fully erupted, unworn, and feature well-developed roots, which reach the ventral region of the dentary. The crown of m1 is present in crypt and its trigonid is visible dorsally since the anterior part of the bony roof of the crypt has disappeared. The trigonid is likely to have been totally covered by gum only and its largest cusps (protoconid and metaconid) are unworn and unlikely to have pierced this gum. The m1 is a germ; it has no root and the crown only has developed

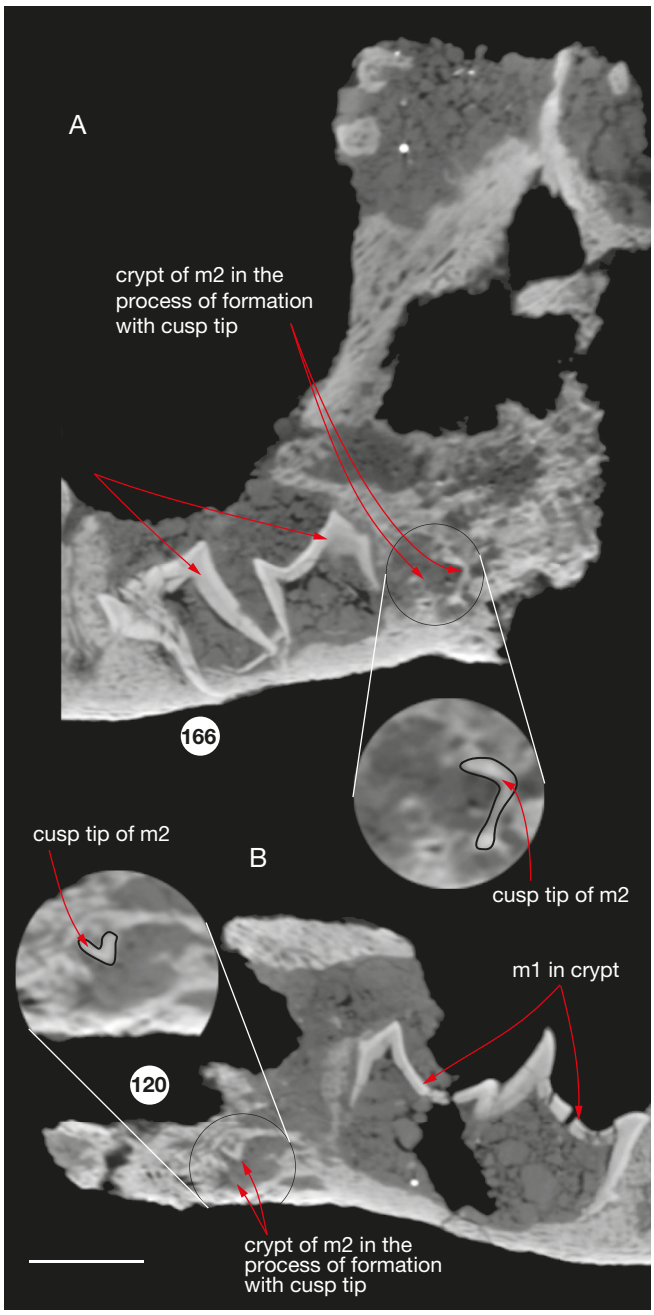

Fig. 3. — Mandibles of the perinatal specimen (MHNC 8373) showing the crypt of m2 in formation with a cusp tip: **A**, left mandible; **B**, right mandible. The number for each illustrated slice refers to the position within the sequence of 772 images (resolution binned images voxel size = 0.01857481 mm) for A and 247 images (resolution binned images voxel size = 0.01857481 mm) for B. Scale bar: 2 mm.

(Fig. 2). Posterior to the crypt for m1, a much smaller cavity is observed. It contains a small cusp tip and represents the future crypt for m2 in the process of formation (Figs 3; 4). Although incomplete this cusp is interpreted here as the protoconid in the light of observations made on MHNC 13859, an individual in which the cusp is more recognizable (Fig. 6). This interpretation follows Jernvall (1995: 26 and references therein) who states that the protoconid is generally the first cusp to develop in the lower molars.

In MHNC 13859 the development of dental eruption is slightly more advanced than in MHNC 8373 (Fig. 4). The germ of dp1 is more developed and its apex is higher in the alveolus. On dp2, the crown is almost fully erupted and the root is slightly longer and extends below mid-height of the dentary, up to the ventral third of bone. At the posterior end of the dentary a small crypt for m2 is also present, in which a very thin cusp tip can be observed and better preserved than on MHNC 8373 (Figs 5; 6). Because of its shape (labial side strongly convex without cristid and lingual side flat) and because of the presence of a slight cingulid (precingulid) on its anterior edge, we interpret this cusp as the protoconid. Because of its position in the fossil, it is likely that this cusp has been displaced lingually before filling of the crypt with sediment. It is noteworthy that the differences noted above between the two specimens are minor and may well be the result of some individual variation. This stage in *Alcidedorbignya* probably corresponds to IDAS stage 0 (foetus) or early IDAS 1 (newborn) of Anders *et al.* (2011), since the m1 is still in crypt and does not present any wear facet. One of the specimens in this stage (MHNC 8373) being a possible near-term foetus (because of its position between the limbs of MHNC 8372; Muizon *et al.*, 2015) rather argues for IDAS 0. Furthermore, if this interpretation is correct, then MHNC 13859, the dental eruption of which is slightly more advanced, could be a newborn individual and would correspond to early IDAS 1. Be that as it may, both specimens are regarded as perinatal. In fact, because differences of dental eruption between a near-term foetus and a newborn individual are minimal, it makes more sense to include both in a single stage (our stage 1) including perinatal specimens. Stage 1 corresponds to late IDAS 0 and early phase of IDAS 1, but the difference with late IDAS 0 should be minimal (Fig. 1).

Stage 2

Dental ontogenetic criteria for this stage are 1) M1 partly erupted (apices of proto-, para- and metacone out of crypt, but styles and stylar shelf still covered by the maxilla); 2) trigonid of m1 partly erupted but talonid still in crypt; 3) crypt of m2 much larger than on stage 1 (almost definitive size) with trigonid of m2 formed and at least one tip of cusp (hypocone) of talonid present; 4) dP1 and dp1 still in crypt but with apex close to alveolar border; 5) dP2 and dp2 fully erupted; 6) tip of permanent canine in crypt (Figs 7-10).

Sixteen specimens are included in this stage: MHNC 8423, a partial skull and associated mandibles: the skull is missing the premaxilla, most of the occipital, and part of the left ear region, right maxilla bearing dC, dP1 starting to erupt, dP2-4, M1 erupting, left maxilla bearing dP1 starting to erupt, dP2-4, M1 erupting, ectotympanic and ear ossicles in situ, left mandible with di2, dc, dp1 in crypt, dp2-4, trigonid of m1 erupting, right mandible with di2-3, dc, dp1 in crypt, dp2-4, trigonid of m1 erupting (Figs 7-10); MHNC 13863, partial right mandible with dp3-4; MHNC 13865, left partial mandible with m1 (trigonid erupting and talonid in crypt; MHNC 13866, anterior part of left mandible with roots of di2-3; dc, dp1 in crypt, root of dp2, dp3; MHNC 13948 left maxilla with dc, dp1 in crypt, dp3-4 (Fig. 11A);

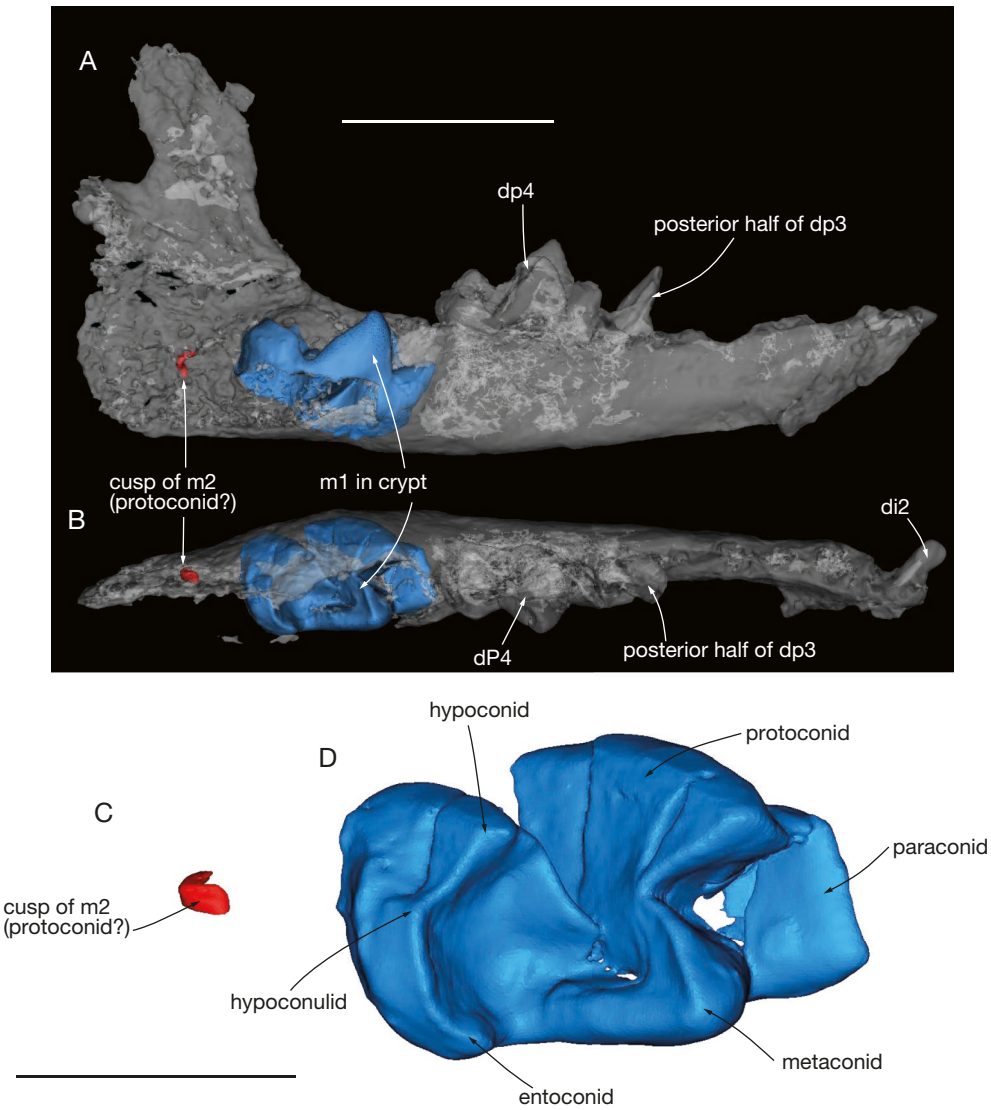

FIG. 4. — **A**, Transparent lateral view of left mandible (MHNC 8373) of juvenile *Alcidedorbignya inopinata* (stage 1) showing left m1 and the tip of a cusp of m2 in crypt (probably the protoconid); **B**, the same in occlusal view; **C**, occlusal view of left m1 in crypt and partial cusp tip of m2 (probably the protoconid). Scale bars: A, B, 5 mm; C, 2 mm.

MHNC 13949, right maxilla with dC, dP1 in crypt, dP3-4, M1 erupting (Fig. 11B); MHNC 13950, fragment of right maxilla with roots of dP3, dP4, M1 just starting to erupt from crypt; MHNC 13955, fragment of right maxilla with unworn dP4 and crypt of M1 above posterior edge of dP4; MHNC 13961; partial left mandible with alveoli of dp4 and m1 erupting; MHNC 13967 (possibly), partial left mandible with dp3; MHNC 13968 (possibly stage 2), partial left mandible with dp3; YPFB Pal 6374, left maxillary fragment with alveolus of dP2, dP3-4 (unworn); YPFB Pal 6380 (possibly stage 2), partial maxilla with crypt of dP1, dP2-4. YPFB Pal 6387, part of right mandible with erupting m1, YPFB Pal 6399, part of left mandible with talonid pf dp4 and erupting m1; YPFB Pal 6449, fragment of a left maxilla with dP4 and crypt of M1 above posterior edge of dP4. These specimens correspond to a minimum of six different individuals based on the presence of six specimens with a left dp3 and/or dp4.

In MHNC 8423, the upper incisors are not preserved (Fig. 7). The right dC is present; on the left side dC is not preserved. Anteromedial to the alveolus of the left dC is the crypt of the left permanent canine, in which is preserved the apex of permanent C, which has been turned upside down during fossilisation (i.e., the apex is facing dorsally; see Fig. 8A). No trace of the permanent C is observed on the right side. However, because the anterior part of right maxilla is broken, the crypt of the right permanent canine is open anteriorly and, if present, the germ of the tooth may have been lost. The dP1 is erupting with only the tip of the crown visible, being slightly ventral to the edges of the alveolus (Fig. 8B).

In MHNC 13948 and 13949, dP1 is emerging but the apex of the crown is slightly dorsal to the edge of the alveolus (Fig. 11), in contrast to the condition observed in the skull of MHNC 8423. The dP2 is fully erupted in the two specimens, in which it is preserved (MHNC 8423 and 13949).

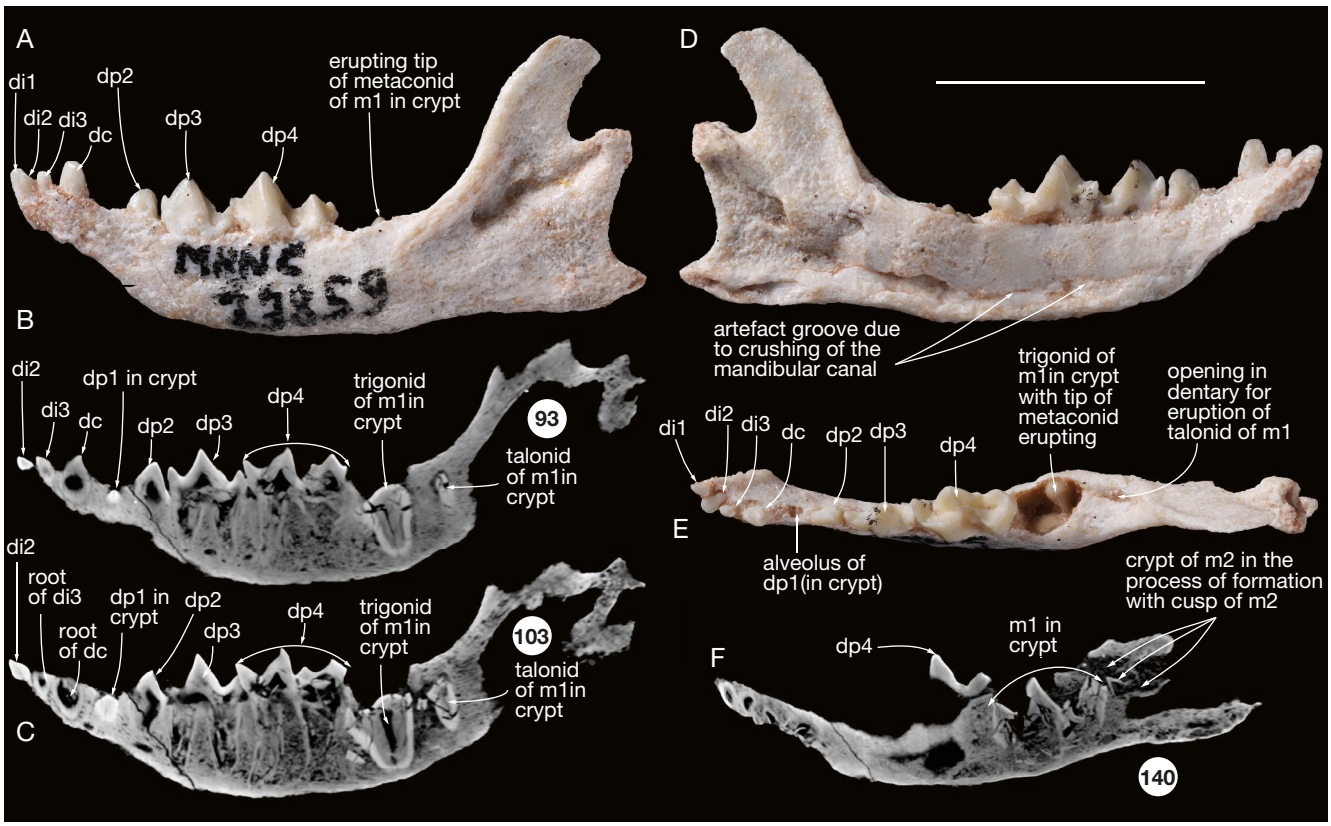

FIG. 5. — Left mandible (MHNC 13859) of juvenile *Alcidedorbignya inopinata* (stage 1): **A**, lateral view; **B**, **C**, slices no. 93 and 103 of the lateral CT-scan of the specimen; (slice 93 is lateral to slice 103); **D**, medial view; **E**, occlusal view; **F**, slice no. 140 of the lateral CT-scan of the specimen (slice 140 is medial to slice 103). The number for each illustrated slice refers to the position within the sequence of 213 images for A and D (resolution binned images voxel size = 0.02781842 mm). Scale bar: 10 mm.

The root of dP2 is as long as the crown and almost closed dorsally. The dP3 and dP4 are erupted and functional. At the mesiolingual edge of dP3 and dP4 is a small pit in the maxilla, through which will erupt, in later stages, the tip of the protocone of P3 and P4 respectively (see below, stage 5 YPFB 6363). Dorsal to dP3 and dP4 there is no indication that the tip of the cusps of P3 and P4 are present and no crypt is developed yet. The M1 is still in crypt but erupting and, even if its lateral edge (stylar shelf) is still covered by the maxilla, the apex of protocone, paracone and metacone were probably piercing (or were close to) the gum (also observed in MHNC 13950). Behind M1, the maxilla is well preserved, no breakage is observable. On both sides, just posterior to the protocone of M1 the maxilla is slightly excavated, which probably indicates that the crypt of M2 is starting to develop. However, no cusp tip has been discovered posterior to M1 during preparation of the skull MHNC 8423. If they were actually present in life, they may have been lost post-mortem. However, the fact that the ectotypmanic and ear ossicles are preserved in situ (with the right one in life position) indicates that the individual has encompassed very little post-mortem disturbance of its elements. It is therefore possible that no cusp of the M2s had yet mineralised in this individual. On the other hand, the fact that the anteromedial angle of the crypt of M2 is starting to develop could also indicate that some cusp tips of m2 may have been already present. Therefore, this point remains unelucidated.

On the mandible of MHNC 8423, di2-3 are preserved on the right side and di2 on the left side, which suggests that the upper incisors were also deciduous. The crown of dp2 is fully erupted and its root is two to three times as long as the crown. It is moderately open ventrally. The condition of the other deciduous teeth is similar to that observed on the skull and no cusps of p3-4 nor crypt are observed. In contrast to the condition of the dP1, the apex of dp1 is not emerging being slightly ventral to the edges of the alveolus (Fig. 9). The m1 is partly erupted; the cusps of the trigonid are slightly more erupted than the proto-, para-, and metacone and were probably emerging through the gums. In contrast, the talonid is still embedded in the crypt and its cusps were likely covered by gum during life. The roots are not formed yet and the pulp cavity is still widely open ventrally. The crypt of m2 is present and features a small dorsal circular opening, through which can be observed the first elements of the trigonid cusp in process of mineralisation. The CT scan slices on Fig. 9 and the transparent view of Fig. 10, reveal that the trigonid and talonid of m2 were in early stage of mineralisation. The three cusps of the trigonid are formed but are incompletely fused in the centre of the trigonid basin and posterior to the trigonid, a single

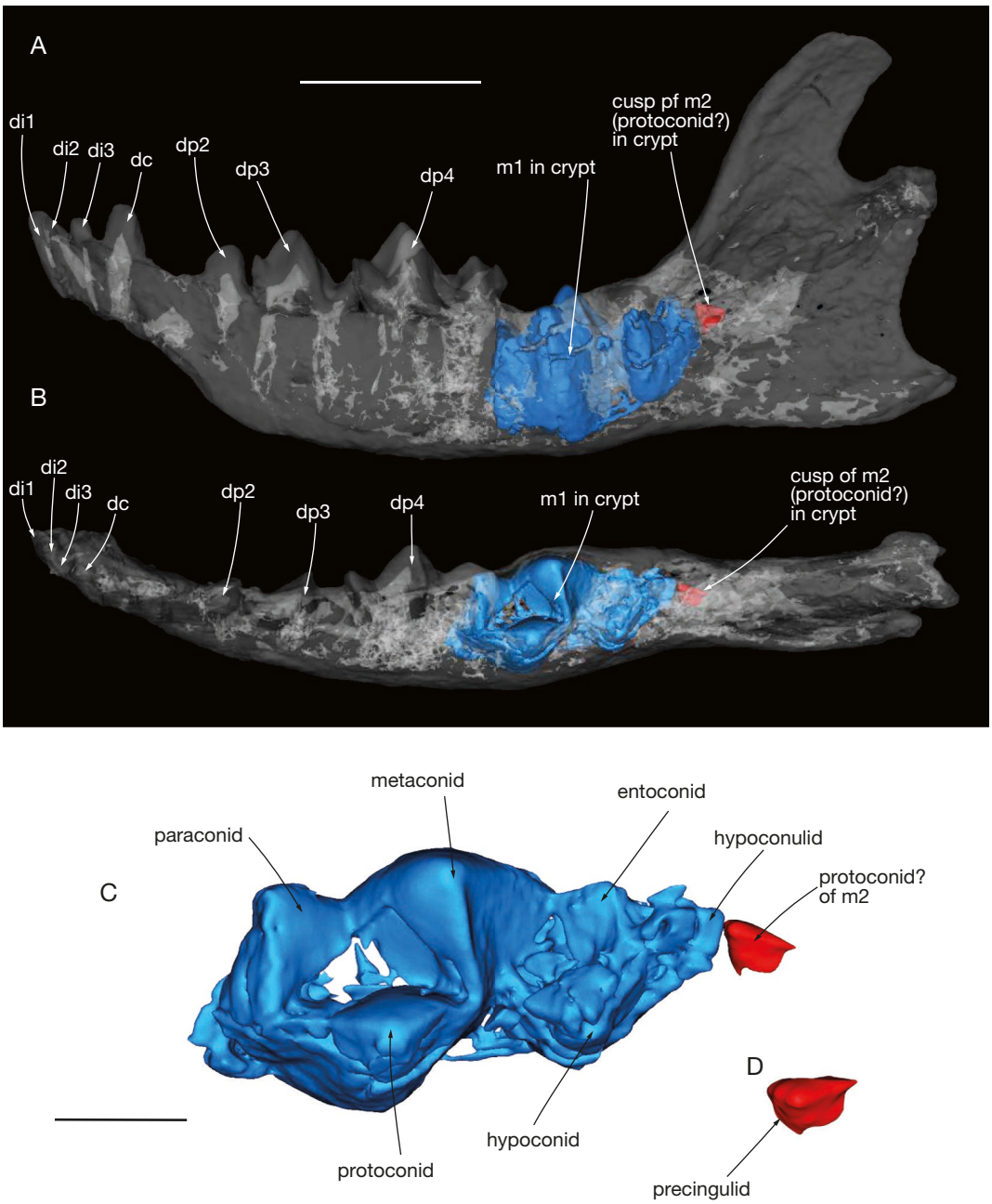

FIG. 6. — **A**, Transparent lateral view of left mandible (MHNC 13859) of juvenile *Alcidedorbignya inopinata* (stage 1) showing left m1 and the tip of a cusp of m2 in crypt (probably the protoconid); **B**, the same in occlusal view; **C**, occlusal view of left m1 in crypt and cusp tip of m2 interpreted here as the protoconid (the cusp has been slightly displaced and rotated clockwise *c.* 45°); **D**, occlusal view of the protoconid of m2 in its probable natural position. Scale bars: A, B, 5 mm; C, 2 mm.

cusp is present, referred here to the hypoconid. On MHNC 13865, a partial mandible with erupting m1, the crypt is observed through a small breakage on the medial aspect of the dentary just anterior to the mandibular foramen. Peering through this opening some poorly mineralised cusps of m2 are visible. No dorsal opening of the crypt of m2 is observed posterior to erupting m1 and anterior to the base of the coronoid process, as in MHNC 8423. If our interpretation of the absence of crypt and cusps of M2 on the skull is correct, then the formation of m2s slightly predates that of M2s. On upper and lower deciduous premolars (dP/dp 2-4), wear facets, when observed, are extremely faint and we suggest that they are rather attrition (tooth to tooth) than abrasion (tooth to food) facets. Stage 2 corresponds to early IDAS 1 but later in IDAS 1 than our stage 1 (see Fig. 1).

STAGE 2 +

Dental ontogenetic criteria for this stage are 1) eruption of M1 and m1 more advanced than on stage 2; 2) M1 with parastyle still covered by the maxilla and alveolar border of maxilla almost reaching the labial cingulum of stylar shelf; 3) m1 with trigonid almost fully erupted and talonid erupting; 4) wear facet on deciduous premolars, when present, are extremely faint.

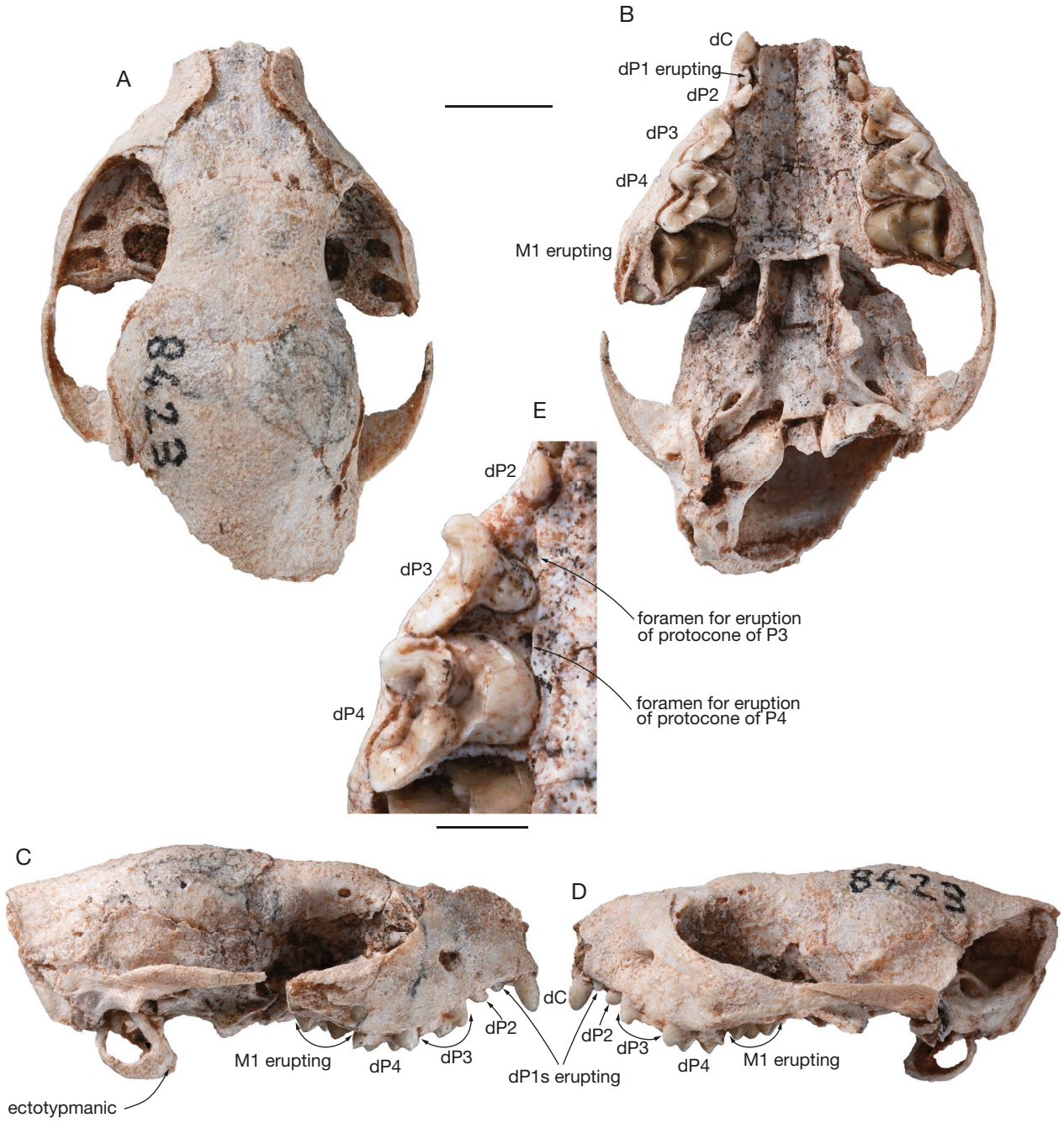

FIG. 7A-E. — Partial skull and mandibles (MHNC 8423) of juvenile *Alcidedorbignya inopinata* (stage 2): **A**, dorsal view of skull; **B**, ventral view of skull; **C**, enlargement of part of right palate; **D**, right lateral view of skull; **E**, left lateral view of skull. Scale bars: A-D, 5 mm; E, 2 mm.

Three specimens are referred to this stage: MHNC 1213 left mandible with di2, dc, dp1 in crypt, dp4, m1 almost fully erupted (Fig. 12); MHNC 13969, partial maxilla with roots of dP4 and almost fully erupted M1, but less than in stage 3, since parastyle is clearly above metastyle of dP4; YPFB Pal 6352, left almost complete mandible with dc; dp1 in crypt, d2-4, m1 almost fully erupted. These specimens correspond to at least two different individuals based on the presence of two specimens with the left m1.

This stage differs from the preceding one in the more advanced eruption of m1. The trigonid cusps are at the occlusal level of those of dp4 and the three talonid cusps are out of the crypt and distinctly overhanging the alveolar border. Therefore, the tooth is almost fully erupted, whereas it was only partly erupted in stage 2. Roots of m1 are barely present and the pulp cavity is widely open ventrally. Therefore, the ventral edge of the crown (i.e., the cemento-enamel junction) is still below the alveolar border. However, the difference with stage 2 is not major since dp1 is not more erupted with its apex still slightly below alveolar edge. When observed, wear facets on dP/dp 3-4 are very small. One is present on the oblique cristid of the dp4 of YPFB Pal 6352.

Stage 2+ also corresponds to early IDAS 1 but slightly later in IDAS 1 than our stage 2 (see Fig. 1).

FIG. 7F-K. — Partial skull and mandibles (MHNC 8423) of juvenile *Alcidedorbignya inopinata* (stage 2): **F**, lateral view of left mandible; **G**, occlusal view of left mandible; **H**, medial view of left mandible; **I**, Lateral view of right mandible; **J**, occlusal view of right mandible; **K**, medial view of right mandible. Scale bar: 5 mm.

STAGE 3

Dental ontogenetic criteria for this stage are 1) M1 and m1 fully erupted (or almost), but without wear facet; 2) crypts of M2 and m2 almost totally formed with the major cusps of M2 and m2 already mineralised and connected; 3) M2 and m2 still totally in crypt; 4) dP1 and dp1 still in crypt but apex close the alveolar border; 5) tips of crown of I3 and i3 present in crypt, at least on one side; 6) conspicuous wear facets present on deciduous premolars (Figs 13-19).

Thirteen specimens are referred to this stage: MHNC 8416, a partial skull with braincase distorted, missing the right premaxilla, exoccipitals and supraoccipital, with associated mandible; on the left side dI1-2, dC, dP1 in crypt, dP2-4, M1, protocone of M2 in crypt, on the right side dC, dP2-4, M1, crypt of M2 above posterior half of M1, on the left mandible, di1-3, dc, dp1 starting to erupt, dp2-4, M1 fully erupted; M2 in crypt, right mandible as for the left but missing dp2 (Figs 13-19); MHNC 8418 left mandible fragment with dp4, m1; MHNC 1212, anterior part of right mandible with root of di1, di3, root of dc, dp1 erupting, dp2-4, anterior alveoli of m1; MHNC 13864 right mandible fragment with root of dp2, dp3-4; MHNC 13953 (possibly stage 3), fragment of right maxilla with dP3-4 and medial and mesiolabial alveoli of M1; MHNC 13957, fragment of left mandible with m2 in crypt; MHNC 13962, fragment of right mandible with alveoli of m1 and trigonid of m2 in crypt; MHNC 13965, fragment of right mandible with distal alveolus of dp4, alveoli of m1 and trigonid of m2 in crypt; YPFB Pal 6353, part of right mandible with m1 and unerupted m2 (this specimen could also be referred to stage 3 + since the degree of eruption of its dp1 is unknown – see below) ; YPFB Pal 6367, part of left maxillary with dp4 and m1; YPFB Pal 6370, fragment of right maxillary with dP4-M1; YPFB Pal 6379, left mandible with root of dc, dp1 erupting, and dp2-3; YPFB Pal 6457, left maxillary fragment with dP3, with a distinct wear facet on posterior edge of metacrista. These specimens correspond to a minimum of five different individuals based on the presence of five specimens with a left dP3

As seen on the skull and mandible MHNC 8416, all deciduous teeth are present and functional at this stage. Conspicuous wear facets are observed on dP/dp 3-4, in contrast to the condition observed on stages 2 and 2+. As seen on CT data of the skull and mandible, the germs of permanent I1, I2, i1, and i2 are not present. However, the germ of permanent I3 and i3 is present (Fig. 15A, D). I3 is observed on the left side only since right premaxilla is not preserved on the specimen. On the mandible, the germ of i3 is present only on the right side and the crypt of the left deciduous i3 bears no tooth germ

FIG. 8. — Slices of CT-scan of skull (MHNC 8423) of juvenile *Alcidedorbignya inopinata* (stage 2): **A**-**D**, slices (70, 121, 297, 529) of the frontal CT-scan (slice 70 is anterior and slice 529 is posterior); **E**, slice 593 of the coronal CT-scan. The number for each illustrated slice refers to the position within the sequence of 1630 images for A-D and 922 images for E (resolution binned images voxel size = 0.0159858 mm). Scale bar: 5 mm.

(which has probably not developed yet) (Fig. 16C). On the skull, anterodorsomedial to dC, is the germ of the permanent canine in crypt (Figs 15A; 16A). It has no root and its crown is widely open dorsally. It is barely larger than the deciduous canine. A similar condition is present on the mandible (Fig. 16B, E). The dP1 and dp1 are unerupted. However, the

apex of dP1 is slightly dorsal to the alveolar edge (Fig. 17A, B), being internal to the alveolus, whereas, on the mandible, the apex of dp1 is slightly dorsal to alveolar edge (Fig. 17C, D), emerging from the alveolar border. The dP1 has no root in this specimen, whereas, on the mandible, a distinct root of dp1 is present and extends below mid-height of the dentary (Fig. 17A). Therefore, the eruption of dp1s slightly precedes that of dP1s. This condition of dP1 in MHNC 8416 is reversed from that observed on the skull of stage 2 (MHNC 8423), in which the apex of dP1 is emerging whereas that of dp1 is still within the crypt thus indicating that the eruption of dP1 precedes that of dp1. This condition indicates that some variation exist in the relative timing of eruption of dP1 and dp1.

On the palate, pits for eruption of the protocones of P3 and P4 are present in the maxilla at the mesiolingual edge of the alveoli of dP3 and dP4 (Fig. 14A). The M1 and m1 are almost fully erupted and may have been functional but no wear facet is observed. They have well-developed roots, which almost reach the mandibular canal on the left mandible. The germ of M2 and m2 are present in their crypts (Figs 17-19). The M2 shows two post-mortem *c.* 90° rotations: a clockwise rotation in right lateral view of the skull and another clockwise rotation in anterior view of the skull. As a result of these turns, the protocone is facing more or less dorsally, the paracone dorso-posteriorly and the metacone ventro-posteriorly (Fig. 19). The upper crypt is observed on the right side of the skull; its anterior edge is located above the level of the ectoflexus of M1. The germ of M2 is missing on the right crypt. It is only partially complete on left crypt, since the stylar shelf is apparently missing, but all major cusps are mineralised (paracone, metacone, protocone, paraconule, metaconule) and connected at their base. Only the protocone and conules are observed in the floor of the left orbit (the tooth has been displaced post-mortem and is not in anatomical position) and the rest of the tooth (i.e., paracone and metacone) is still in matrix and has been reconstructed from CT data (Fig. 19). On the mandible, a small opening is observed on the anterior roof of the crypt only above the trigonid of m2 but no cusp of the tooth is emerging; the tooth is in its crypt and slightly crushed (Figs 14; 17D). All cusps are mineralised on the m2, with no part of the crown missing (Fig. 19). Roots are not formed in either M2 or m2 on this specimen. Stage 3 corresponds to late phase of IDAS 1 (Fig. 1).

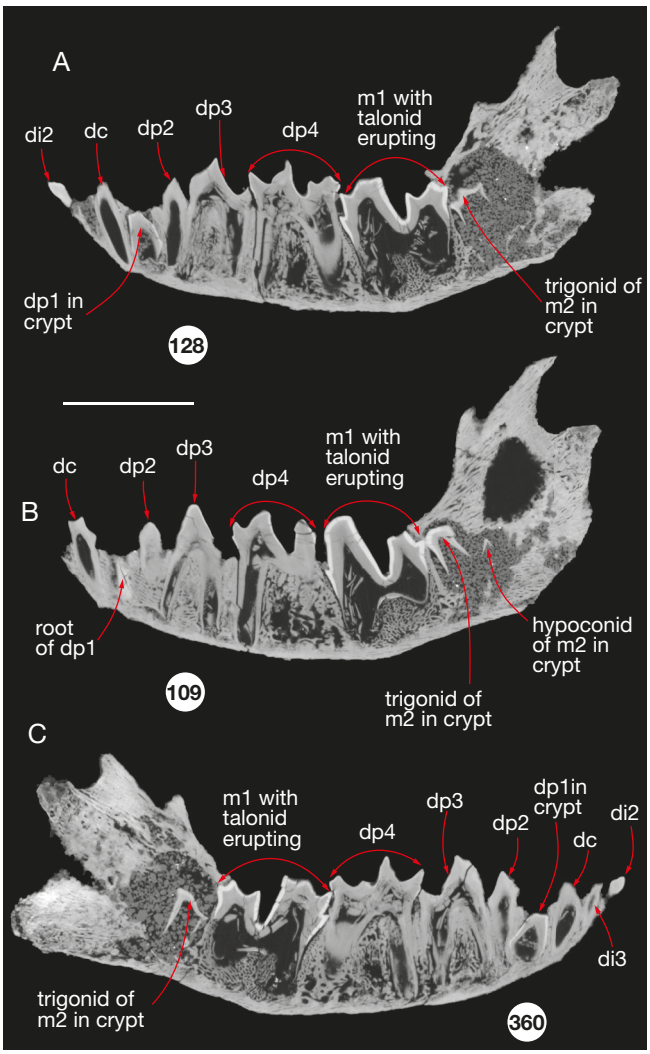

Fig. 9. — Slices of the lateral CT-scan of the mandibles (MHNC 8423) of juvenile *Alcidedorbignya inopinata* (stage 2): **A**, **B**, slices (128, 109) of the left mandible (slice 109 is lateral to slice 128); **C**, slice 360 of the right mandible. The number for each illustrated slice refers to the position within the sequence of 699 images for A and B and 720 images for C (resolution binned images voxel size = 0.0159849 mm). Scale bar: 5 mm.

Stage 3+

Dental ontogenetic criteria for this stage are 1) dp1 partly erupted and 2) m2 starting to erupt with tips of protoconid visible out of the crypt (Figs 20-23).

Nine specimens are referred to this stage: MHNC 8279, a complete left mandible with di1 broken at base, di2-3, dc, permanent c in crypt, dp1 erupting (one third to one half of the crown), dp2-4, m1 fully erupted, tip of protoconid of m2 visible (but not emerging) through a small opening in the roof of the crypt (Fig. 20); MHNC 8298, an almost complete right mandible with di1-3, dc, permanent c in crypt, dp1 erupting (*c.* one third of the crown is erupted), dp2-4, tip of protoconid (?) in crypt below dp4, m1 fully erupted, roof of the crypt of m2 open dorsally but no cusp emerging (Figs 21; 22); MHNC 13952 (possibly stage 3+), fragment of left maxilla with dP3-4 (with distinct wear facets) and medial and mesiolabial alveoli of M1; MHNC 13954, fragment of right maxilla with dp1 erupting (apex well below alveolar edge) (Fig. 23), dp2-3; MNHN 13956, right mandible fragment with alveoli of m1 and m2 in crypt; MNHC 13958, ramus of left mandible with m2 in crypt; YPFB Pal 6379, part of left mandible with root of dc, dp1 erupting dp2-3; YPFB Pal 6385, part of left maxillary with dc, dp1 erupting, dp2 and anterior roots of dp3; YPFB Pal 6430, right mandible with dp1 erupting alveolus of dp2, and dp3-4. These specimens correspond to a minimum of four different individuals based on the presence of four specimens with a right m1 or m2 and morphological differences between their dentaries.

This stage essentially differs from stage 3 in the greater degree of eruption of dp1, which is erupted on one third to

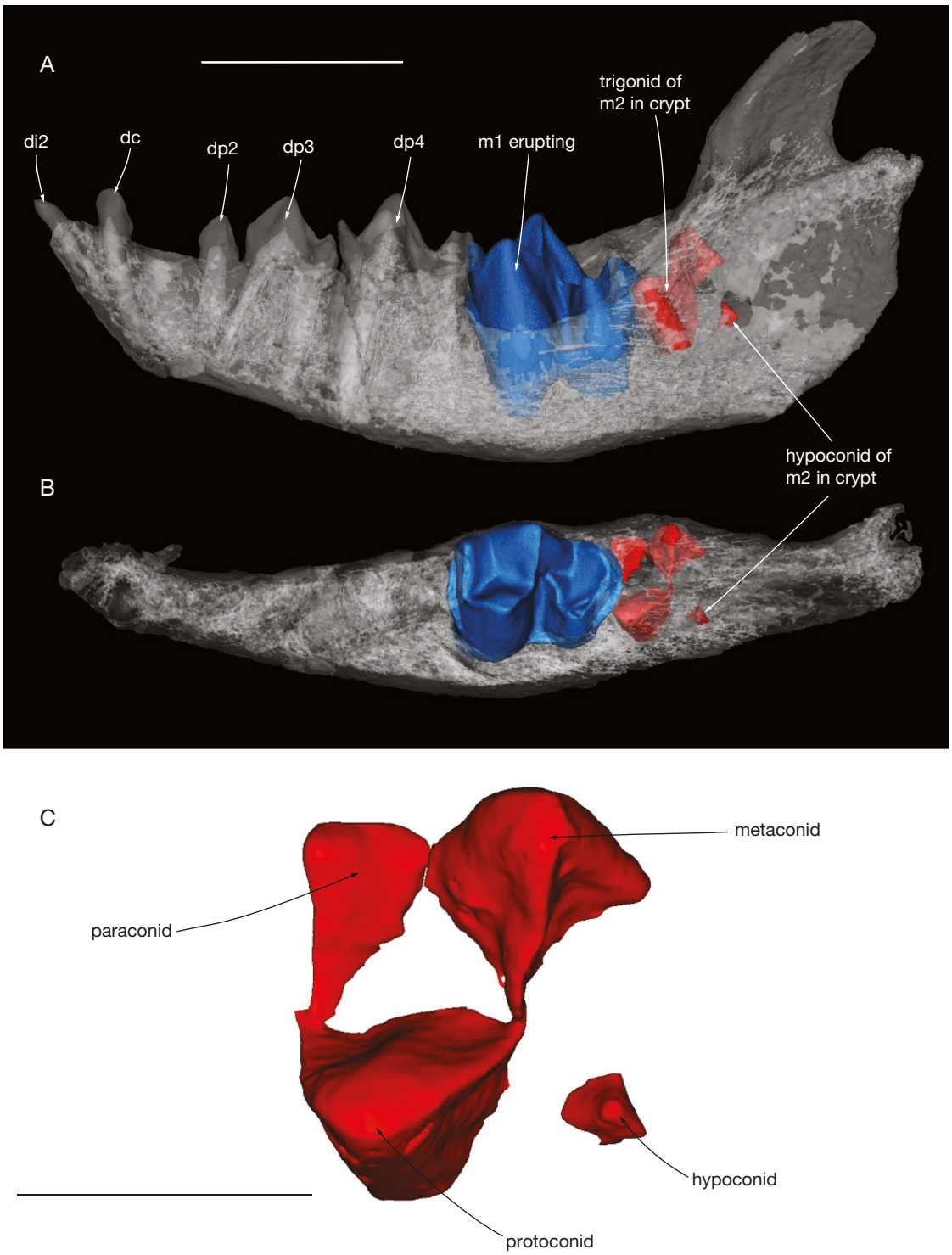

FIG. 10. — **A**, Transparent lateral view of left mandible (MHNC 8423) of juvenile *Alcidedorbignya inopinata* (stage 2) showing left m1 erupting and m2 in formation in crypt; **B**, the same in occlusal view; **C**, occlusal view of left m2 in crypt showing the trigonid with its three cusps partially formed but not completely fused in the centre of the trigonid basin and, posterior to the protoconid, the tip of a cusp interpreted as the hypoconid. Scale bars: A, B, 5 mm; C, 2 mm.

one half of the height of its crown (Figs 20-22), whereas its apex remains at the edge of the alveolus on stage 3 (Fig. 17). Furthermore, as seen in MHNC 8298 and 8279 (Figs 20; 22), the roots of m1 are more developed than in MHNC 8416 (stage 3). Furthermore, m2 is also starting to erupt in MHNC 8279: the roof of the crypt bears two openings (dorsal to trigonid and talonid) and the tip of the protoconid is emerging from a third small opening in the roof of the crypt labially to the large one above the lingual cusps of trigonid (Fig. 20). In MHNC 8298 only one opening is present in the roof of the crypt above the trigonid of m2 indicating a slightly less advanced condition in the eruption of m2 (Fig. 17).

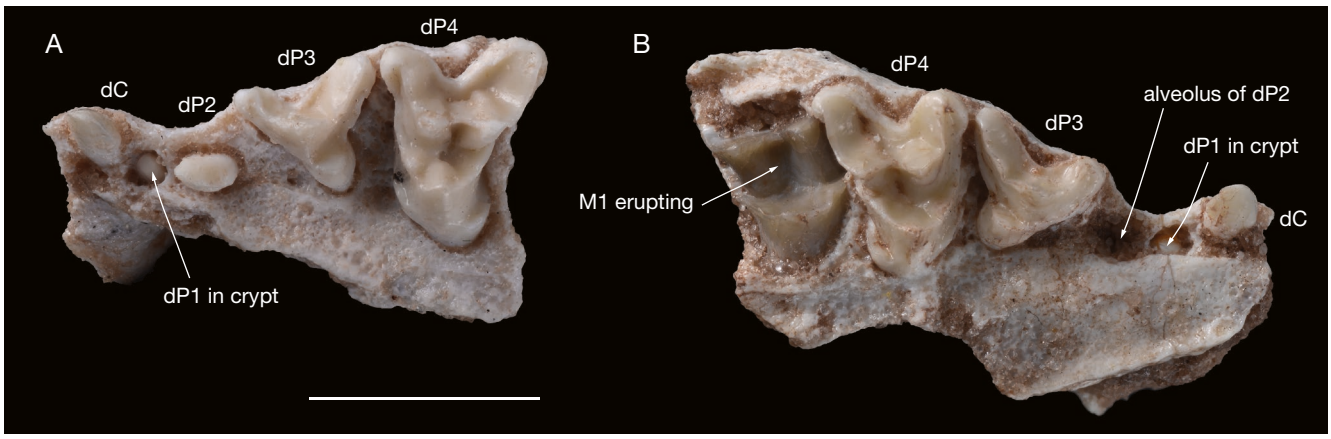

FIG. 11. — Occlusal views of maxillae (stage 2) of juvenile *Alcidedorbignya inopinata*: **A**: left maxilla (MHNC 13948); **B**, right maxilla (MHNC 132949). Scale bar: 5 mm.

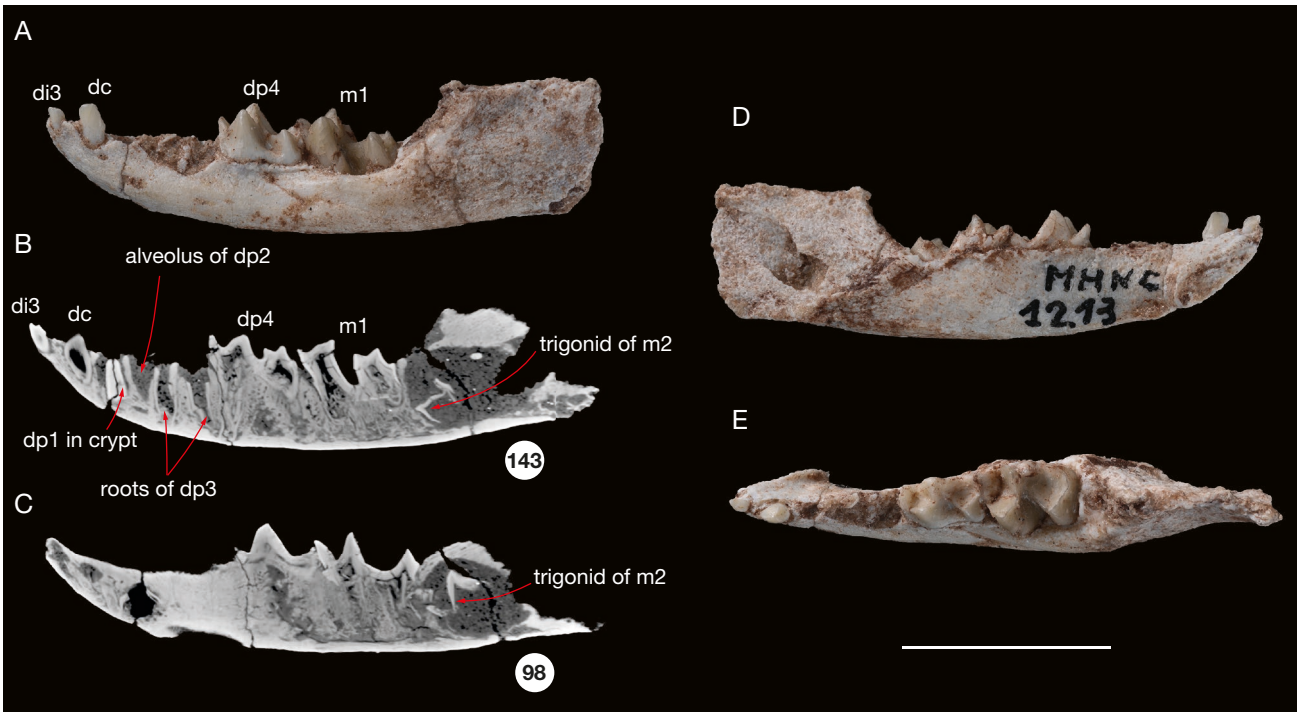

FIG. 12. — Left mandible (MHNC 1213) of juvenile *Alcidedorbignya inopinata* (stage 2+): **A**, lateral view; **B**, **C**, slices 98 and 143 of the lateral CTscan (slice 98 is medial to slice 143); **D**, medial view; **E**, occlusal view. The number for each illustrated slice refers to the position within the sequence of 258 images for B and C (resolution binned images voxel size = 0.02781842 mm). Scale bar: 10 mm.

No indication of crypts and mineralised cusps of p3-4 is observed in MHNC 8279 (stage 3+), a condition similar to that of MHNC 8416 (stage 3), (Fig. 20). However, in MHNC 8298 a tiny tip of a cusp is present below dp4 lingually (Fig. 22), but no mineralised cusp of p3 is observed below dp3. The cusp below dp4 is referred to the protoconid because it bears a flat lingual side, oblique relative to the axis of the tooth row (with a distolingual-mesiolabial orientation) and a strongly convex labial side (Fig. 21C). This condition clearly corresponds to the morphology and orientation observed for the protoconid of the p4 and departs from that of the para- and metaconid. In contrast to what is observed above concerning the eruption of m2, MHNC 8298 would be slightly more advanced than MHNC 8279 as far as the p4 is concerned. As in MHNC 8416, the permanent canines are present in their crypts.

A partial maxilla with erupting dP3, dP2 and dP1 erupting (with dP1 apex distinctly below the alveolar border), has been referred to stage 3+ because the degree of eruption of its dP1 is more advanced than in MHNC 8416 (stage 3+) and less than in MHNC 13857 (stage 4) (Fig. 23). No wear facet is observed on m1, but substantial facets are present mainly on the protoconid of dp3 and protoconid and hypoconid of dp4. These facets are clearly more developed than on the skull and mandible of MHNC 8416 (stage 3). Similar to Stage 3, Stage 3+ corresponds to late phase of IDAS 1 (Fig. 1).

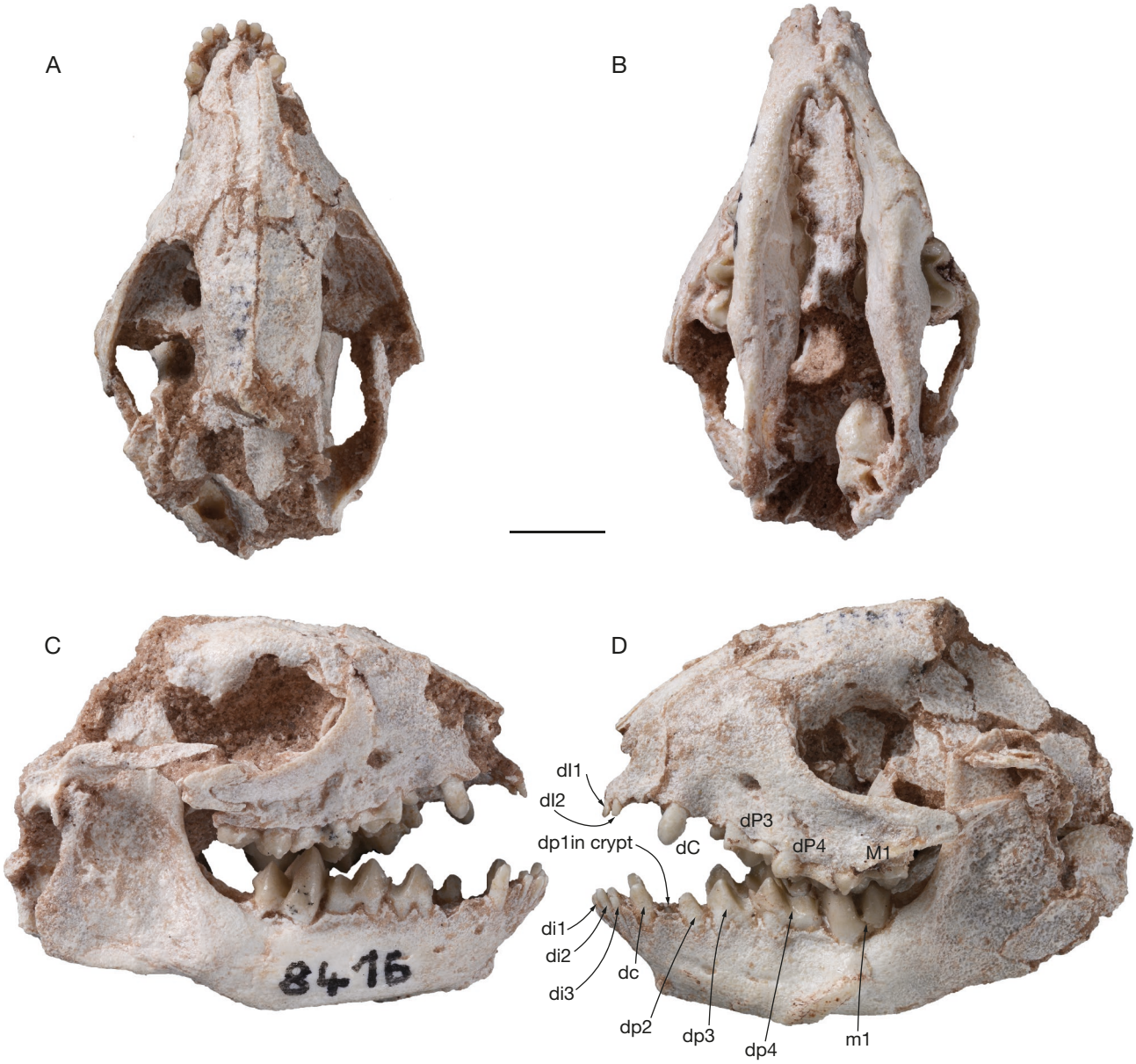

FIG. 13. — Partial skull and mandibles (MHNC 8416) of juvenile *Alcidedorbignya inopinata* (stage 3): **A**, dorsal view of skull; **B**, ventral view of skull and associated mandibles; **C**, right lateral view of the skull and mandible; **D**, left lateral views of the skull and mandible. Scale bar: 5 mm.

STAGE 4

Dental ontogenetic criteria for this stage are 1) Wear facet on M1 and m1; 2) M2 in crypt but starting to erupt (protocone probably piercing the gums); 3) proto-, para-, and metacone and conules of M2 fully mineralised but mineralisation of stylar shelf not completed; 4) trigonid of m2 erupting but talonid still in crypt; 5) germ of P4 in crypt, totally mineralised; 6) trigonid of p4 partially mineralised (protoconid and metaconid); 7) paracone of P3 in crypt in some specimens but absent (not formed yet) in others (i.e., this criterion is diagnostic when the cusp is present); 8) P2 (single cusped) in crypt in some specimens but absent (not formed yet) in others (i.e., this criterion is diagnostic when the cusp is present) (Figs 24-34).

Eleven specimens are referred to this stage: MHNC 13857, right maxilla with C (well-developed but with apex slightly above the alveolar border), dC, dP1 erupting, dP2-4, paracone of P3 in crypt, complete P4 in crypt, M1, M2 erupting with mesial, lingual and labial part of tooth still covered by the floor of the crypt (Figs 24-27); MHNC 13861, right maxilla fragment with C erupting (apex slightly below alveolar border), alveoli of dP1 and dP2, dP3-4, anterior edge of medial and mesiolateral alveoli of M1 (Figs 24; 28); MHNC 8286, left partial mandible with dp4, m1, m2 with trigonid partly erupted and talonid still in the alveolus (Figs 29-31); MHNC 8417, fragment of right mandible with dp3-4, m1 fully erupted (Figs 32; 33) ; MHNC 13964, partial left mandible with talonid of dp4 and m1 and anterior region of crypt of

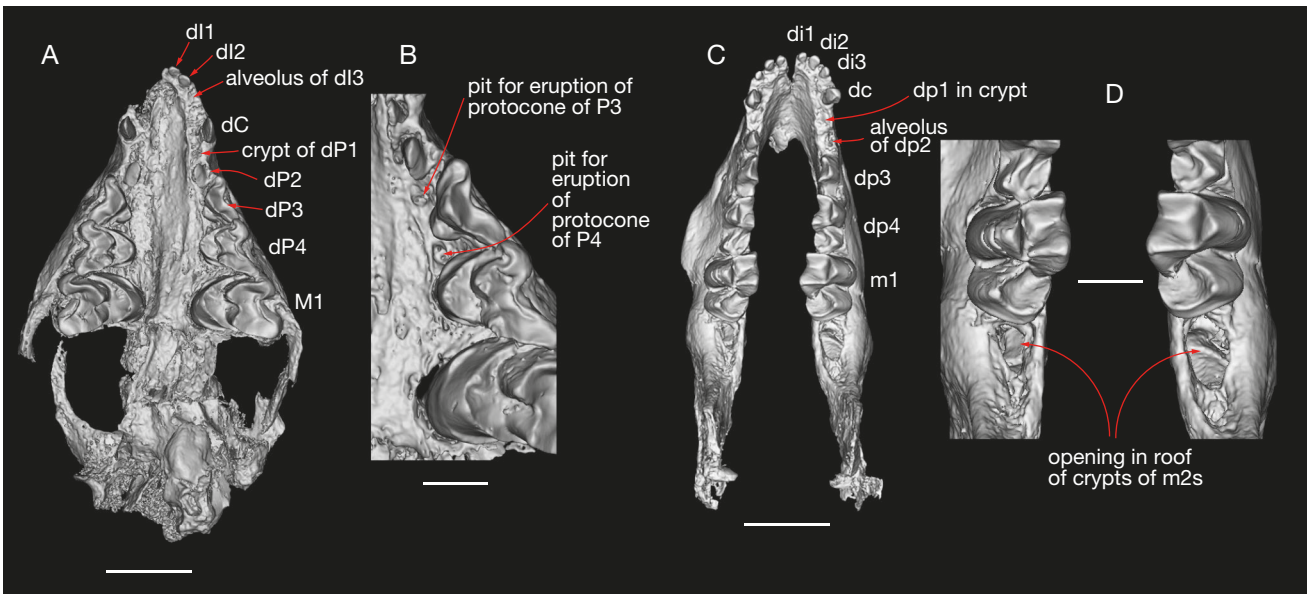

Fig. 14. — Digital rendering of the skull and mandibles (MHNC 8416) of juvenile *Alcidedorbignya inopinata* (stage 3): **A**, ventral view of the skull; **B**, enlargement of part of the left palate; **C**, dorsal view of the mandible; **D**, enlargement of the posterior region of the mandible, showing the opening in the roof of crypts of M2. Scale bars: A, C, 5 mm; B, D, 2 mm.

m2; MHNC 13960, partial left maxillary with roots of dP4, M1 almost fully erupted, and anterior part of crypt of M2 located above posterior edge of M1, indicating an erupting tooth; YPFB Pal 6369, partial right maxilla with dP1 erupting (more than half of the crown), dP2-4; YPFB Pal 6373, right maxillary with dP1, dP2-4; YPFB pal 6381, left mandible with dp1, dp2-3; YPFB Pal 6378 (possibly stage 4) fragment of a right maxilla with dP3-4; YPFB Pal 6448, maxillary fragment with dP4 and P4 in crypt. These specimens correspond to a to a minimum of five different individuals based on the presence of five specimens with a right dP4.

No specimen preserving the incisors is known for this stage. The upper canine is starting to (or about to) erupt since its tip has reached the level of the alveolar border or is slightly above (i.e., most of the tooth is still within the alveolus). The alveolus of the permanent upper canine is mesiolingual to that of the deciduous canine. The deciduous canine has been shed (or lost post mortem) on MHNC 13861, but its alveolus is still visible on the distolabial edge of the alveolus of the permanent canine (Fig. 24B, C). The deciduous canine is present on MHNC 13857, in which the eruption of the permanent canine is slightly less advanced than in MHNC 13861. The dP1 is about three-quarters erupted in MHNC 13857; it is not preserved in MHNC 13861 (Fig. 24). The dP3 and dP4 are still functional and, as observed on stages 2 and 3, small pits are observed in the maxilla, at their mesiolingual edges for eruption of the protocone of P3 and P4 respectively (Fig. 24). The development of P2, P3, and P4 varies on the two relatively complete maxillae available for this study. On the CT slices of MHNC 13857 (Figs 25; 26), the germ of P4 is clearly formed and almost complete in the crypt, whereas P3 has only the paracone starting to mineralize in crypt (we interpret this cusp as the paracone because it is labio-lingually more flattened than the protocone as compared to the condition on P4 of the same specimen) (Fig. 27). The dP2 of MHNC 13857 is clearly functional but there is no indication that the crypt of P2 has even started to develop in this individual. On MHNC 13861, the germ of P4 is also completely mineralised in crypt, but the crypt of P3 is empty. In contrast, P2 is well developed in crypt and dP2 has, either been shed or has been lost post mortem; P2 is visible externally peering into the alveolus of dP2 on its distolingual edge (Fig. 24C). The degree of eruption of P2 is almost comparable to that observed on YPFB Pal 6363, a specimen that has been referred to stage 5 below. Therefore, if P4 is probably the first upper premolar to erupt, the relative timing of eruption of P3 and P2 may have been variable.

The M1 of MHNC 13857 is fully erupted and functional. It shows discrete but clear wear facets on the conules, on the preparaconular crista and on the preparacrista. On this specimen, M2 (the only one available for this stage) is just starting to erupt. It is still in an "open crypt" (transitional to alveolus) and is positioned well above M1. The paracone and paraconule are covered by the anterior roof of the crypt. The protocone is slightly emerging below the lingual edge of the cavity, but is likely to have still been covered by gums during life. That tooth is a germ and has no roots. In MHNC 13960, the M1 is preserved and bears a distinct wear facet on the mesial edge of the paraconule and on the preparaconular crista (Fig. 33A, B). On this specimen, the crown of dP4 has been lost post-mortem but the roots are still present in the maxilla (i.e., the tooth has not been shed). Above the root is a large crypt for P4 open anteriorly because of the breakage of the specimen. Therefore, the P4 was unerupted and still in crypt but the germ is likely to have been complete because of the large size of the crypt.

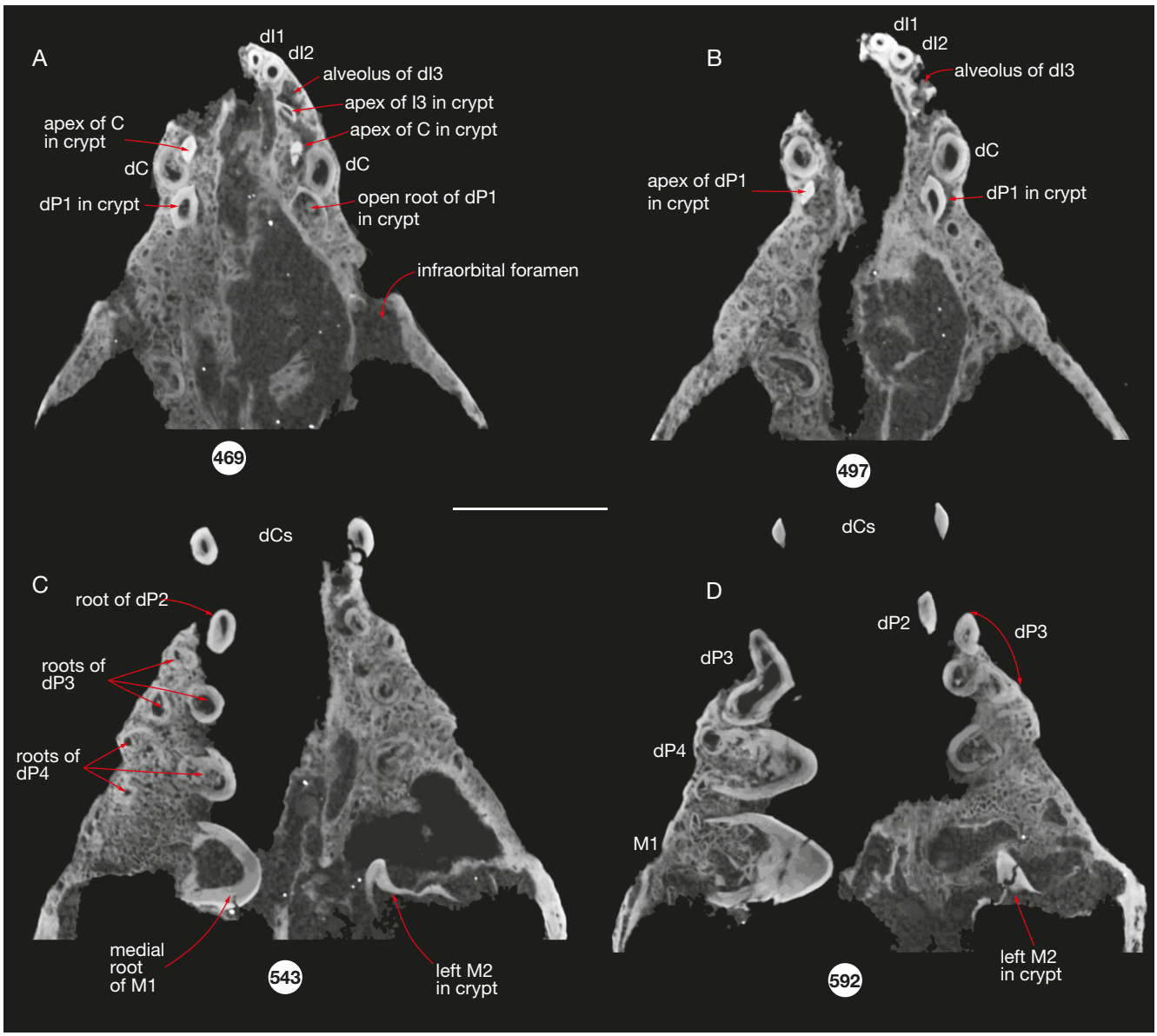

FIG. 15. — Slices of the coronal CT-scan of the anterior part of the skull (MHNC 8416) of juvenile *Alcidedorbignya inopinata* (stage 3): **A**-**D**, slices 469, 497, 543, 592 (slice 469 is the most dorsal and slice 592 is the most ventral). The number for each illustrated slice refers to the position within the sequence of 1165 images (resolution binned images voxel size 0.01900180). Scale bar: 5 mm.

In MHNC 8286, the anterior part of the mandible is missing. The specimen bears dp4, m1 and m2 erupting (Figs 29-31). The partially mineralised trigonid of p4 is observed below dp4 at the broken anterior end of the specimen (Fig. 30B-D). The protoconid has a characteristic triangular section and the metaconid is attached distolingually to it. At the mesiolingual angle of the protoconid, a small element of enamel could represent the paraconid, just starting to mineralize. No talonid cusp of p4 is observed. The m1 is functional and bears a weak wear facet on the posterior edge of the protocristid and on the anterior edge of the protoconid. The m2 is starting to erupt and the three cusps of the trigonid are dorsal to the edge of the alveolus, but well below those of m1 and slightly below the cusps of the talonid of m1. The talonid of m2 is still embedded in the alveolus with the tip of the hypoconid at the level of (but not above) the alveolar edge. Posterior to the crypt of m2 is the crypt of m3 in which two small cusps can be observed. The larger cusp resembles the protoconid in its triangular morphology, but, if this interpretation is correct, it has been displaced medially and rotated in the crypt post-mortem. Because this is a frequent condition in our juvenile sample, we refer this cusp to the protoconid. Furthermore, a tiny cusp is present posteroventrally to the protoconid and is referred here to the metaconid. This cusp is upside down and, as for the protoconid, has been displaced before filling of the crypt with sediment (Fig. 31).

On MHNC 8417 no cusp of p3 is observed below dp3. Below dp4 a partially mineralised trigonid of p4 is present but has been rotated counter clockwise in anterior view of the mandible during fossilization. This trigonid includes two

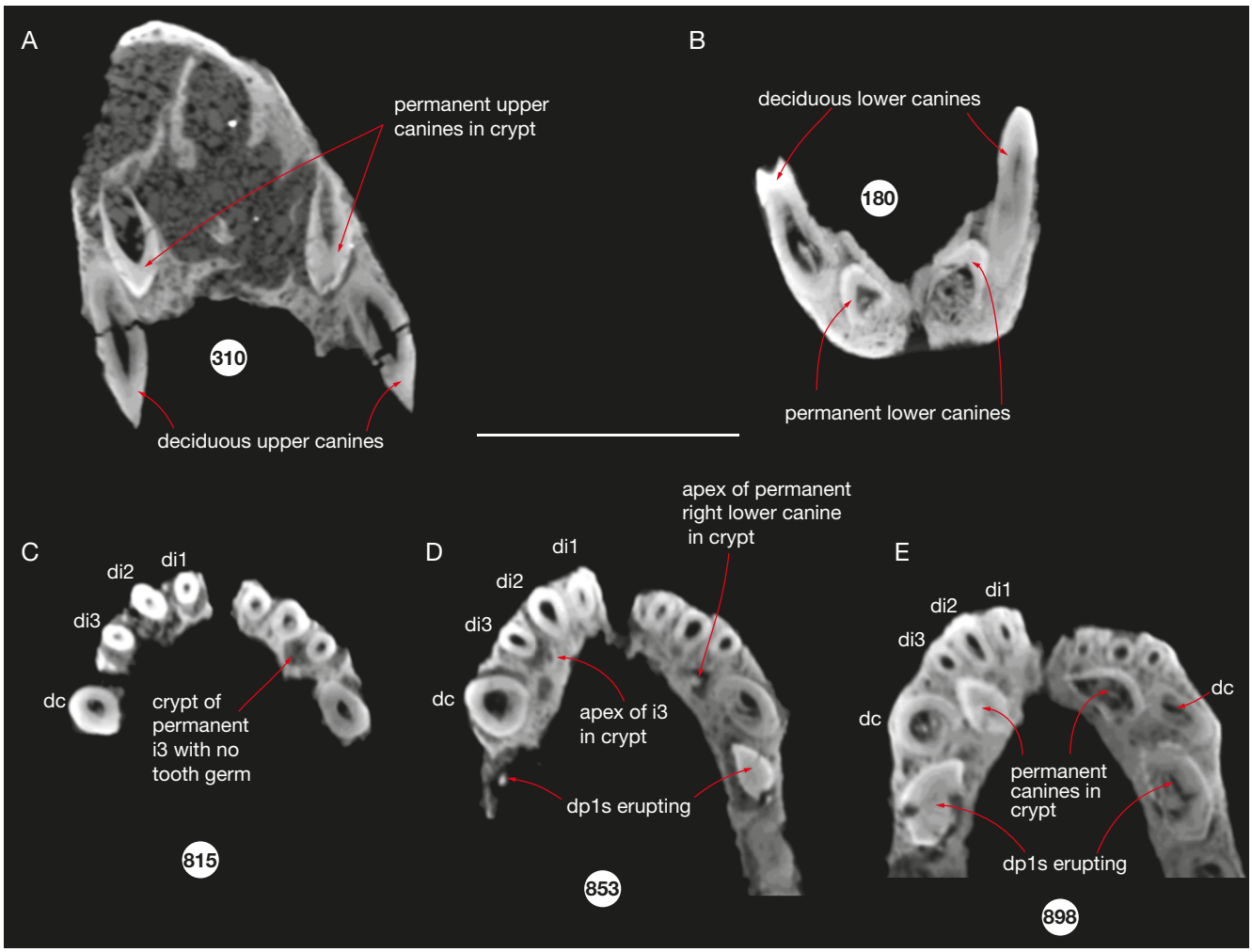

Fig. 16. — Slices of the CT-scan of the anterior part of the skull and mandible (MHNC 8416) of juvenile *Alcidedorbignya inopinata* (stage 3): **A**, slice 310 of frontal CT-scan of rostrum; **B**, slice 180 of frontal CT-scan of symphyseal region of mandible; **C**-**E**, slices of coronal views anterior region of mandible (slice 815 is dorsal and slice 898 is ventral). The number for each illustrated slice refers to the position within the sequence of 1644 images for A and B, and 1165 images for C-E (resolution binned images voxel size = 0.02781842 mm). Scale bar: 5 mm.

cusps, the larger with a distinct triangular section is referred to the protoconid. If one rotates the trigonid to its original position, the other cusp places itself disto-lingually to the protoconid and is therefore referred to the metaconid. This cusp is much smaller in volume than the protoconid and has a drop-like section, which corresponds to that of the metaconid (Fig. 32; 33). Furthermore, at the anterior part of the crypt is a tiny cusp, which we regard as the paraconid, appressed against the posterior edge of the anterior root of dp4 and well separated from the proto-metaconid. This condition indicates that the paraconid is the last cusp of the trigonid to mineralize.

Weak wear facets are observed on the posterior edge of the protocristid of the m1 of MHNC 8417 (Fig. 34C, D) and 13964. On MHNC 8417 a small circular facet is also present at the apex of the hypoconid.

This stage corresponds to an early phase of IDAS 2, which starts with the first wear facets on the first molars and often corresponds, according to Anders *et al.* (2011), to recently weaned juvenile individuals (Fig. 1).

Stage 5

Dental ontogenetic criteria for this stage are 1) M2/m2 fully erupted; P2/p2 well mineralised, still in crypt, but about to erupt or partly erupted; 3) P4 starting to erupt or almost erupted; 4) p4 still in crypt but fully formed; 5) P3 starting to erupt; 6) p3 in crypt and incompletely formed (only one cusp observable); 7) permanent upper canine erupting; 8) permanent lower canine still in crypt. (Figs 35-39).

Eight specimens are referred to this stage. MHNC 13860 right maxilla with C partially erupted (apex below the apex of dP1), dP1 fully erupted, alveolus of dP2, P3 just starting to erupt, P4 almost fully erupted, M1, M2, and anterior part of crypt of M3 above posterior half of M2 (Fig. 35); YPFB Pal 6363, left partial maxilla with C erupting (apex above the apex of dP1), P2 in alveolus (apex above alveolar edge), apex of protocone of P3 visible in the alveolus but not emerging yet, dP4, apex of protocone of P4 erupted (visible above protocone of dP4), M1, alveoli of M2, and anterior part of crypt of M3 above posterior half of M2 (Fig. 36); MHNC 13858, left mandible with c erupting (but with apex below alveolar

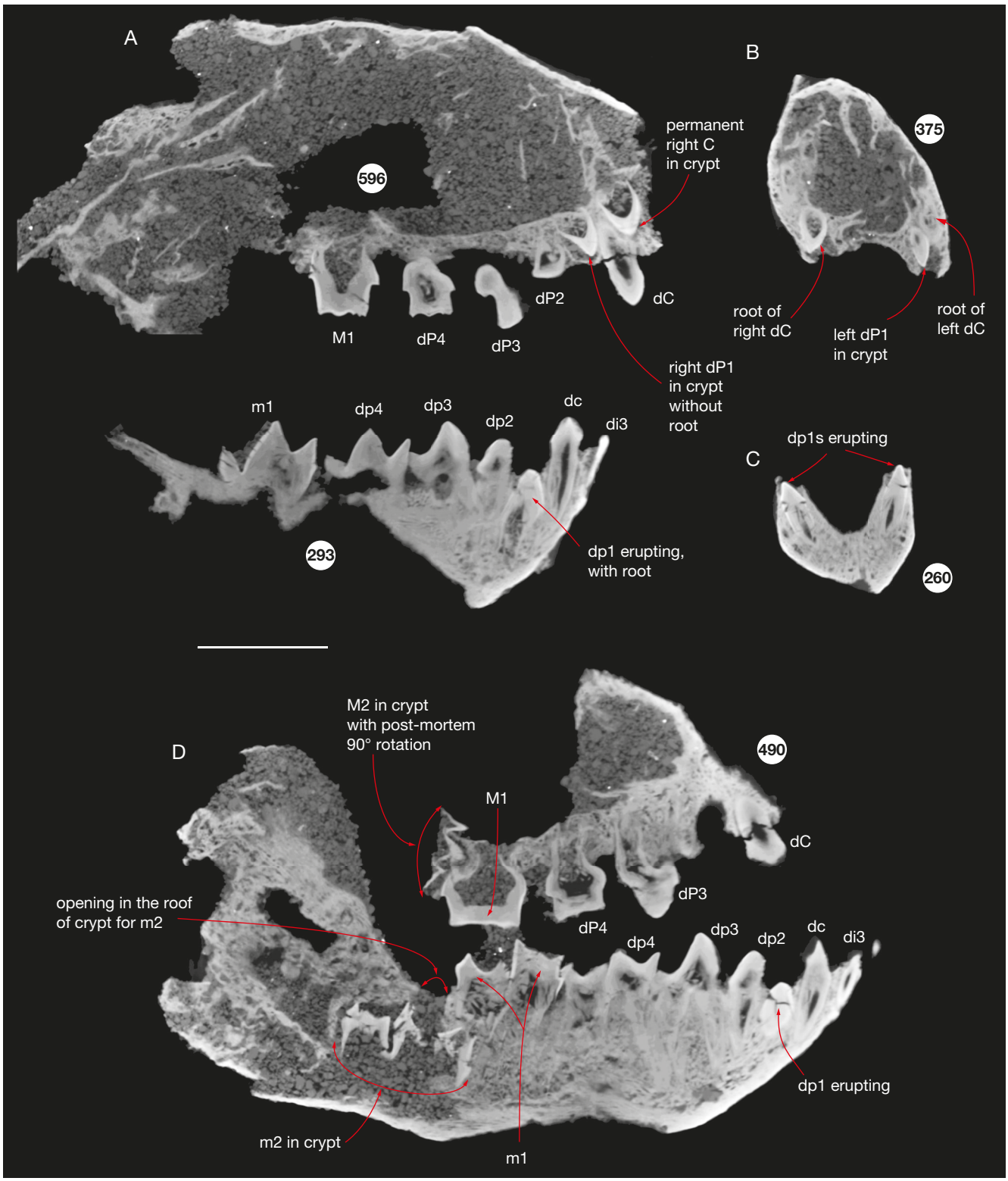

FIG. 17. — Slices of the CT-scans (lateral and frontal) of the skull (MHNC 8416) of juvenile *Alcidedorbignya inopinata* (stage 3): **A**, slices of the original lateral CT-scan (slice 596 is in the right maxilla of the skull and slice 293 is in the left mandible); **B**, slice 375 (in the skull) of the frontal CT-scan (right side of the figure is left side of the skull); **C**, slice 260 (in the mandible) of the frontal CT-scan (right side of the figure is left side of the skull); **D**, slice 490 of the resliced lateral CT-scan in the left side of the skull. The number for each illustrated slice refers to the position within the sequence of 974 images for A and D and 1644 images for B and C (resolution binned images voxel size = 0.02781842 mm). Scale bar: 5 mm.

edge) dc, dp1 fully erupted, apex of p2 just emerging at the level of the alveolar edge, dp3-4, protoconid of p3 in crypt, p4 in crypt, m1, alveoli of m2 (which was fully erupted), m3 in crypt (apices of trigonid cusps well below the roof) (Figs 37; 38); MHNC 13963, left mandible fragment with dp3 and p3 in crypt; YPFB Pal 6351, left mandible with i3 erupting,

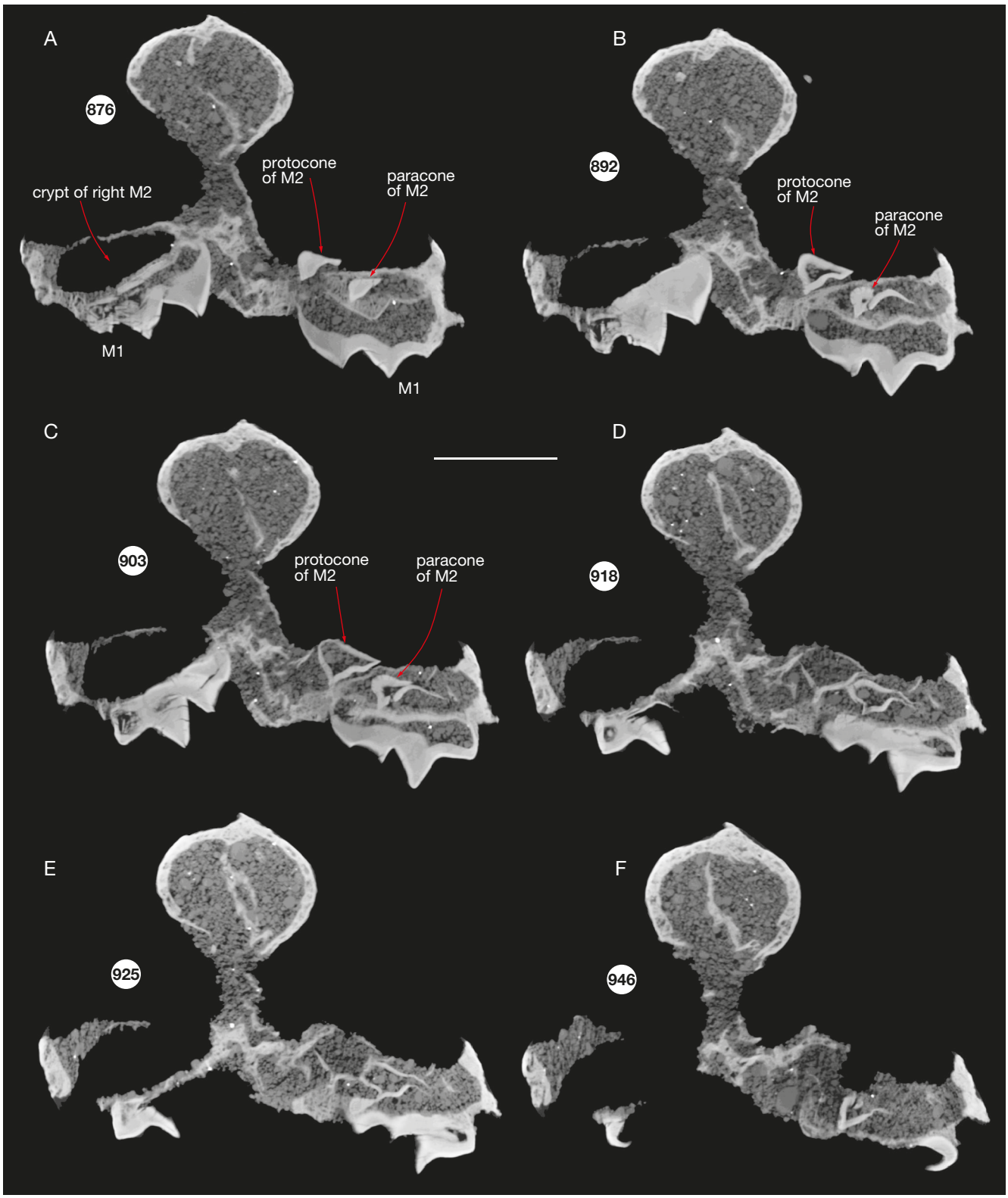

FIG. 18. — Slices of the frontal CT-scans of the skull (MHNC 8416) of juvenile *Alcidedorbignya inopinata* (stage 3): **A**-**F** slices 876, 892, 903, 918, 925, 946 (**A**, slice 876, is anterior and **F**, slice 946 is posterior; the left side of the skull is the right side on the figure). The number for each illustrated slice refers to the position within the sequence of 1644 images (resolution binned images voxel size = 0.02781842 mm). Scale bar: 5 mm.

c still in the alveolus, dp1 almost fully erupted, dc, dp2-4, m1, trigonid of m2 erupting (but at the level of the talonid of m1), (Fig. 39); YPFB Pal 6384, part of left mandible with alveoli of i1-3, alveolus of dc, tip of c visible in alveolus (below alveolar edge) but not erupting yet, dp1, and anterior root of dp3; YPFB Pal 6386, part of right mandible with roots of

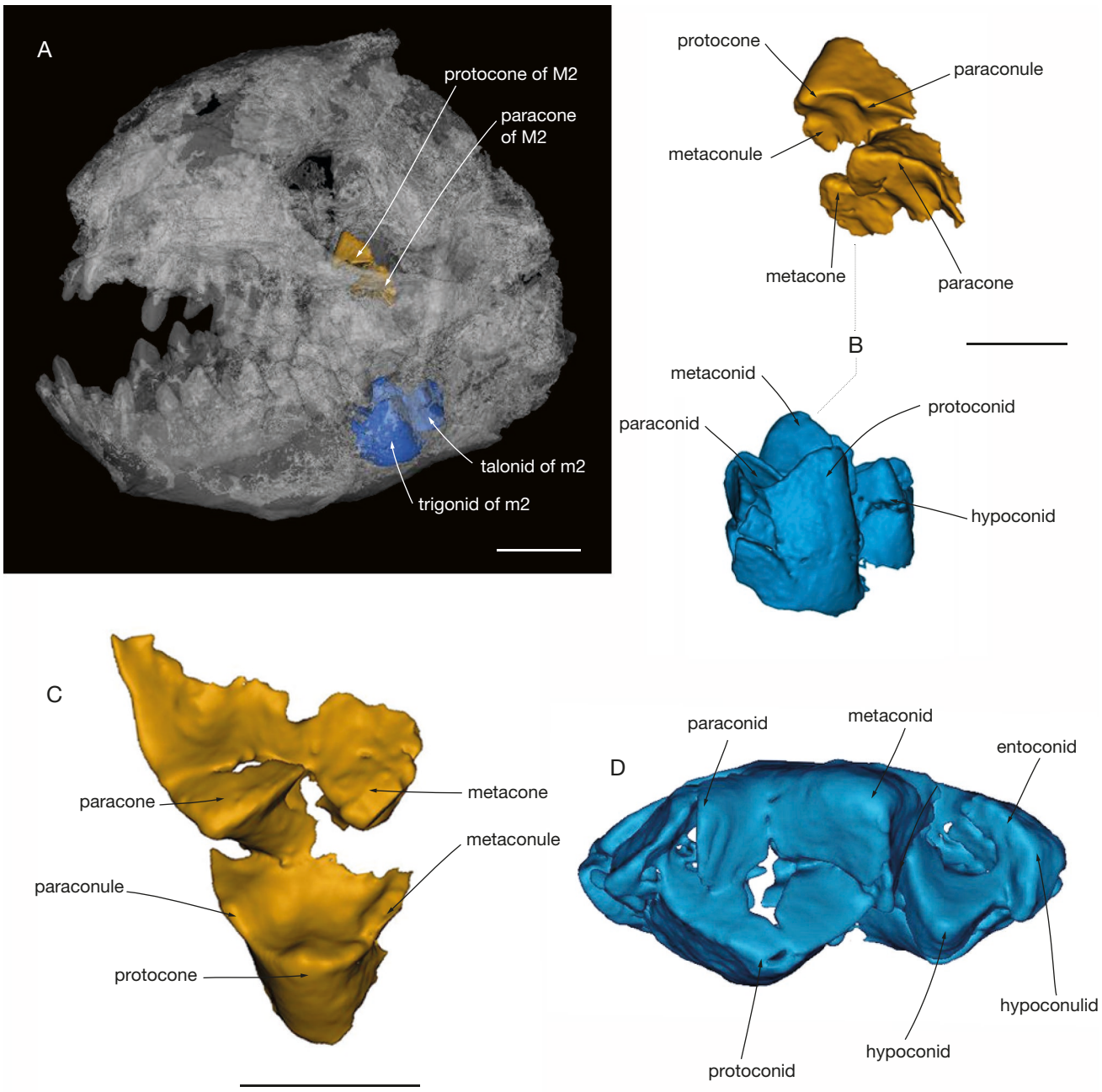

FIG. 19. — **A**, Transparent anterolateral view of the skull and mandible (MHNC 8416) of juvenile *Alcidedorbignya inopinata* (stage 3) showing left M2 and m2 in their respective crypt; **B**, left M2 and m2 in their relative position as preserved in the specimen (i.e., M2 has suffered two 90° rotations, one in an anteroposterior axis and the other in a transverse axis); **C**, left M2 in occlusal view; **D**, left m2 in occlusal view. Scale bars: A, 5 mm; B-D, 2 mm.

dp1, p2, p3 erupting, alveoli of P4; YPFB Pal 6376, partial right mandible with root of dp1, p2 erupting dp3, and root of dp4. It is noteworthy that YPFB Pal 6351 and 6363 were not available for CT scanning during this study; observations were made through casts and photographs as published by Muizon & Marshall (1992). These specimens correspond to a minimum of three different individuals based on the presence of three specimens with a right dp1 or p2.

We have included in this stage all specimens in which M2/m2 are at or close to full eruption but which have not reached the full adult dentition with all permanent teeth (i.e., including M3/m3) fully erupted. As compared to the condition in stage 4, this stage is mainly characterised by the degree of eruption of M2 and m2. In three specimens M2 or m2 is either fully erupted (MHNC 13860) or its fully formed alveolus indicates that the tooth was so (MHNC 13858, YPFB Pal 6363). In one mandible specimen (YPFB Pal 6351), m2 is incomplete and only the paraconid and protoconid are preserved. These cusps are not considerably overhanging the talonid of m1 and the paraconid is only very slightly dorsal to the entoconid of m1, whereas it greatly overhangs it in full adults. However, the eruption of m2 in this specimen is conspicuously more advanced than in stage 4 (MHNC 8286), in which the trigonid of m2 is ventral to the talonid of m1.

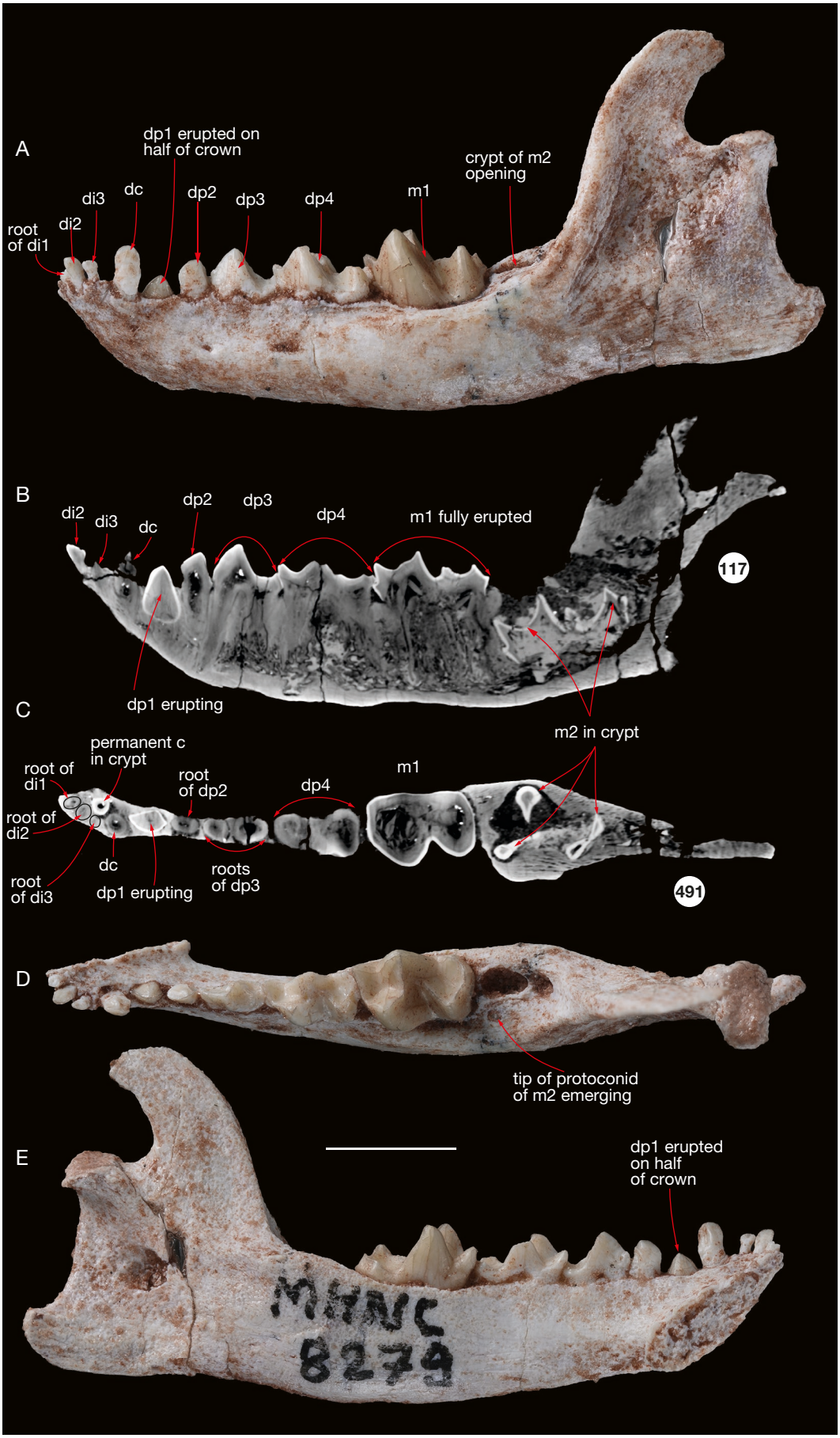

FIG. 20. — Left mandible (MHNC 8279) of juvenile *Alcidedorbignya inopinata* (stage 3+): **A**, lateral view; **B**, slice 117 of the Lateral CT-scan, **C**, slice 491 of the coronal CT-scan; **D**, occlusal view; **E**, medial view. The number for each illustrated slice refers to the position within the sequence of 262 images for B and 742 images for C (resolution binned images voxel size = 0.02781842 mm). Scale bar: 5 mm.

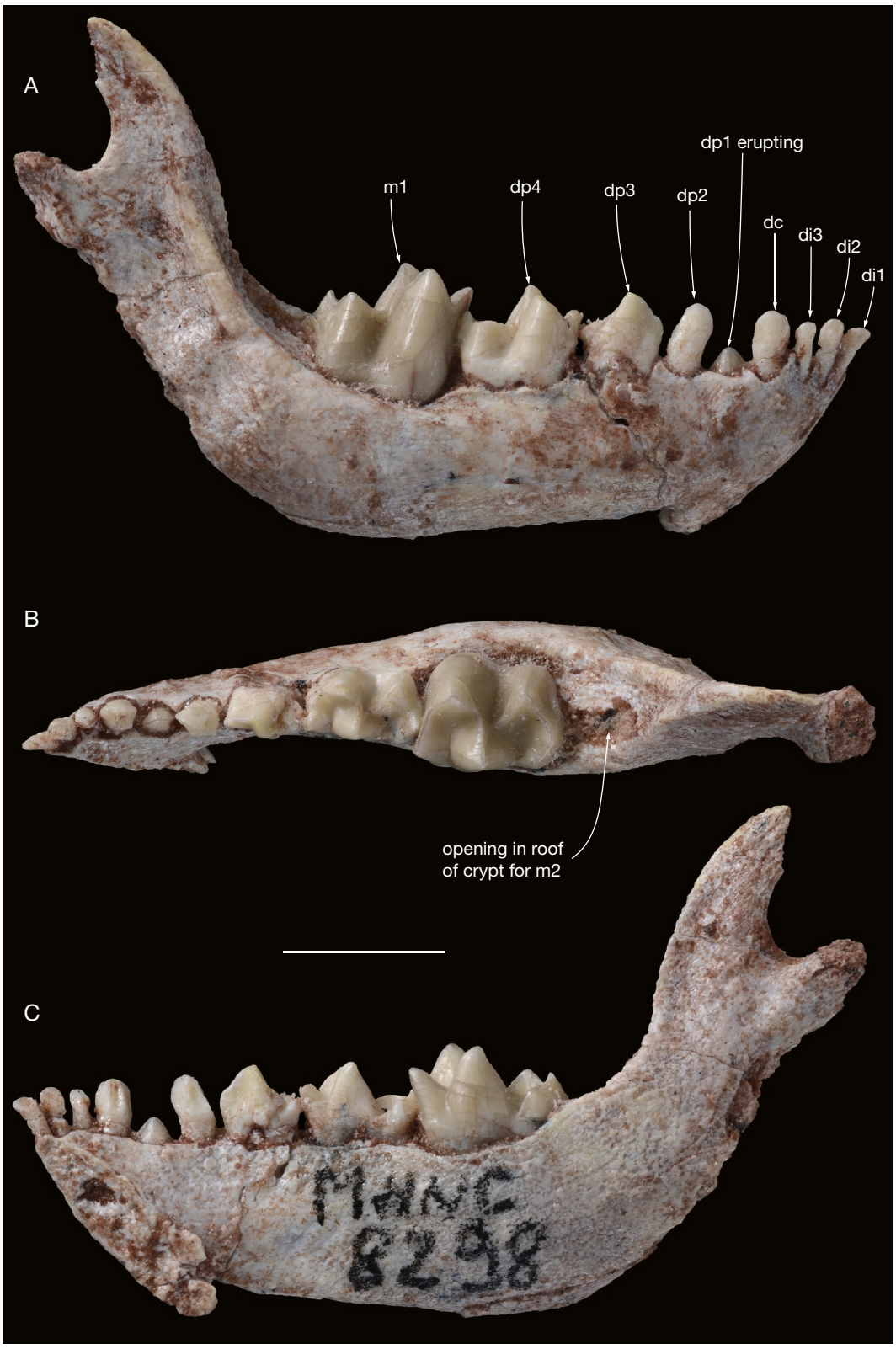

Fig. 21. — Right mandible (MHNC 8298) of juvenile *Alcidedorbignya inopinata* (stage 3+): **A**, lateral view; **B**, occlusal view; **C**, medial view. Scale bar: 5 mm.

In stage 5, the M3 and m3 are still in their crypts and not even close to eruption. This condition is observed in MHNC 13858, a mandible that presents a vertical break of the dentary through the crypt of m3 (Figs 37; 38). On this specimen, the m3 exhibits a section of the protoconid and metaconid; it is poorly mineralised and is deeply embedded

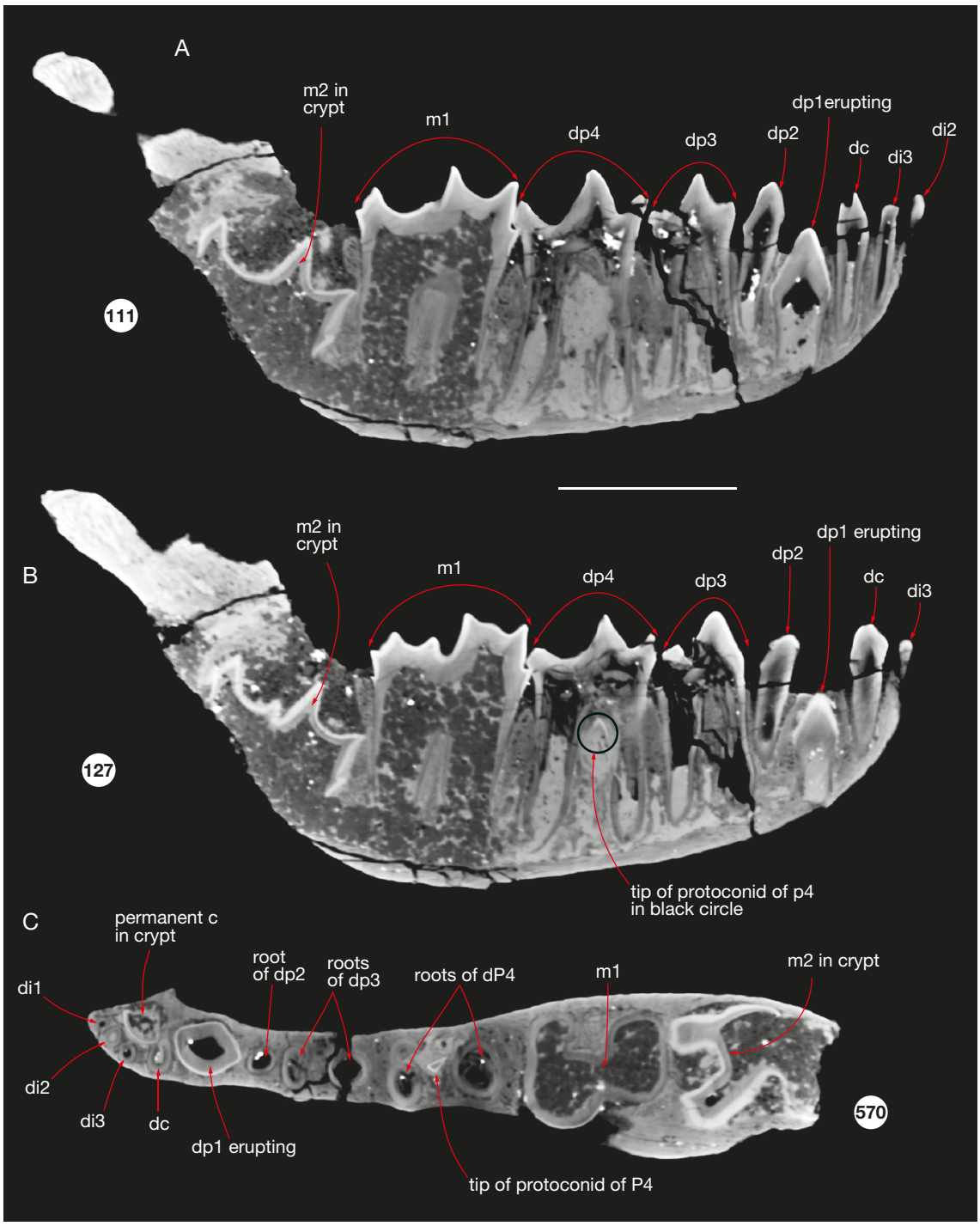

FIG. 22. — Slices of the CT-scans (lateral and coronal) of the mandible (MHNC 8298) of juvenile *Alcidedorbignya inopinata* (stage 3+): **A**, **B**, slices 111 and 127 of the lateral CT-scan; (slice 127 is lateral to slice 111); **C**, slice 570 of the coronal CT scan. The number for each illustrated slice refers to the position within the sequence of 260 images for A and B and 804 images for C (resolution binned images voxel size = 0.02781842 mm). Scale bar: 5 mm.

in the crypt. Nevertheless, in dorsal view, on the lingual edge of the dentary, a distinct opening is observed in the anterolingual region of the roof of the crypt, thus indicating that m3 was close to eruption. Furthermore, on the maxilla MHNC 13860, the anterior part of the crypt of M3 is located above the paracone, thus indicating that the last molar is not close to eruption (Fig. 35). Therefore, stage 5 is characterized by a fully erupted M2/m2 and an unerupted M3/m3 . However, in our sample two specimens are clearly more advanced than the others. In the two maxillae (MHNC 13860 and YPFB Pal 6363) the canine and P3-4 have started to erupt (Figs 35; 36). In both specimens, dC has been shed and its alveolus resorbed, in contrast to the condition observed in MHNC 13861 (stage 4 [Figs 24; 28]), in which the permanent canine

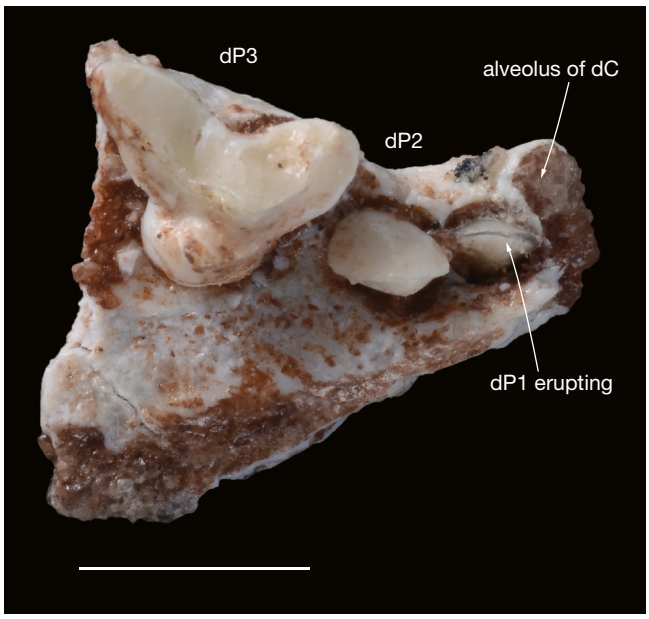

FIG. 23. — Occlusal view of a right maxilla (MHNC 13954) of juvenile *Alcidedorbignya inopinata* (stage 3+). Scale bar: 5 mm.

has started to erupt but which still retains the alveolus of dC. The process is more advanced in MHNC 13860 (Fig. 35), in which the apex of the canine is ventral to that of dP1, P4 is erupted and P3 erupting (dP3-4 have been shed), whereas in YPFB Pal 6363 (Fig. 36), the apex of the canine is dorsal to that of dP1, P4 is erupting (above dP4) and P3 is still in its alveolus but dP3 has been shed. In YPFB Pal 6363, dP2 has been shed and P2 is clearly visible in its alveolus although its apex remains dorsal to the alveolar edge (Fig. 36). In MHNC 13860, an alveolus is observed posterior to dP1 and anterolingual to erupting P3; because no tooth germ is observed above this alveolus (as seen on the CT scan; Fig. 34D) it is likely to be that of a fully erupted P2, a tooth that has been lost post-mortem (Fig. 35). In the two mandibles (MHNC 13858 and YPFB 6151) the canine has not started to erupt but is close to its alveolar border and dc is still present (Figs 37-39). The timing of eruption of M3 relative to premolars is clear for P4 only, since in MHNC 13860 P4 is fully erupted whereas the position of the crypt of M3 indicates that the last molar was clearly not close to eruption (Fig. 36). P3 of MHNC 13860 is distinctly erupting and apices of protocone and paracone were probably piercing the gums. Therefore, it is reasonable to hypothesize that P3 was erupting slightly before M3.

On the mandible MHNC 13858, below dp4, a fully mineralised germ of p4 is present and a single cusp is observed below dp3. This cusp has been rotated (post-mortem) upside down and its shape (oblique crest) is identical to the protoconid of p4, a cusp to which it is referred (Fig. 38D). On this specimen, on the lingual edge of dp3-4 between the roots, the dentary bears a small elongated foramen through which will start the eruption of the permanent premolars (probably with the metaconid), resembling the condition observed on the maxilla at the mesiolingual edge of dP3-4 on MHNC 8423, 8416, 13857, and 13861. This condition was also apparently present, but less pronounced, in other mandibles of stages 2-5. This stage also corresponds to IDAS 2, since the permanent dentition is not fully erupted (Anders *et al.* 2011) (Fig. 1).

STAGE 6

The ontogenetic criteria for this stage is 1) P3-M2 fully erupted and 2) M3 erupting.

Only one specimen represents this stage: MHNC 13853 left maxilla with roots and base of protocone of P3, P4-M1, M2 missing the metacone and anterolingual part of crypt of M3. Although the M3 is not preserved the anterior border of the crypt, which is almost vertical and located above the posterior edge of M2, indicates that this tooth had probably started to erupt. It is therefore more advanced than the maxillary MHNC 13860 of stage 5, in which the anterior part of the crypt is more anterior, above the postparacrista of M2. Furthermore, on the stage 6, P3 is fully erupted whereas it is still erupting in stage 5 (Fig. 40). On MHNC 13853, although P4 is fully erupted, this tooth is in a pathological position since it is rotated 45° clockwise in occusal view. Its metastyle is located approximately dorsomesial to the paracone of M1. Therefore, this specimen of stage 6 confirms the hypothesis made from stage 5 (e.g., MHNC 13860) that M3 was the last permanent upper cheek tooth to erupt. This stage corresponds to a late phase of IDAS 2 (Fig. 1).

STAGE 7

Stage 7 corresponds to the fully erupted adult dentition as illustrated by Muizon & Marshall (1992) and Muizon *et al.* (2015). In our sample collected at the quarry (the site where almost all the *Alcidedorbignya* specimens were collected) most of the adult specimens are either almost unworn or very slightly worn (Fig. 41). The adult specimens of stage 7 (i.e., excluding those of stage 8, see below) correspond to a minimum of 20 different individuals based on the presence of 20 maxillaries with a left M2. This stage corresponds to an early phase of IDAS 3 (Fig. 1).

STAGE 8

Six specimens feature a significant wear of the proto- para-, and metacone, which are abraded approximately on half of their height, which justifies the definition of this stage. On the maxillaries MHNC 8400 and 8401, the enamel of the floor of the trigon and stylar shelf basins is still preserved on all molars (Fig. 42). On the maxillary fragment figured by Muizon & Marshall (1992: fig. 6 [7]) (YPFB Pal 6364), M2 features a wear slightly more advanced than on the two aforementioned specimens. The M1 of this specimen is not preserved; however, it is unlikely that it was completely worn out. Three mandible fragments feature a similar wear. On MHNC 13975 the trigonid and talonid of m2 are deeply excavated by wear; on MHNC 13873, molars are not preserved but the significant wear of p4 indicates that it was probably more advanced on m1, whose eruption precedes that of p4; on MHNC 8413 m1 is not preserved but the conspicuous wear of the hypoconid of m2, suggest that m1

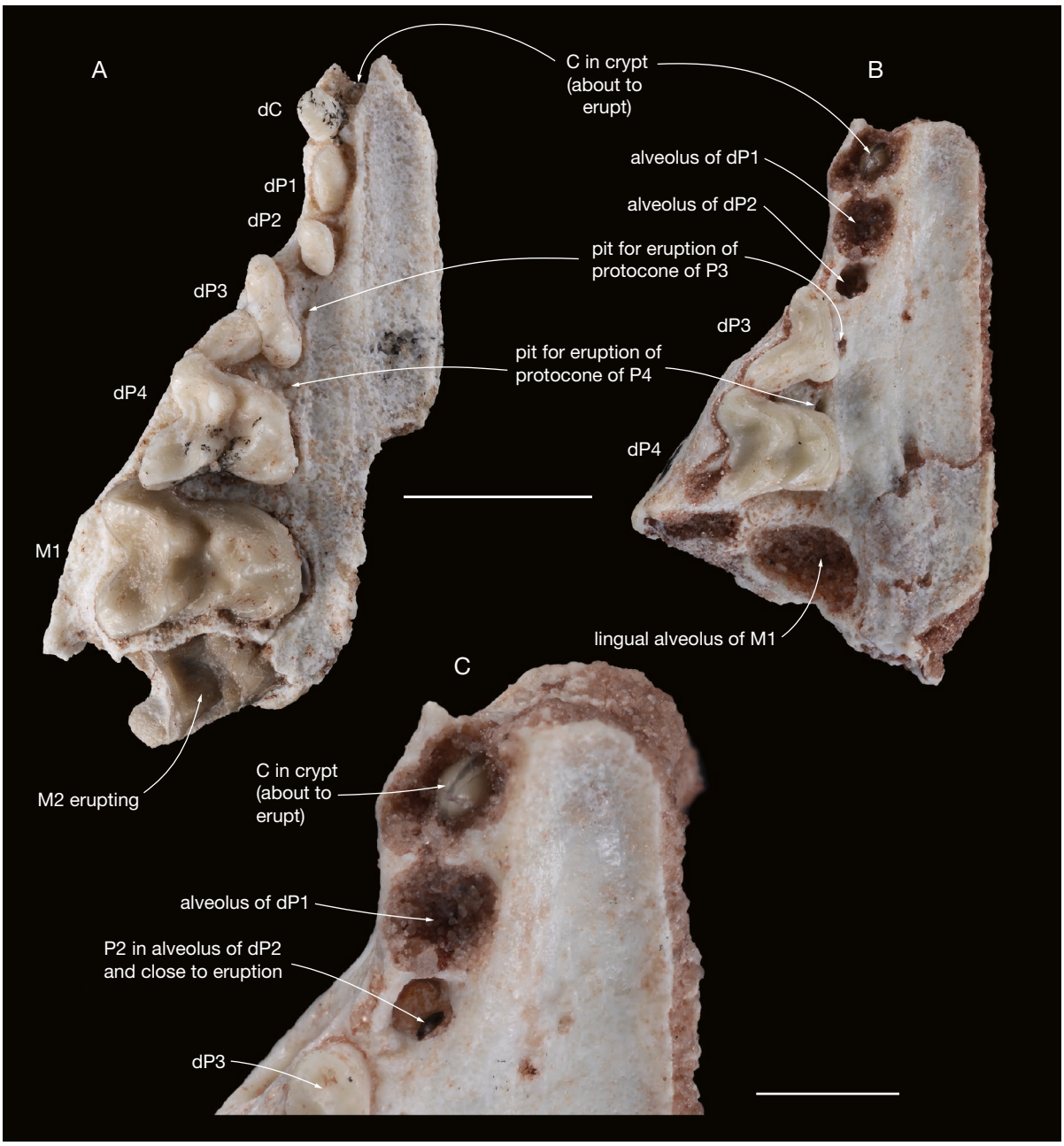

Fig. 24. — Maxillae of juvenile *Alcidedorbignya inopinata* (stage 4): **A**, MHNC 13857 right maxilla in occlusal view; **B**, MHNC 13861, right maxilla in occlusal view; **C**, anteromedial view showing the germ of P2 close to eruption. Scale bars: A, B, 5 mm; C, 2 mm.

was also strongly worn. Pronounced wear (although less than in MHNC 8400) is also observed on the partial skull and mandible (MHNC 13931) figured by Muizon *et al.* (2015: 591), which is therefore also included in stage 8.

This stage corresponds to a late phase of IDAS 3, within which there is a minimum of three individuals represented by maxillae. Our sample does not include specimens with worn out M1/m1 or M2/m2; thus, no later stage is documented. These specimens, although not from the same side (two right and one left) have significant differences in the tooth row length (C-M3): 33.17 mm in MHNC 13931, 29.05 mm in MHNC 8401, and 27.10 mm in MHNC 8400. Furthermore, the two specimens, in which the size difference is the smallest (8400 and 8401), show notable morphological differences in molar proportions and morphology.

Therefore, our jaw sample of adult specimens corresponds to a total minimum number of 23 adult individuals (stages 7 + 8). In comparison, the minimum number of juvenile individuals is 30 when adding the minimal number of individuals of stages 1 to 6.

Dental eruption sequence (Fig. 43)

The upper tooth eruption sequence (excluding dI1-3, I1-2, for which we have almost no data) for *Alcidedorbignya* is as follows: dC-dP2-4 (probably erupted at birth, order unknown), M1,

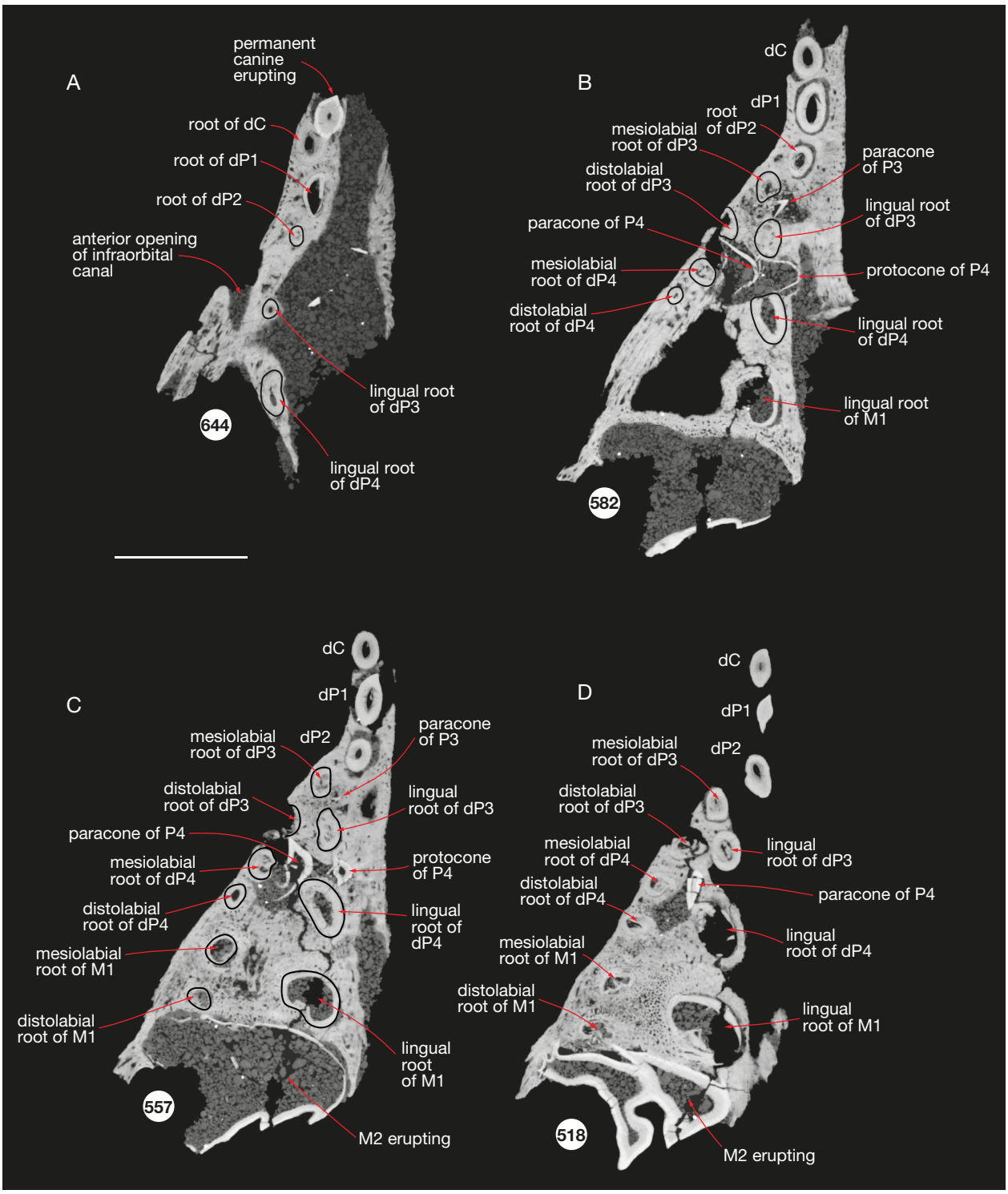

FIG. 25. — Slices of the coronal CT scan of the maxilla (MHNC 13857) of juvenile *Alcidedorbignya inopinata* (stage 4): **A-D**, slices 644, 582, 557, 518 (slice 644 is the most dorsal and slice 518 is the most ventral). The number for each illustrated slice refers to the position within the sequence of 1021 images (resolution binned images voxel size = 0.0186471 mm). Scale bar: 5 mm.

dP1, M2, I3, C, P4, P2-P3, M3. The sequence of eruption of P2 and P3 seems to be variable. As observed, eruption timing may be, either both teeth together, or P3 before P2, or P2 before P3. In MHNC 13857 (stage 4), P3 has started to mineralize in crypt but there is no indication of P2 in crypt (Figs 25; 26). This would be an indication that P3 could erupt before P2. In MHNC 13861 (stage 4) the germ of P2 is clearly developed in crypt, whereas the crypt of P3 is empty (Fig. 28), which would indicate that P2 erupts before P3. In YPFB Pal 6363, P2 and P3 appear to be at a similar degree of eruption, an indication

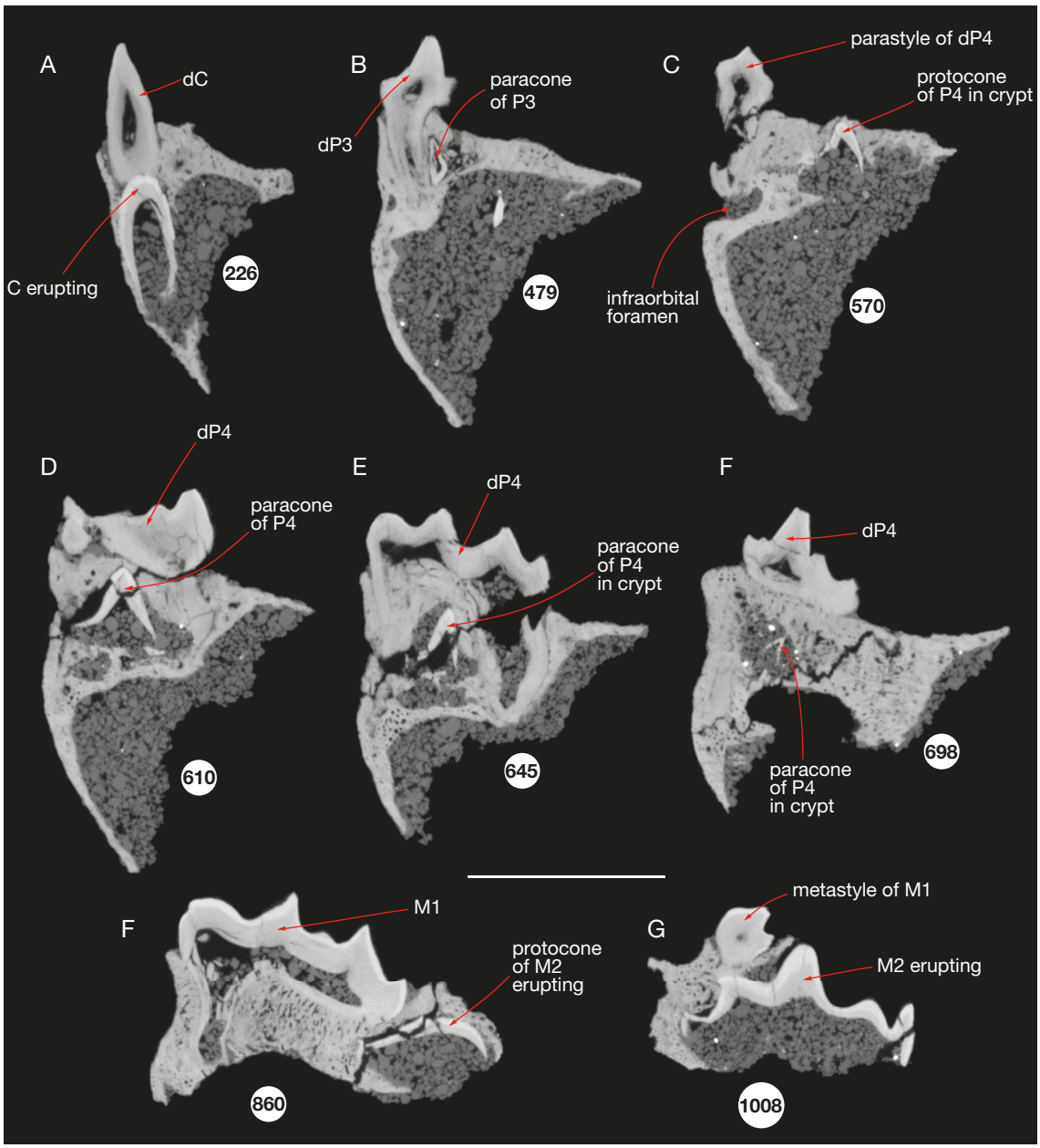

FIG. 26. — Slices of the frontal CT-scan of the maxilla (MHNC 13857) of juvenile *Alcidedorbignya inopinata* (stage 4): **A**-**H**, slices 226, 479, 570, 610, 645, 698, 860, 1008 (slice 226 is the most anterior and slice 1008 is the most posterior). The number for each illustrated slice refers to the position within the sequence of 1168 images (resolution binned images voxel size = 0.0186471 mm). Scale bar: 5 mm.

that both teeth probably erupt jointly (Fig. 36). Finally, in MHNC 13860, P2 is probably fully erupted (although lost post-mortem) and P3 just starting to erupt (Fig. 35). Another interpretation could be that P3 starts to mineralize before P2 but that P2 mineralises and erupts faster than P3, therefore being functional earlier. Be that as it may, our observations indicate that eruption of P2 and P3 of *Alcidedorbignya* are probably very close in time and that their order of eruption may vary.

The lower tooth eruption sequence (excluding i1-2 for which we have no data) for *Alcidedorbignya* is as follows: di1-3-dc-dp3-4 (probably erupted at birth, order unknown), dp2, m1, dp1, m2, i3, c, p2, p4, p3, m3. In the case of the lower teeth, our sample only includes one specimen that provides information on the relative sequence of eruption of p2-p4. On MHNC 13858, p2 is erupting (its apex is at the edge of the alveolar border), whereas the germ of p4 is well formed but still in crypt below dp4 and one single cusp (protoconid?) of p3 is visible in crypt below dp3 (Fig. 38). As for their upper counterparts, it is possible that the eruption of p2-4 happens in a very short period and thus with some variation in their sequence.

Whatever the relative eruption sequence of P2-P4/p2-p4, according to our sample, it is highly probable that M3 and m3 are the last permanent cheek teeth to erupt. This hypothesis is confirmed by the wear facets observed on several adult individuals, in which M3 is un- or barely-worn and the P4 and P3 bear distinct to large wear facets thus indicating an earlier

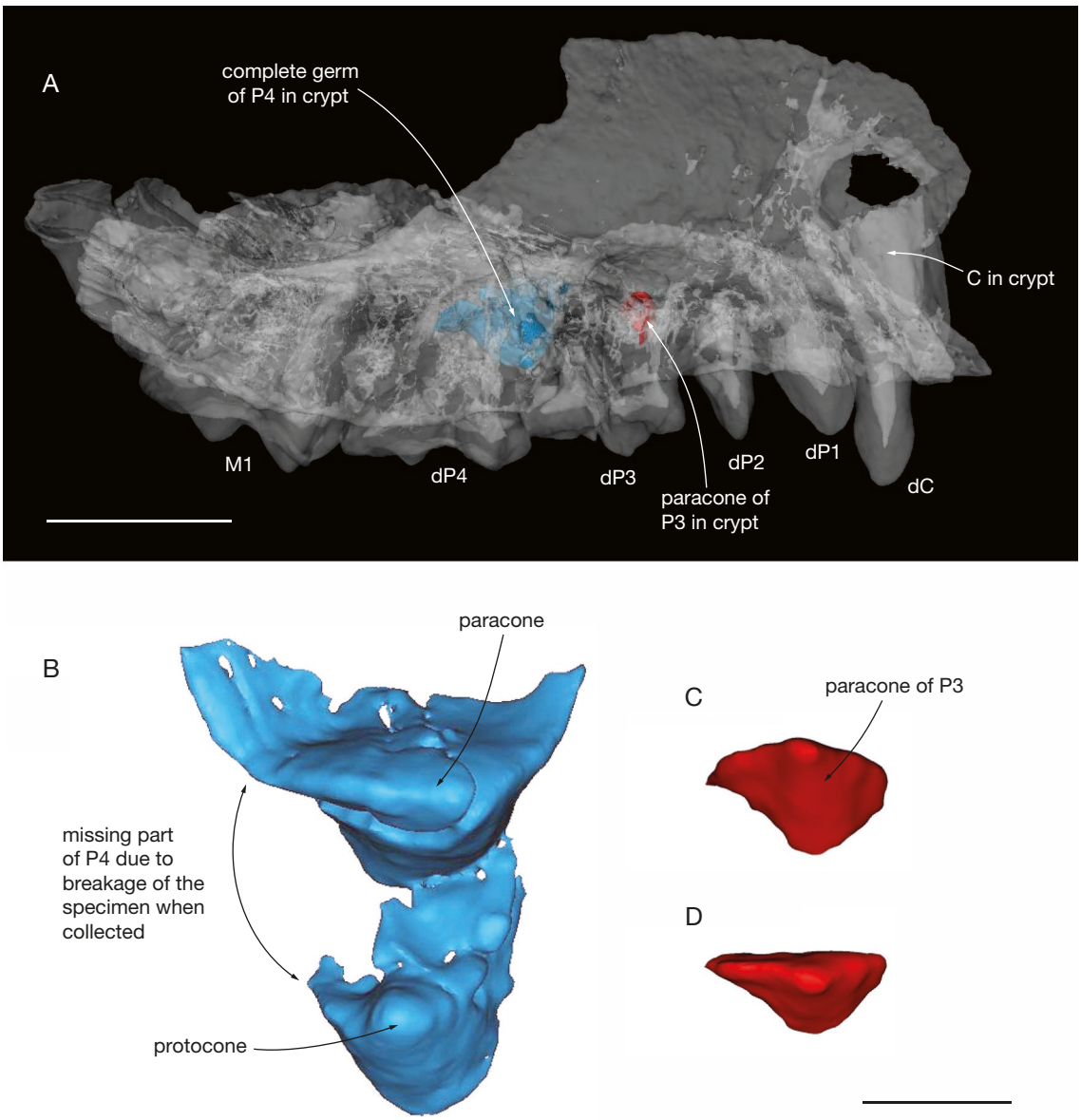

FIG. 27. — **A**, transparent anterolateral view of the maxilla (MHNC 13857) of juvenile *Alcidedorbignya inopinata* (stage 4) showing unerupted right P3 and P4 in their respective crypt; **B**, occlusal view of P4 (the missing part in posterior edge of the tooth is due to the breakage of the maxilla at that level, with loss of some fragments of P4); **C**, paracone of P3 in occlusolingual view; **D**, paracone of P3 in occlusal view. Scale bars: A, 5 mm; B-D, 1 mm.

eruption (e.g., MHNC 8372, 8399, 8402, 8404) than the last molar. A similar condition is observed on the lower jaws (MHNC 8372, 8399; 8402; 8403). Furthermore, in some of these specimens, wear facets are slightly more pronounced on P4 than on P3 (MHNC 8399, 8402, 8403).

Moreover, as in the great majority of eutherians, the first premolar of *Alcidedorbignya* is characterised by a single dental generation, (i.e., with no replacement or no deciduous tooth) (Luckett 1993). As mentioned in the Material and Methods section above, we hypothesized that the first premolars of *Alcidedorbignya* are retained dP1/dp1 following the statement of Luckett (1993) that a successor of dP1/dp1 is normally absent in most genera of eutherians. However, as mentioned above, this condition is not constant within placentals, since, in the dog, in which the primary dental lamina lacks a tooth bud of the dP1, the first premolar has been interpreted as a permanent premolar with no precursor (Williamson & Evans 1978; McKay *et al.* 2022: fig. 6). Furthermore, according to Luckett (1993: 186 and references therein), in the genus *Tapirus* there is a clear evidence for normal replacement of dP1 by P1. A dP1 replaced by P1 is also observed in dorudontine basilosaurids (Uhen 2000) and in hyracoids (Gheerbrant *et al.* 2007; Asher *et al.* 2017 Gomes-Rodrigues *et al.* 2020). This condition, with two generations of the first premolars, is clearly absent in *Alcidedorbignya*.

The dental eruption sequence observed here in *Alcidedorbignya* is almost identical to that postulated by Lucas & Schoch (1990) for the pantodont *Coryphodon*, which was confirmed by McGee & Turnbull (2010). Among others, our interpretation of the first premolars of *Alcidedorbignya* follows that of

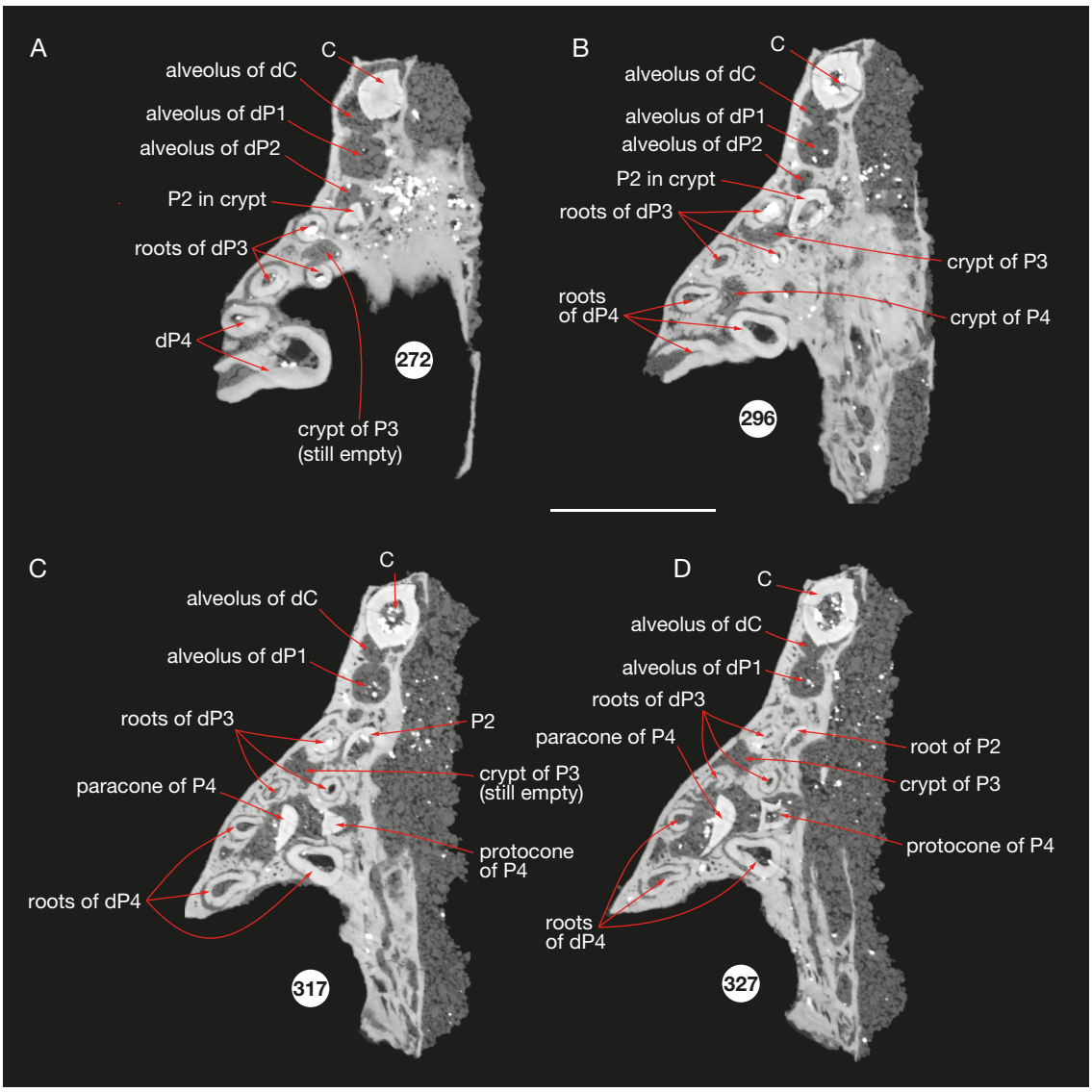

FIG. 28. — Slices of the coronal CT-scan of the maxilla (MHNC 13861) of juvenile *Alcidedorbignya inopinata* (stage 4): **A**-**D** slice 272, 296, 317, 327 (slice 272 is the most ventral and slice 327 is the most dorsal). The number for each illustrated slice refers to the position within the sequence of 783 images (resolution binned images voxel size = 0.0186471 mm). Scale bar: 5 mm.

McGee & Turnbull (2010), who regard these teeth in *Coryphodon* as dP1/dp1. Furthermore, the M3 of *Coryphodon* is the last cheek tooth to erupt and P4 erupts before P3 (McGee & Turnbull 2010). The specimen described by these authors (PM 39385, class 3, young adult), which bears an erupting M3, whereas the other cheek teeth are full erupted perfectly fits our stage 6 represented by MHNC 13853 (Fig. 40).

In several Paleocene eutherians, (e.g., *Phenacodus* Cope, 1873 [West 1971], *Hyopsodus* Leidy, 1870 [West 1979], *Meniscotherium* Cope, 1874 [Williamson & Lucas 1992], and *Leptictis* [West 1972]), the M3 is not the last cheek tooth to erupt since it is fully erupted when dP4 is still functional (see also Gomes-Rodrigues *et al.* 2019: fig. 2). This condition is also present in "the vast majority of Paleogene families of cetartiodactyls" (Gomes-Rodrigues *et al.* 2019) and is regarded by these authors as the plesiomorphic condition for cetartiodactyls. It is present in the four taxa ("*Hyracotherium*" Owen, 1840, *Phenacodus, Meniscotherium*, and *Leptictis* Leidy, 1869) they retained as outgroup (Gomes-Rodrigues *et al.* 2019: fig. 2).

In the Late Cretaceous *Kennalestes*, M3 and P3 are just starting to erupt when P4 and P2 are functional. In a slightly later stage, M3 is fully erupted and P3 is still erupting (Luo *et al.* 2004: fig. 4D). In contrast, in *Ukchudukodon* Archibald & Averianov, 2006 (*Daulestes* Trofimov & Nesov, 1979 in Luo *et al.* 2004), m3 is still in its crypt, whereas dp4 is still functional and p3 and p2 are erupting (Luo *et al.* 2004). Therefore, the condition of *Kennalestes* Kielan-Jaworowska, 1968 resembles that of *Alcidedorbignya* in the slightly delayed eruption of P3 (as compared to P4), but differs from it in the M3 not being the last tooth to fully erupt, thus resembling the condition in *Leptictis*, *Phenacodus*, and *Meniscotherium*. The condition of *Ukchudukodon* appears inconclusive as far

as the relative eruption of m3 is concerned, but it differs from *Alcidedorbignya* in p3 erupting before p4, a condition which is reversed in *Alcidedorbignya*.

Among extant mammals, Asher & Olbricht (2009) observed that the last molars of *Macroscelides* A.Smith, 1829 (M2/m2) and *Erinaceus* Linnaeus, 1758 (M3/m3) are not the last cheek teeth to erupt. Slaughter *et al.* (1974: table 1) observed a similar condition in several taxa of Tenrecidae, Leptictidae, Erinaceidae, and Macroscelididae. These authors also observed a similar condition in most of the carnivorans considered (46 species), in which the last molar (M3/m3 or M2/m2, or M1/m1) is not the last cheek tooth to erupt, with some exception however (*Mephitis* Geoffroy Saint-Hilaire & Cuvier, 1795*, Conepatus* Gray, 1837*, Dusicyon* C.E.H.Smith, 1839*, Selenarctos* Heude, 1901*, Arctogalidia* Merriam, 1897*, Paradoxurus* F.Cuvier, 1821, and possibly *Paguma* Gray, 1831). Moreover, Monson & Hlusko (2018a) observed that, within primates, the third molars erupt before one or more of the premolars in the early diverging primates such as strepsirhines and tarsiiforms.

Similarly, in most ruminants (for example) the M3/m3 erupt before the premolars (Smith 2000; Veitschegger & Sánchez-Villagra 2016; Monson & Hlusko 2018b; Gomes-Rodrigues *et al.* 2019). However, variation exists. For instance, in cervids, several authors have also observed that M3/m3 are the last cheek teeth to fully erupt (or erupt jointly with the premolars) in *Cervus elaphus* Linnaeus, 1758 (Lowe 1967: 151; Azorit *et al.* 2002); *Cervus canadensis* Erxleben, 1777 (Quinby & Gab 1957: table 4); *Dama dama* (Linnaeus, 1758) (Chaplin & White 1969: 128, table 1, and personal observations in the MNHN collections); *Muntjacus reevsi* (Ogilby, 1839) (Chapman *et al.* 1985: 213); *Odocoileus virginianus* (Zimmermann, 1780) (Severinghaus 1949: Table 1). In *Rangifer tarandus* (Linnaeus, 1758), although eruption of M3/m3 starts slightly before that of premolars, it is apparently slower and full eruption is either simultaneous or slightly later than that of premolars (Miller 1972: table 2).

In contrast, in hyracoids, most anthropoid primates, early diverging notoungulates, astrapotheres and suoids (for example), M3/m3 erupt last, after P4/p4 (Smith 2000; Billet & Martin 2011; Kramarz & Bond 2013; Asher *et al.* 2017; Monson & Hlusko 2018a; Gomes-Rodrigues *et al.* 2017, 2019). It therefore appears that M3/m3 erupting last may be a derived condition, which evolved many times within several groups of eutherians (e.g., primates, cetartiodactyls, perissodactyls, notoungulates, astrapotheres) as suggested by several authors (Smith 2000; Veitschegger & Sánchez-Villagra 2016; Monson & Hlusko 2018a; Gomes-Rodrigues *et al.* 2019). The occurrence of this character state in one of the earliest pantodonts (*Alcidedorbignya*) and in one of the latest (*Coryphodon*) would indicate that it likely represents a synapomorphy of this order (Muizon *et al.* 2015).

The late eruption of molars compared with permanent premolars (i.e., M3/m3 after P2-4/p2-4) was reportedly associated with a slow pace of growth in some mammals (e.g., humans, hippos, rhinos) (Smith 2000) but this relationship, generally known as the Schultz's rule, cannot be generalized to all mammals (Godfrey *et al.* 2005; Veitschegger & Sánchez-Villagra 2016). Therefore, it is uncertain whether the delayed eruption of the third molars in comparison to permanent premolars in *Alcidedorbignya* can be indicative of a slow life history.

Tooth mineralisation timing in crypt

Interesting observations can also be made on the degree of mineralisation of the tooth germs or cusps before eruption (i.e., in crypt) (Fig. 43). At Stage 1, we have no indication on the permanent upper cheek teeth development but, on the dentary dp1 is starting to mineralize in the bottom of crypt, the crown (no root present) of m1 is fully mineralised (germ) in crypt and a single cusp of m2 only is observed in crypt posterior to m1 (Figs 2-6). This cusp is strongly convex labially (but with no crest), almost flat lingually, and feature an anterior cingulid (precingulid), a morphology that resembles that of the protoconid, to which it is referred.

At Stage 2, on the skull, the tip of C is mineralised and M1, although not fully erupted, is completely mineralised (with no roots), but we have not observed any cusp of M2 (which may have been lost post-mortem). On the dentary, dp1 fills its crypt but is not erupting. The m1 is erupting and trigonid and talonid of m2 are formed in crypt but still separated (Figs 8-10). As seen on Fig. 10, the three cusps of the trigonid are well formed but incompletely fused; a single cusp of the talonid is present referred to the hypoconid because of its shape and labial position in the crypt.

At stage 3, the apex of I3 and crown of C and dP1 are mineralised (Figs 15; 16); three main cusps of M2 are formed but apparently imperfectly mineralised since the enamel is very white (see McGee & Turnbull 2010: 5) and thin (as seen on MHNC 8416); furthermore, the stylar self is absent (Figs 15; 17-19). On the dentary, the apex of i3 is present and crowns of permanent canines are well mineralised (Fig. 16). The m2 crown is a fully mineralised germ with fused trigonid and talonid (Fig. 19). On one specimen of Stage 3+ the tip of protoconid of p4 is mineralised in crypt (Fig. 22).

At stage 4, only the paracone of P3 is mineralised and P4 is almost fully mineralised except the labial edge of the stylar shelf (Figs 26-28); on one specimen the crown of P2 is present and well mineralised (Figs 24; 28). On the dentary only the trigonid of p4 is mineralised (protoconid [clearly more developed than in stage 3+], paraconid, and metaconid), and tips of protoconid and metaconid of m3 are present in crypt (Figs 30-33).

At stage 5, we have no indication of the mineralisation of M3 which has not been preserved in the crypt of the maxilla MHNC 13860 (Fig. 35). On the dentary (MHNC 13858) a single cusp (protoconid) of p3 is present below dp3 and p4 is fully mineralised in crypt; the trigonid of m3 is well mineralised and the talonid was not observed because of the breakage of the posterior part of the specimen. However, given the degree of mineralisation of the trigonid, it is likely that the talonid was also present (Fig. 37).

At stage 6 all deciduous cheek teeth have been shed, P4 is almost fully erupted and M3 is erupting (Fig. 40). At stage 7, all permanent teeth are present (fully erupted), (Fig. 41).

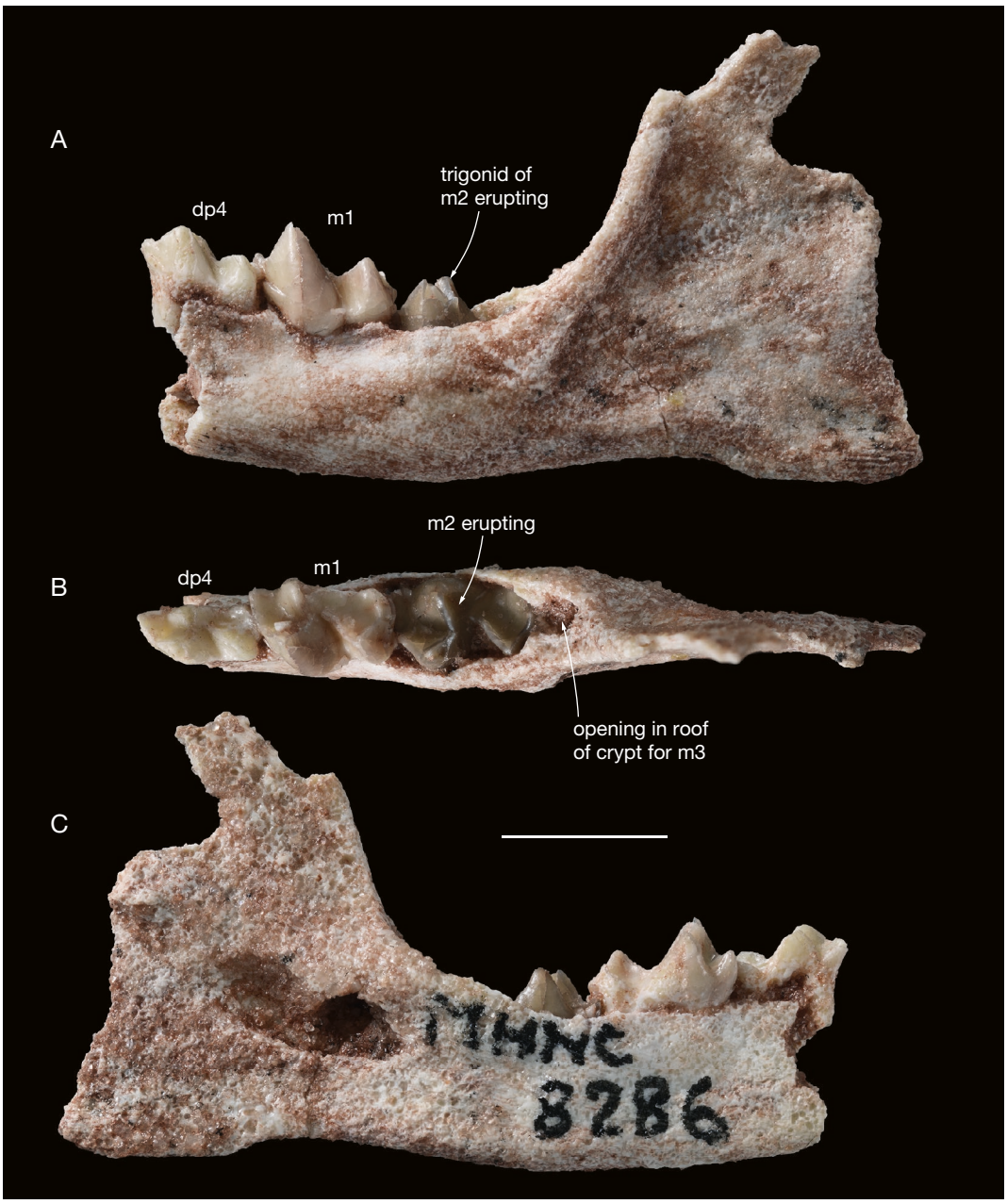

FIG. 29. — Left mandible (MHNC 8286) of juvenile *Alcidedorbignya inopinata* (stage 4): **A**, lateral view; **B**, occlusal view; **C**, medial view. Scale bar: 5 mm.

The formation of p4 anterior to that of p3 has also been observed in *Phenacodus* (West 1971: 30, fig. 23). However as mentioned by West (1971) in phenacodontids, the tooth eruption does not follow the sequence of tooth mineralisation and the sequence of eruption of the last three lower premolars is p2, p3, p4, whereas the sequence of calcification is p4, p3, p2. Comparison of the premolar eruption sequence in *Alcidedorbignya* with that of phenacodontids is difficult because the studies of West (1971) are based on lower dentition and our observations are based on the upper dentition (MNHC 13860 and YPFB Pal 6363).

In *Alcidedorbignya,* considering that the tooth just posterior to the canine is a retained dP1, not a P1 (see comment in Material and methods section above), the first premolar to erupt is P4 followed by the two anterior premolars (P2-3) with the variation observed above. Furthermore, on MHNC 13858, a stage 5 mandible, the p4 is fully mineralised, whereas a single cusp of p3 is present in crypt. Therefore, we hypothesize that, in *Alcidedorbignya*, the sequence of mineralisation of p4 vs p3 is probably similar to the eruption sequence of the upper premolars, although data indicating full eruption of p3-p4 at stage 6 are missing. However, it is noteworthy that the eruption sequence does not always strictly follow the mineralisation sequence (West 1971; van Nievelt & Smith 2005).

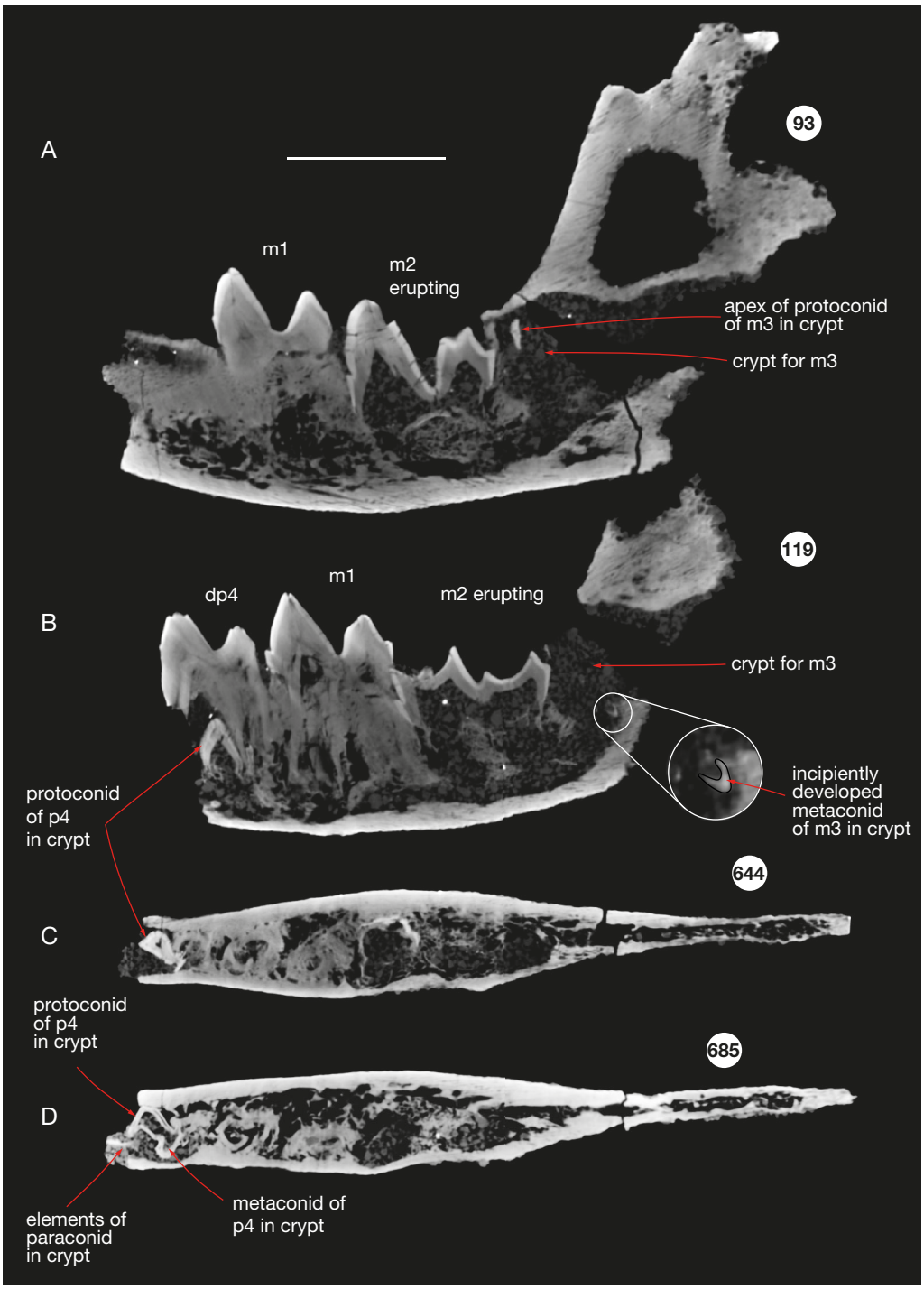

FIG. 30A-D. — Slices of lateral and coronal CT-scans of the mandible (MHNC 8286) of juvenile *Alcidedorbignya inopinata* (stage 4): **A**, **B**, slices 93 and 119 of the lateral CT scan; (Slice 93 is lateral to slice 119); **C**, slice 644 of the coronal CTscan; **D**, slice 685 of the coronal Ctscan (slice 685 is ventral to slice 644). The number for each illustrated slice refers to the position within the sequence of 223 images for A, B and D and 823 images for C and E (resolution binned images voxel size = 0.02781842 mm). Scale bar: 5 mm.

RELATIVE TIMING OF CUSP MINERALISATION

Considering the timing of cusp mineralisation relative to others in the same tooth, it is noteworthy that, in the six cases in which a single cusp of a tooth is present in crypt, this cusp is a labial one: paracone of P3 in MHNC 13857; protoconid of m2 in MHNC 8373 and 13859; hypoconid of m2 in MHNC 8423; protoconid of p3 in MHNC 13858 protoconid of m3 in MHNC 8286. Furthermore, as observed on MHNC 8423, on lower molars, the trigonid develops before the talonid (Fig. 6).

Our observations are congruent with previous statements in many eutherian mammals (Butler 1956 and literature

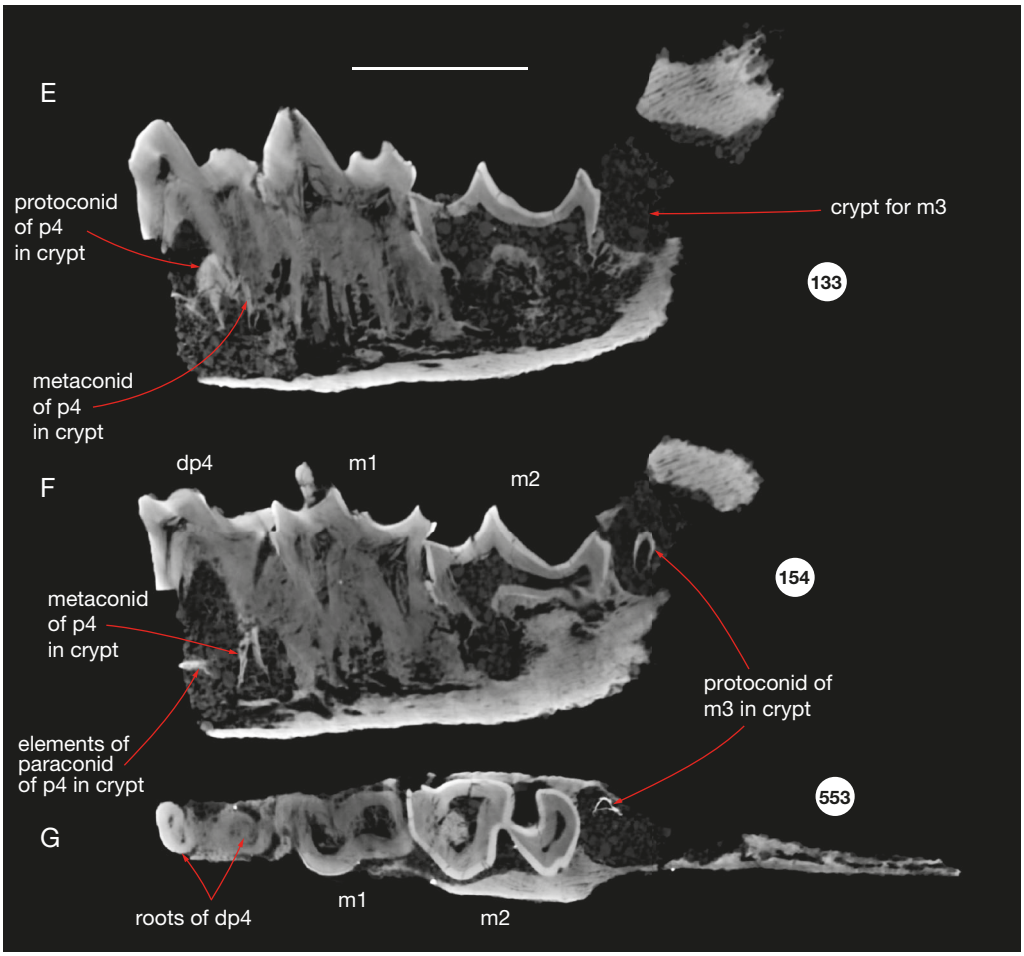

Fig. 30E-G. — Slices of lateral and coronal CT-scans of the mandible (MHNC 8286) of juvenile *Alcidedorbignya inopinata* (stage 4): **E**, slice 133 of the lateral CT-scan; **F**, slice 154 of the lateral CT-scan; **G**, slice 553 of the coronal CT scan (slice 553 is dorsal to slice 644). The number for each illustrated slice refers to the position within the sequence of 223 images for A, B and D and 823 images for C and E (resolution binned images voxel size = 0.02781842 mm). Scale bar: 5 mm.

therein; Hershkovitz 1971; Luckett 1993; Jernvall 1995) that the paracone and protoconid are the first cusps to develop. As stated by Jernvall (1995: 26), the cusps develop from "tip to down" and "the order of initiation of cusp development is the main determinant of relative cusp size". In *Alcidedorbignya*, the early-mineralizing labial cusps mentioned above are among the highest cusp(s) on their respective upper tooth (paracone) or lower tooth trigonid (protoconid) or talonid (hypoconid). However, although most authors regard the hypoconid as the first talonid cusp to develop, variations exist (e.g., *Erinaceus* and *Cynocephalus* Boddaert, 1768; see Butler 1956: 51).

Relative synchrony of tooth eruption: upper vs lower

Relative eruption of mandibular teeth as compared to maxillary teeth is variable among mammals. The former can erupt slightly earlier than the latter as for instance in some cervids (Chapman *et al.* 1985, Severinghaus 1949), in the didelphid marsupial *Monodelphis* Burnett, 1830 (van Nievelt & Smith 2005) or later as in *Giraffa* Brisson, 1762 (Singer & Boné 1960: 384; Hall-Martin 1976: 270) and *Diceros* Gray, 1821 (Goddard 1970).

In *Alcidedorbignya*, relative eruption of dP1 and dp1 is reversed in MHNC 8423 as compared to MHNC 8416. In the former, dP1 starts to erupt before dp1, whereas the contrary is observed in the latter. Furthermore, the degree of eruption is similar in these specimens (although reversed) when MHNC 8423 is a stage 2 individual, in which M1 is barely erupting, whereas in MHNC 8416, a stage 3 individual, M1 is almost fully erupted. These conditions indicate that, in *Alcidedorbignya*, variation exists as regard to the relative eruption of upper and lower teeth.

COMPARISON AND DISCUSSION

Correlation with IDAS of Anders *et al.* (2011)

In our sample of juvenile individuals of *Alcidedorbignya*, we identified six stages (1-6) according to the degree of dental eruption for juvenile individuals and two stages (7 and 8) for adult individuals with fully erupted permanent dentition.

Stage 1 includes one specimen (MHNC 8373, likely a near term foetus or a new born individual), which is tentatively

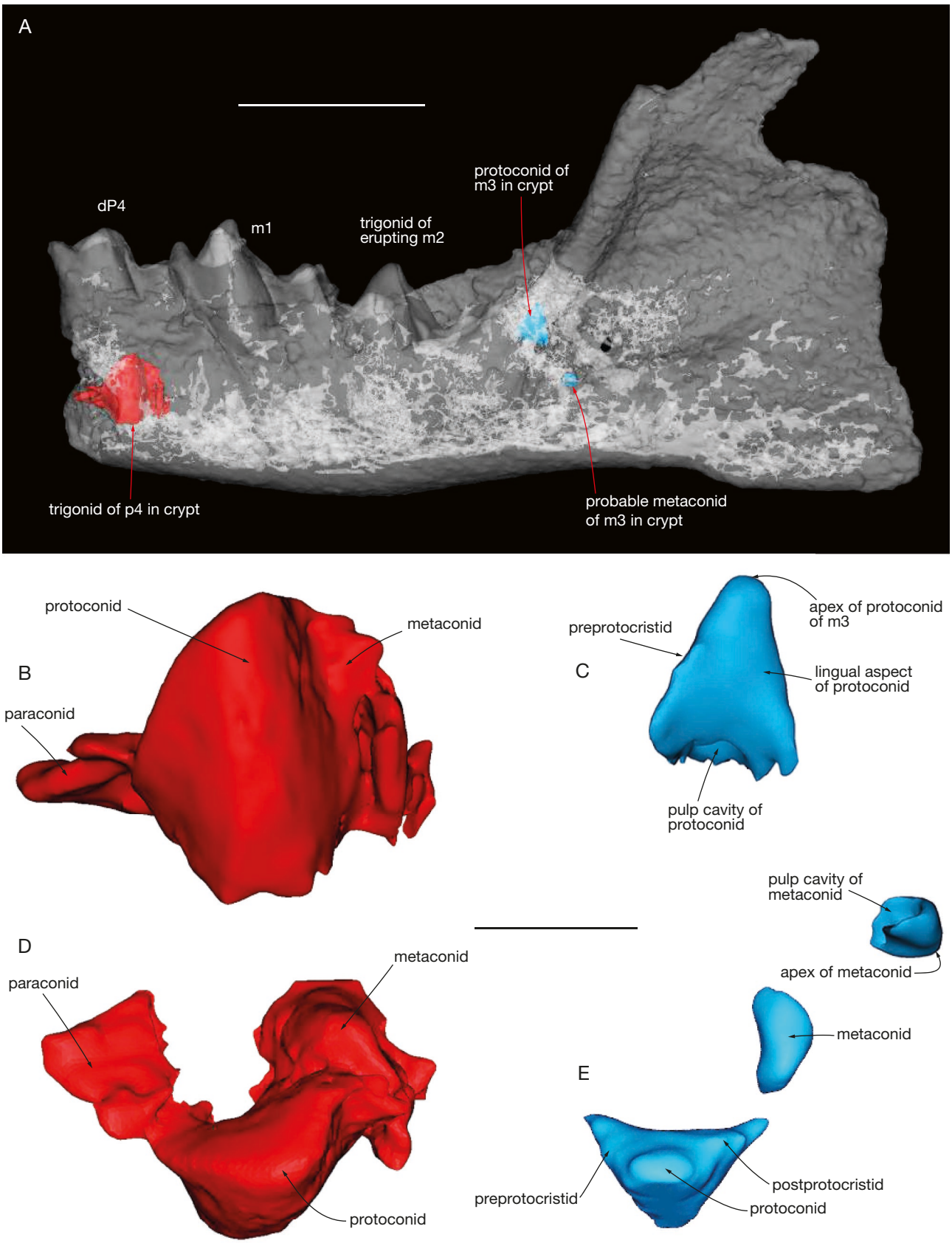

FIG. 31. —**A**, transparent lateral view of the left mandible MHNC 8286 of juvenile *Alcidedorbignya inopinata* (stage 4) showing the trigonid of p4 and protoconid and probable metaconid of m3 in process of mineralisation in their respective crypts; **B**, enlarged view of the trigonid of p4 in the same position as in its crypt; **C**, enlarged view of the protoconid and metaconid of m3 in the same position as in its crypt (the cusps of the trigonid of m3 are not in their natural position since they have been displaced and rotated before filling of the crypt with sediment); **D**, occlusal view of the trigonid of p4; **E**, occlusal view of the protoconid and metaconid of m3, which have been restored in their original positions. Scale bars: A, 5 mm; B-E, 1 mm.

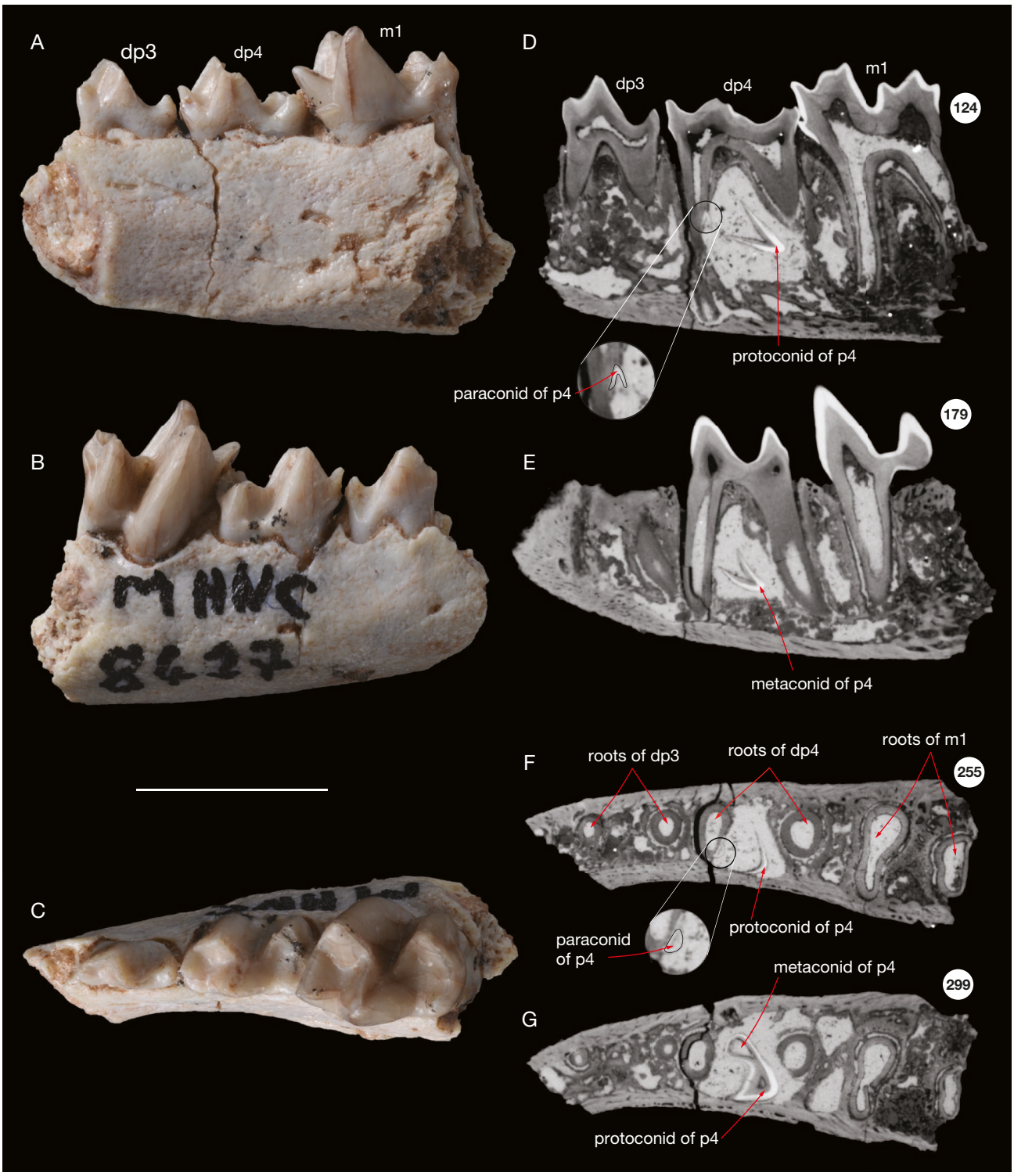

FIG. 32. — Left mandible (MHNC 8417) of juvenile *Alcidedorbignya inopinata* (stage 4): **A**, lateral view; **B**, medial view; **C**, occlusal view; **D**, slice 124 of the lateral CT scan showing the paraconid of p4 in natural position and the metaconid rocked (approximately 130°) posteriorly; **E**, slice 179 of the lateral CT scan, showing section of the protoconid rocked (approximately 130°) posteriorly; **F**, slice 255 of coronal CT Scan showing section of paraconid of p4 mesially and metaconid distally; **G**, slice 299 of coronal CT Scan showing section of fused protoconid and metaconid of p4. Scale bar: 5 mm.

referred to IDAS 0 of Anders et al (2011). In fact, because some specimens of stage 1 are slightly more advanced than this probable near term foetus, our stage 1 (perinatal stage) likely corresponds to late IDAS 0 (MHNC 8373) and very early IDAS 1 (the other specimens referred to stage 1). Nevertheless, it is noteworthy that the difference in dental eruption was probably almost identical between a near term foetus and a newborn individual.

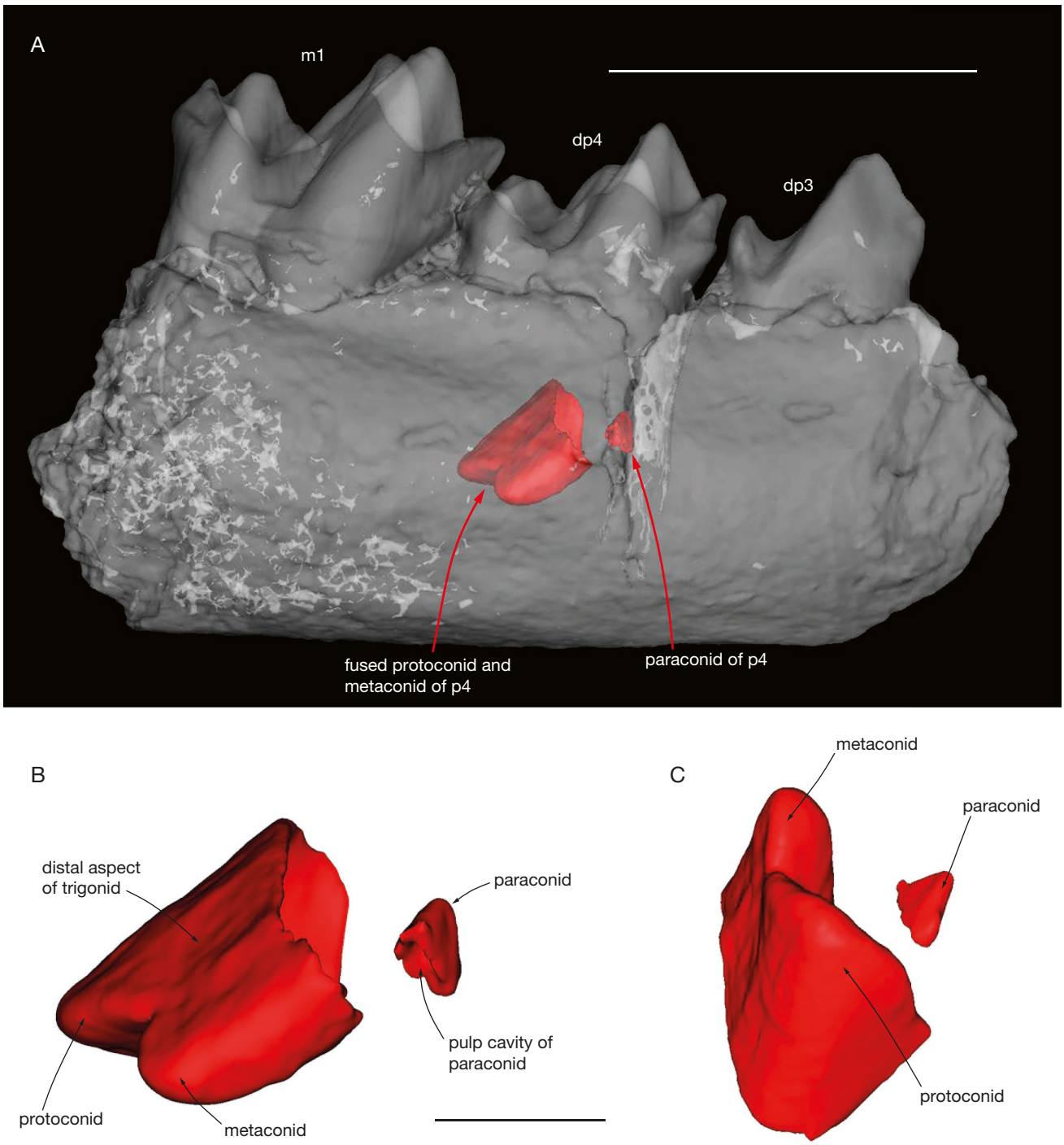

FIG. 33. — **A**, Transparent lateral view of the left mandible MHNC 8417 of juvenile *Alcidedorbignya inopinata* (stage 4) showing unerupted partial trigonid (paraconid anteriorly and fused protoconid and metaconid posteriorly) of p4 in crypt; **B**, view of the partial trigonid of p4 as preserved in crypt (the paraconid is approximately in its natural position but the fused protoconid and metaconid have been rotated along a vertical axis, which has placed the protoconid lingually and the metaconid labially, and along a transverse axis which has rocked the two cusps approximately 130° posteriorly; **C**, occlusal view of partial trigonid of p4 restored in its natural position. Scale bars: A, 5 mm; B, C, 1 mm.

Stage 2, 2+ 3, and 3+, are included in IDAS 1. Anders et al (2011: 4) marked the end of IDAS 1 "with the first attritional facet on the first molar", which is generally related to the end of the lactation period (weaning). In our ontogenetic series, the first wear facet, which is probably attritional, appears on stage 4, when M1 is fully erupted and M2 just starting to erupt. According to Anders *et al.* (2011) P2, P3, P4, M2, and M3 erupt during IDAS 2. Therefore, our stages 4, 5 and 6 are included in the IDAS 2 (Fig. 1).

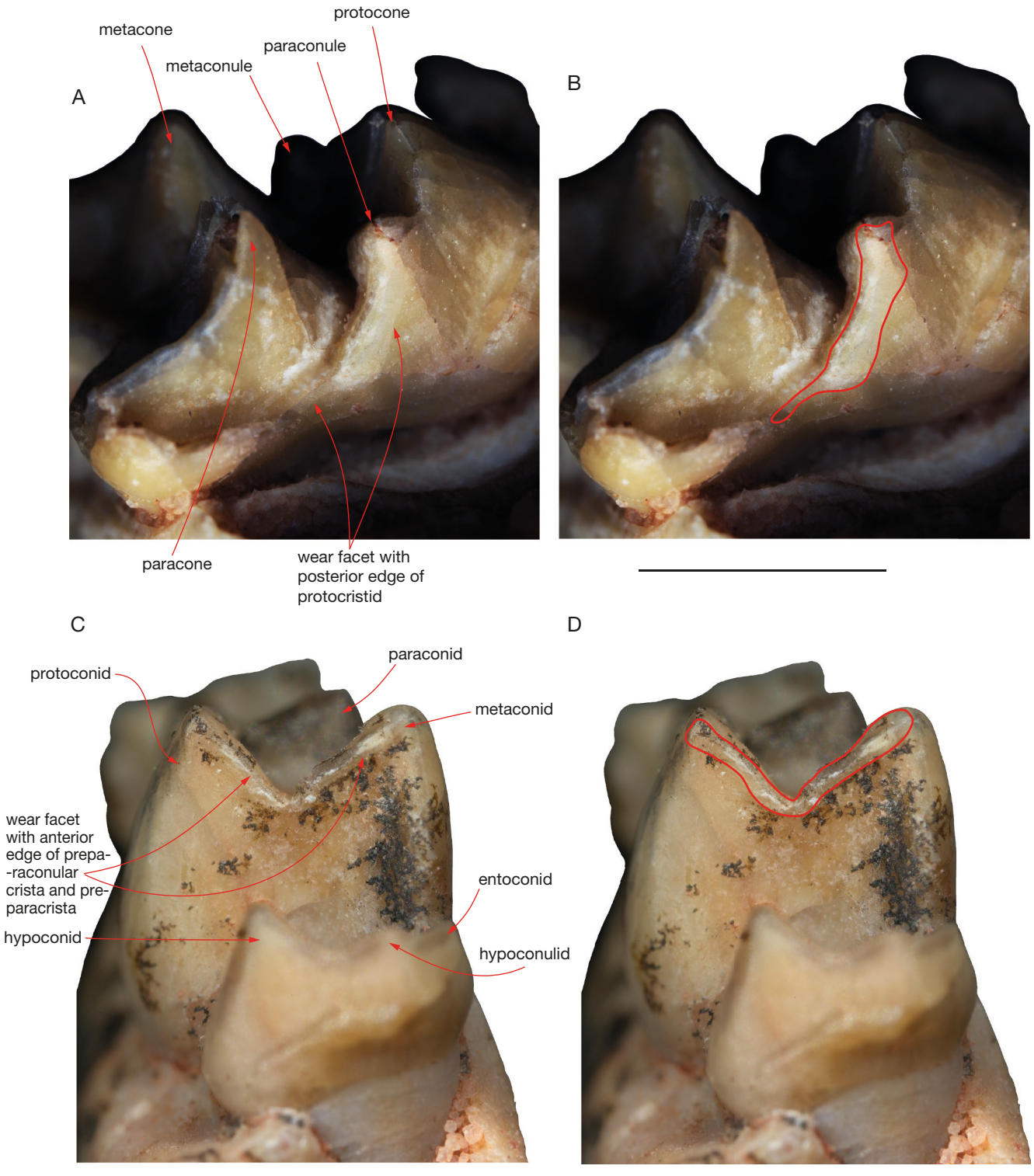

FIG. 34. — Wear facets on the first molars of *Alcidedorbignya inopinata*: **A**, partial left maxillary (MHNC 13960) of juvenile (stage 4) with M1 featuring a small wear facet on the on the mesial edge of the paraconule and on the preparaconular crista; **B**, the same with wear facet outlined with a red line; **C**, partial left mandible (MHNC 13964) of juvenile (stage 4) with m1 showing wear facet on the posterior edge of the protocristid; **D**, the same with wear facet outlined with a red line. The photographs of this figure have been obtained using an RTI (Reflectance Transforming Imaging) setting as indicated by Decombeix *et al.* (2021) with some specifications, as follows: we used a Canon EOS 5DS digital camera equipped with a Canon MP-E 65 mm macro lens (both Tokyo, Japan); and LEDs of the two lower rings of the light dome were used (i.e., 42 LEDs). Snapshots were extracted using the default' mode (for A and B, light source coordinates X = –0.34, Y = –0.34); for C and D, light source coordinates X = –0.31, Y = 0.44). Scale bar: 2 mm.

IDAS 3 is characterised by the use of full permanent dentition (Anders *et al.* 2011) and the shedding of all deciduous teeth. It ends with the strong wear of M1, when it loses its internal occlusal surface and internal enamel structure. Our stage 7 corresponds to early IDAS 3 and is represented by the vast majority of the adult individuals of our sample in which the dental wear is very

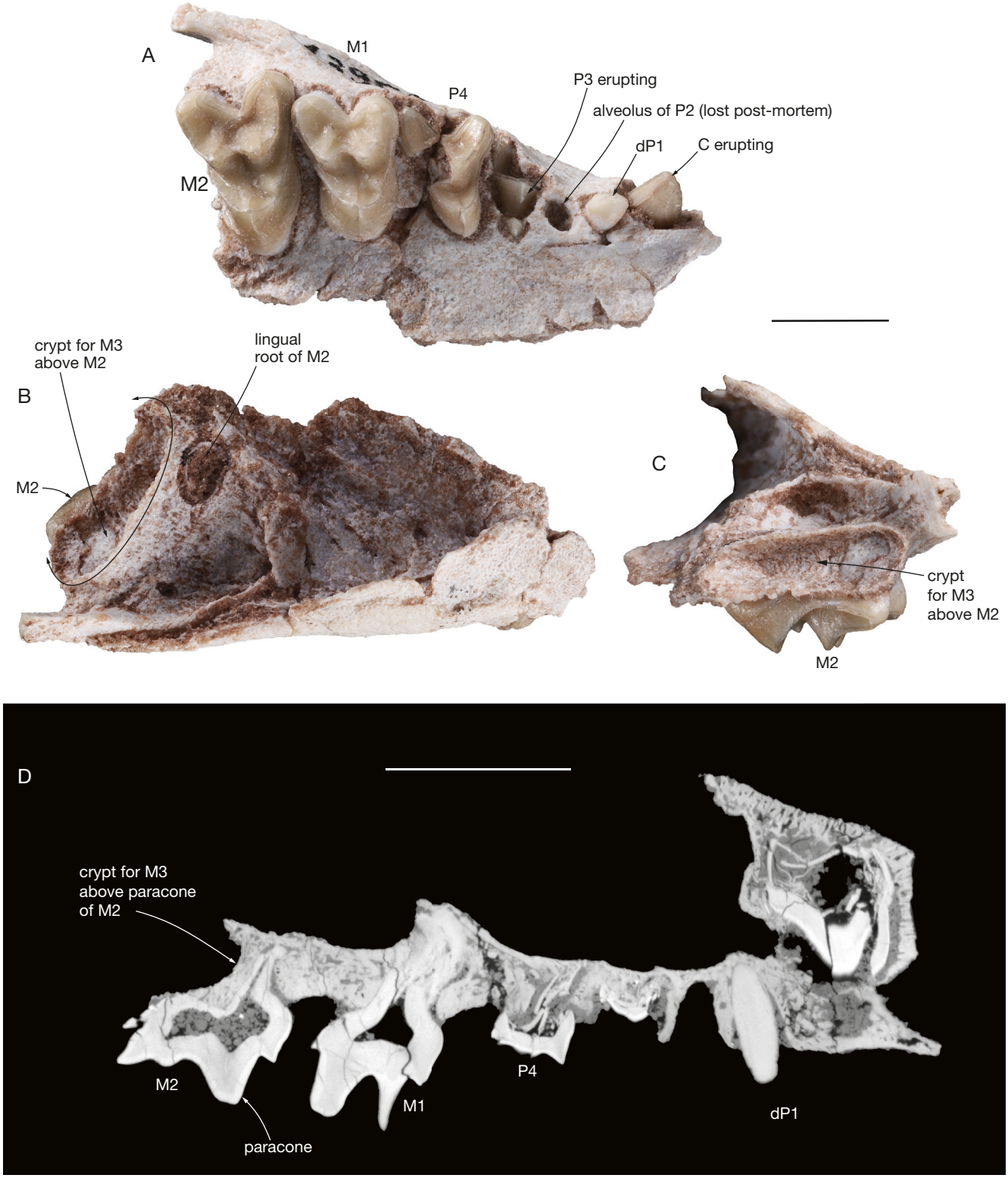

Fig. 35. — Right maxilla (MHNC 13860) of juvenile *Alcidedorbignya inopinata* (Stage 5): **A**, occlusal view; **B**, posterodorsal view, **C**, posterior view showing crypt for M3; **D**, slice 680 of a lateral CT-scan of MHNC 13860, showing the relative position of the crypt for M3 and the paracone of M2. The number for the illustrated slice refers to the position within the sequence of 1004 images (resolution binned images voxel size = 0.0159859 mm). Scale bars: 5 mm.

weak. However, the six specimens mentioned above, included in stage 8 (YPFB Pal 6364, MHNC 8400, 8401, 8413, 13873, and 13975), which show a significant wear of premolars and molars would correspond to a middle to late phase of IDAS 3. We have no specimen that indicate a fully worn M1/m1, and therefore no specimen attributable to a later IDAS.

IDAS 4 is characterised by the wear of M2/m2, which becomes worn out at the end of the IDAS. Similarly, the end of IDAS 5 is defined by the total wear of the tooth row including M3/m3. In our sample, we have no specimens with worn out M2 and M3. Therefore, the two last IDAS, 4 and 5 are not present in our *Alcidedorbignya* population. This does not mean that these phases did not exist in *Alcidedorbignya* (see below). The matching between the stages defined here and the IDAS of Anders *et al.* (2011) is presented on Fig. 1.

Correlation with major life history events

Below we intend to explore two major life history events of the early life of an early placental mammal (*Alcidedorbignya)* based on its sequence of dental eruption: weaning and sexual maturity. For that matter, we have selected models among Recent mammals in which the age of weaning, changes in feeding (from strict suckling to solid food feeder), and acquisition of sexual maturity is relatively easy to obtain. These selected models present a pattern of development of deciduous and permanent cheek teeth at birth and a dental eruption sequence approaching that observed in *Alcidedorbignya*.

Gingerich *et al.* (2009: table 4) provided an overview of the development and mineralisation of deciduous and permanent teeth at birth compared to the developmental maturity categories of Langer (2008) in several Recent mammals. Gingerich identified four categories of developmental maturity from the most altricial (Category I: e.g., *Ursus* Linnaeus, 1758*, Herpestes* Illiger, 1811, *Canis* Linnaeus, 1758) to the most precocial (Category IV: e.g., *Tapirus* Brisson, 1762*, Maiacetus* Gingerich*, Dama* Frisch, 1775*, Giraffa*). Some of the most precocial mammals (Category IV: eyes open, haired, nidifugous at birth) such as *Dama, Muntiacus* Rafinesque, 1815*, Giraffa* have all deciduous teeth erupted at birth and the crown of M1 half or fully mineralised but still in its crypt. In regard to their dental development at birth (all deciduous teeth erupted), they are probably more comparable to our pantodont specimens than mammals of the other precocial categories II and III, respectively suids and primates, which have no erupted teeth at birth. As a matter of fact, the condition of dental eruption at birth in category IV matches the dental development stage 1 described above in MHNC 8373. This specimen was found between the limbs of the adult skeleton MHNC 8372, which has been interpreted as a female individual on the basis of the proportions of the upper canine and height of the snout at the level of anterior edge of M1 (Muizon *et al.* 2015). Besides partial skull and mandibles, MHNC 8373 also includes some postcranial elements (humerus, radius) (Fig. 2E). Therefore, the partial juvenile skull and skeleton MHNC 8373 could be that of a newborn individual. Alternatively, it could also be a near-term foetus since such a well preserved (for instance, the skull still preserves the ectotympanics and ear ossicles articulated), but poorly ossified skeleton might be better explained if it was protected within the uterus of the female. In this context, MHNC 8373 is considered here to belong to a perinatal stage, most likely close before birth, as hypothesised by Muizon *et al.* (2015). According to this hypothesis, *Alcidedorbignya* would

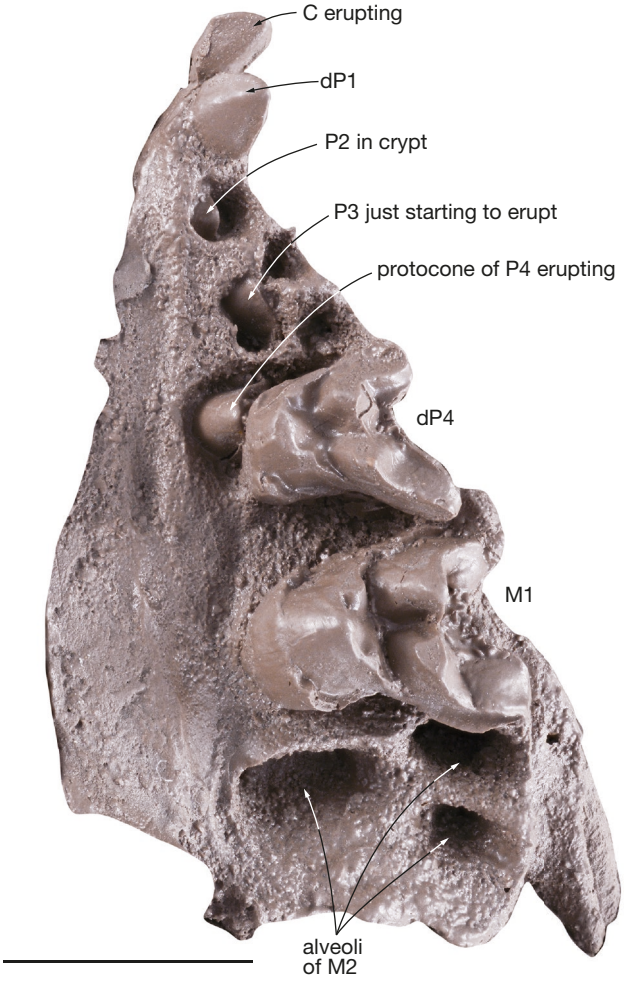

Fig. 36. — Left maxilla (cast of YPFB Pal 6363), of juvenile *Alcidedorbignya inopinata* (stage 5) showing P4 erupting above dP4, which has not shed yet and complete germ of P3 still in crypt: **A**, occlusal view; **B**, mesiolingual view. Scale bar: 5 mm.

then belong to category IV (precocial) of Gingerich *et al.* (2009: table 4) as many Recent ungulates and we prioritize comparisons with these recent taxa of this category. A very detailed comparison of early dental eruption sequence relative to age has been provided in the Reeves' muntjac (*Muntiacus reevesi* (Ogilby, 1839)) and fallow deer (*Dama dama*) (Chapman & Chapman 1970; Chapman *et al.* 1985; Brown & Chapman 1991). These species are the only precocial taxa of category IV of Gingerich *et al.* (2009), for which we found such data in the literature and for that reason we retained them for comparison with *Alcidedorbignya*, in spite of their great phylogenetic distance to pantodonts. Interestingly, these studies indicate similarities between Reeves' muntjac, fallow deer, and *Alcidedorbignya,* although the former two differ from the latter in lacking upper incisors and first premolars (Chapman & Chapman 1970; Chapman *et al.* 1985; Brown & Chapman 1991) and in the fact that M3/m3 are not always the last cheek teeth to erupt. At birth, the two cervids have all their deciduous teeth erupted or erupting and M1/m1 in their crypts, as observed in the perinatal *Alcidedorbignya* specimen MHNC 8373 described above.

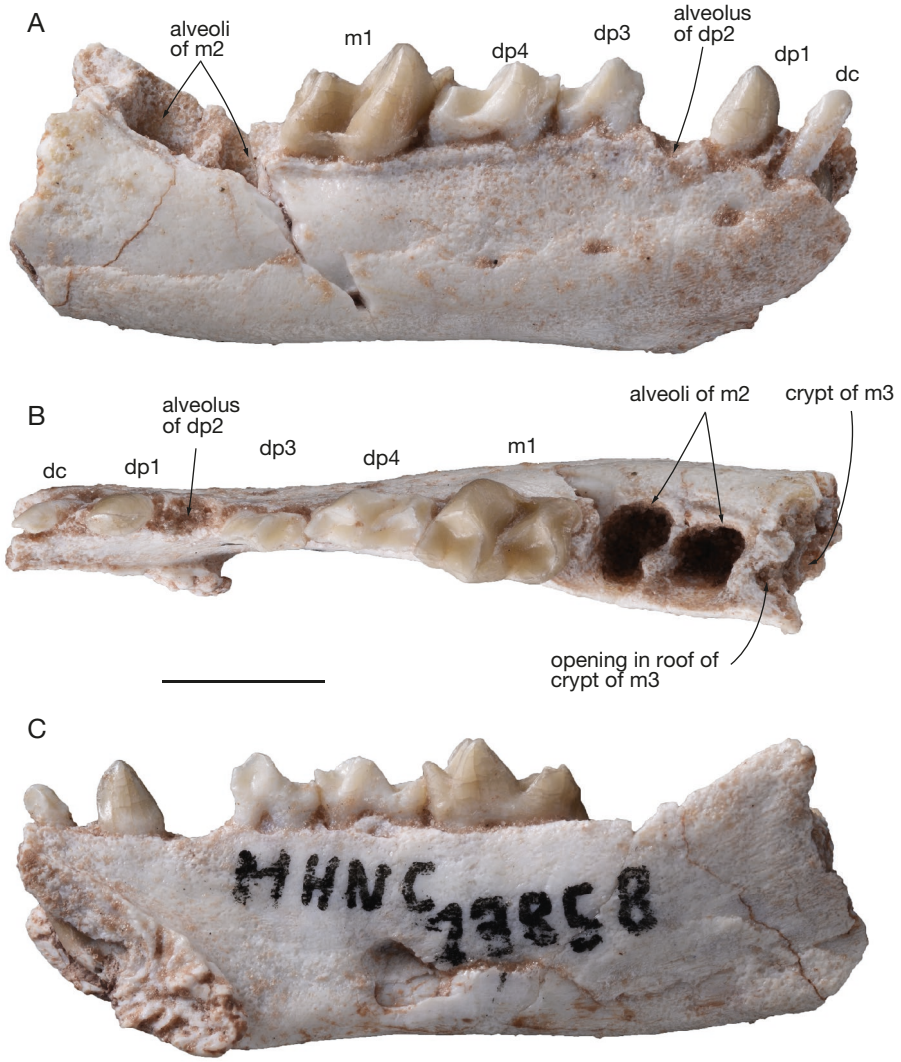

Fig. 37. — Right mandible (MHNC 13858) of juvenile *Alcidedorbignya inopinata* (stage 5): **A**, labial view; **B**, Occlusal view; **C**, lingual view. Scale bar: 5 mm.

Weaning vs dental eruption

Anders *et al.* (2011), have pointed out that, generally, weaning of eutherians takes place when the first molar becomes functional and, therefore, when the first wear facets appear on that tooth (but see below for comparison with dental eruption in extant cervids). They also mentioned that several exceptions are to be taken into account as, for instance, the case of some afrotheres, in which replacement of the deciduous dentition is delayed relative to acquisition of adult size (Asher & Lehmann 2008). In the selected cervids, weaning occurs when M1/m1 are erupting in *Muntiacus reevesi* (at eight weeks, only anterior part of tooth above bone) (Yahner 1978; Chapman *et al.* 1985) or are barely starting to erupt in *Dama dama* (at 11 weeks, tip of molars just showing, but most of the tooth still in crypt) (Pélabon *et al.* 1998; Brown & Chapman 1991).

As a consequence, M1/m1 do not bear wear facets in *Muntiacus reevesi* and *Dama dama* at the age of weaning (personal observations on MNHN collections), (see also Chapman et al 1985: plate I and Brown & Chapman 1991: pl. I). Anders *et al.* (2011: 324) state that "weaning young shortly before or after the emergence of the first permanent molar appears to be widespread in ungulates as well". This statement therefore probably includes cases such as those observed in *Muntiacus* and *Dama*.

Below, in the discussion of the ontogeny of feeding in *Alcidedorbignya*, we consider the appearance of wear facets on dP4/dp4 and dP3/dp3 as compared to those on M1/m1.

We hypothesize that three different ontogenetic phases of feeding in *Alcidedorbignya* are evident in the four first dental stages defined above: stage 1 (perinatal suckling individuals), stages 2-3 (suckling and partly suckling individuals), stage 4 (solid feeders, weaned individuals).

Stage 1 – The best-preserved specimen is MHNC 8373, a partial skeleton including the partial skull with associated mandibles mentioned above and some elements of the postcranial skeleton including a tiny, poorly ossified humerus and partial radius. As mentioned above, this specimen is regarded as perinatal and if newly born, it was certainly suckling only. This individual may correspond to the Individual Dental Age Stage 0 (IDAS 0) of Anders *et al.* (2011) (see above).

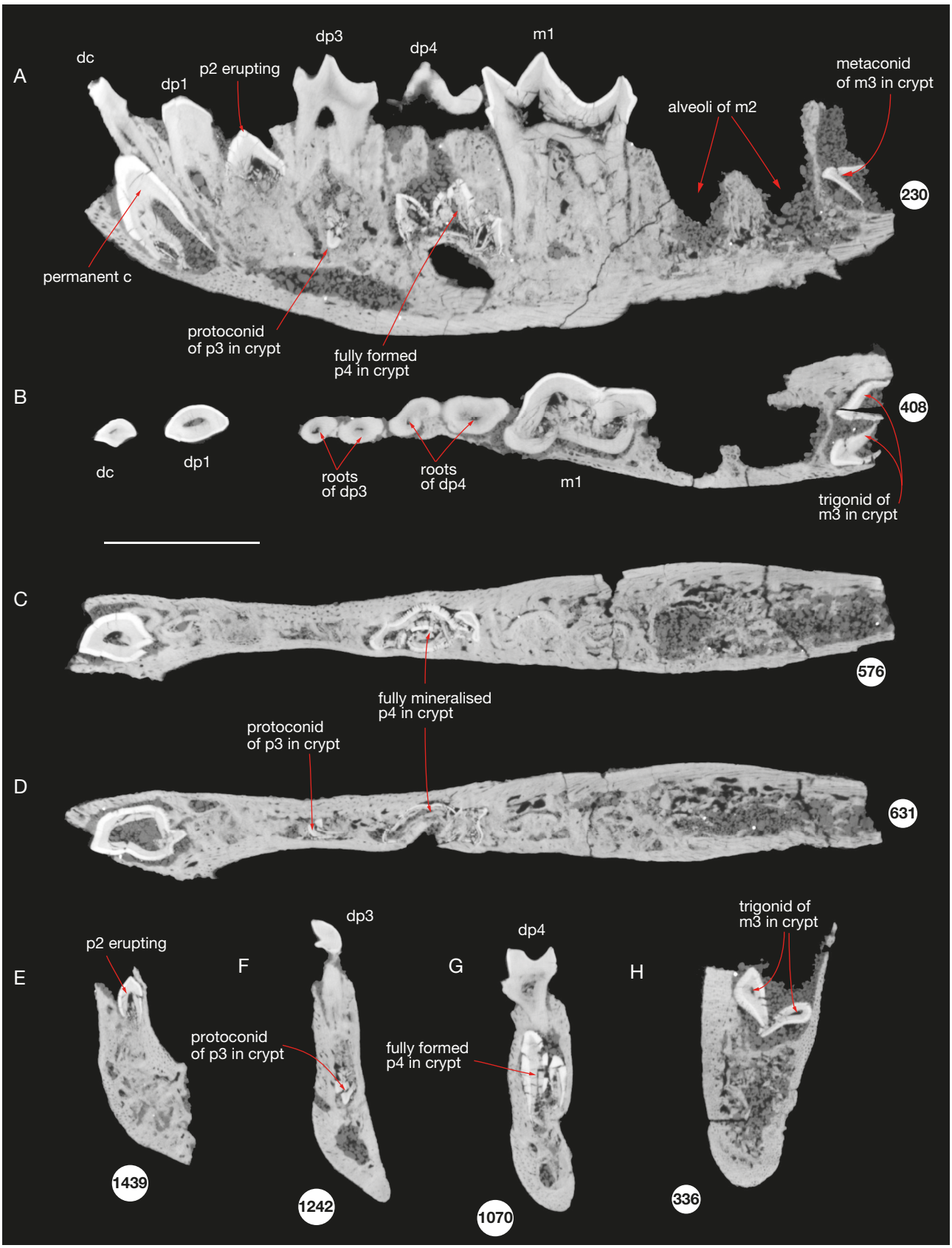

FIG. 38. — Slices of the lateral, coronal, and frontal CT-scans of the mandible (MHNC 13858) of juvenile *Alcidedorbignya inopinata* (stage 5): **A**, slice 230 of lateral CT-scan; **B-D**, slices 408, 576, and 631 of coronal CT-scan (slice 230 is the most dorsal and slice 631 is the most central); **E-H**, slices of frontal CT-scan, 1439, 1242 1070, 336 of CT scan (slice 1439 is the most anterior and slice 336 is the most posterior). The number for each illustrated slice refers to the position within the sequence of 604 images for A, 1003 images for B-D and 1864 images for E-H (resolution binned images voxel size = 0.0159859 mm). Scale bar: 5 mm.

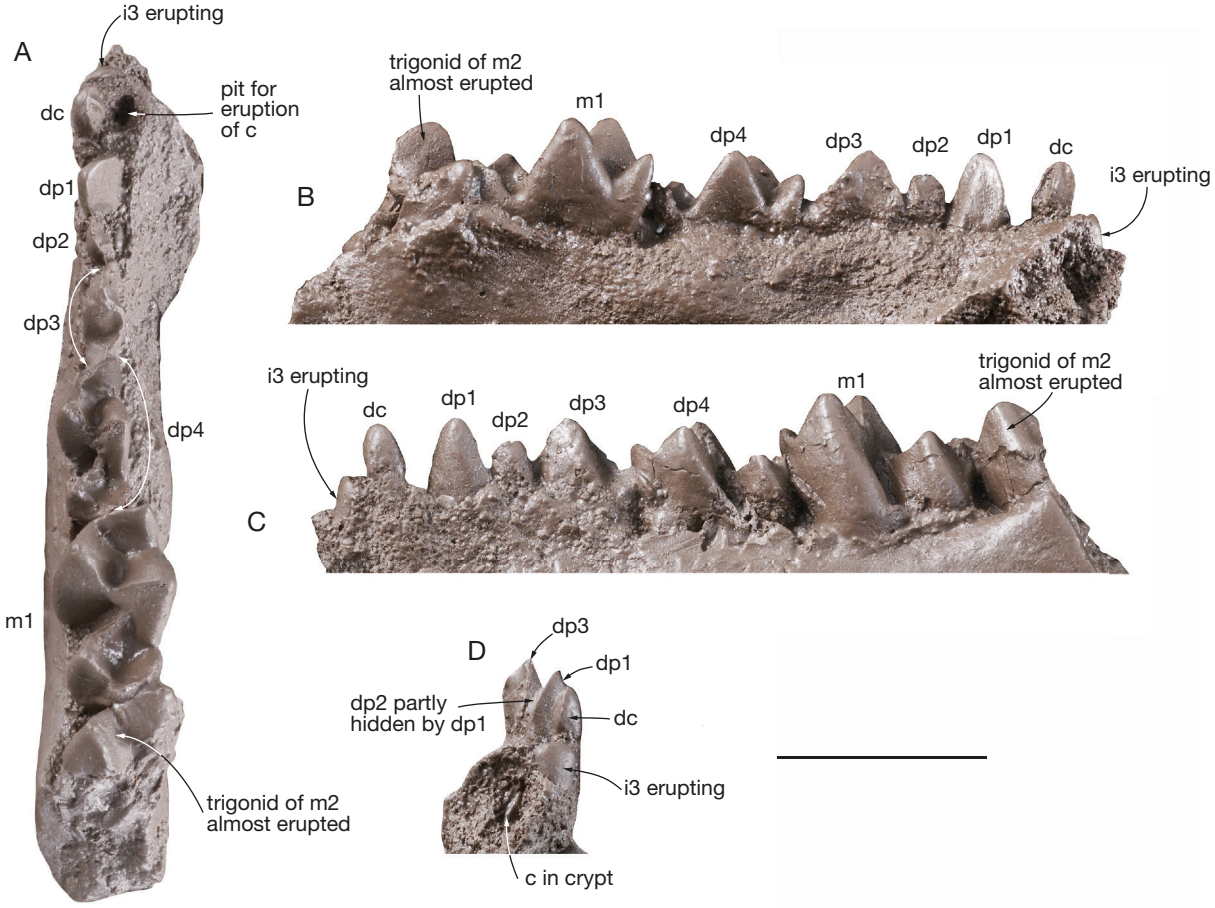

FIG. 39. — Left mandible (cast of YPFB Pal 6351), of juvenile *Alcidedorbignya inopinata* (stage 5) showing trigonid of m2 almost erupted. **A**, occlusal view; **B**, lingual view; **C**, labial view. Scale bar: 5 mm.

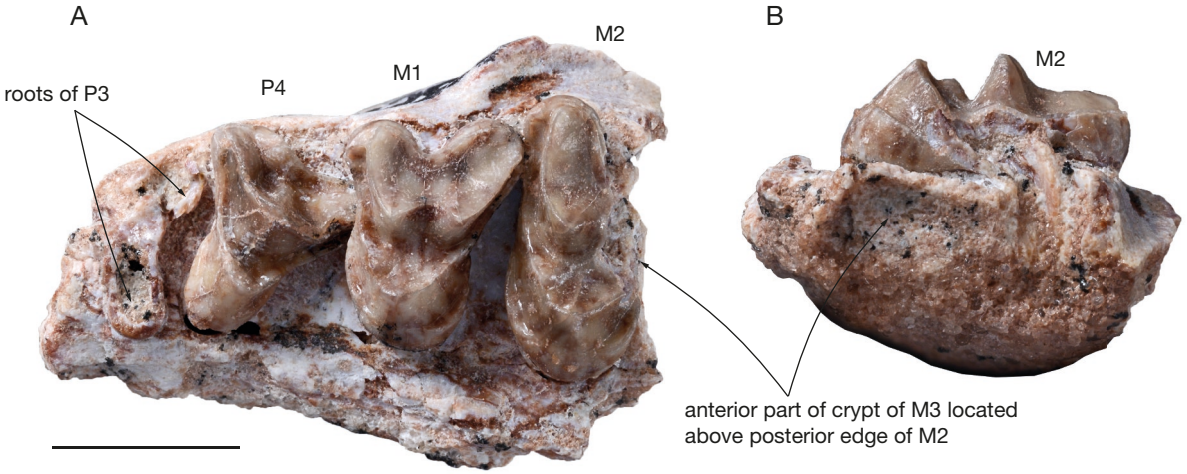

FIG. 40. — Left maxillary (MHNC 13853) of sub-adult *Alcidedorbignya inopinata* (stage 6) with roots of P3 and P4-M2 erupted. M3 is missing but the crypt is present with its anterior border located above the posterior edge of M2 thus indicating that the tooth was erupting. The position of P4 (turned clockwise *c.* 45° and with the metastyle embedded) above the paracingulum of M1 is pathological: **A**, occlusal view; **B**, posterior view showing the anterior part of the crypt of M3. Scale bar: 5 mm.

Individuals of stage 1 and IDAS 0 are regarded here as part (at least) of the "milk-only period" of Langer (2008). As a matter of fact, distinct wear facets are absent on the deciduous premolars of MHNC 8373.

In *Muntiacus*, stage 1 may correspond to week 1 to 3 in terms of degree of eruption of m1 (Chapman *et al.* 1985: appendix, 211). As in *Muntiacus*, dp2 of perinatal *Alcidedorbignya* is still erupting; however, in contrast to *Muntiacus*,

FIG. 41. — Permanent right dentition of *Alcidedorbignya inopinata* (MHNC 8372) in occlusal view (stage 7): **A**, upper dentition; **B**, lower dentition. Scale bar: 10 mm.

dp3-4 are fully erupted whereas, in the cervid, these teeth are not fully erupted yet (Chapman *et al.* 1985: 211, appendix).

Stage 2 (and stage 2+) may approximately correspond to the beginning of IDAS 1 of Anders *et al.* (2011), in which the first permanent molar has just started to erupt and is not functional (it is fully erupted at the end of IDAS 1, which corresponds to our stage 3). At our stages 2 and 2+, we hypothesize that suckling was still the main feeding resource of the juvenile *Alcidedorbignya* since in this stage the deciduous premolars show almost no wear facets, therefore indicat-

Fig. 42. — Permanent right dentition of *Alcidedorbignya inopinata* with moderate wear in occlusal view (stage 8). **A**, left maxilla with canine and cheek teeth (MHNC 8400); **B**, right mandible fragment with m1 (MHNC 13975). Scale bar: 10 mm.

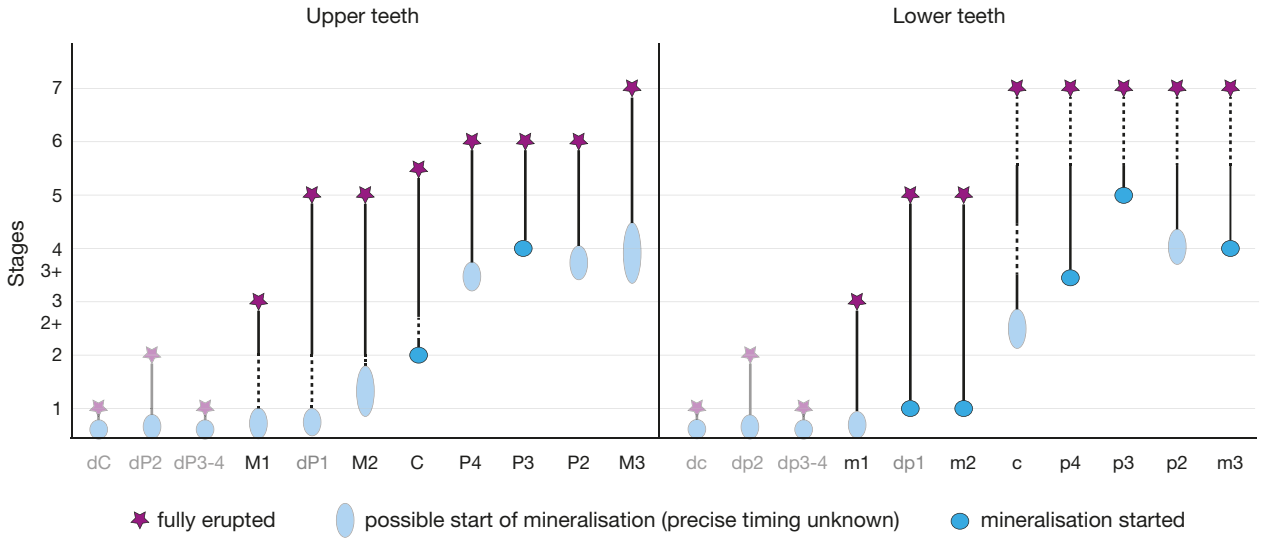

Fig. 43. — Dental ontogeny in *Alcidedorbignya inopinata*. Graphic representation of dental development (mineralisation and eruption) showing on the y-axis the dental stages 1-7 defined in this study. Tooth positions are represented on the x-axis. The teeth are listed from left to right following a possible developmental sequence; this order is only tentative (dotted line indicates missing data).

ing that no (or very little) solid food was ingested. Stages 2 and 2+ probably also correspond to the milk-only period of Langer (2008) or close to the end of this period. In the muntjac, an eruption dental stage similar to our stages 2 and 2+ is reached at approximately 9-12 weeks (Chapman *et al.* 1985: 211, appendix), an age posterior to weaning (which occurs at *c.* eight weeks; Yahner 1978). As a matter of fact, at this stage, dp2-dp4 of muntjac feature pronounced wear facets, thus indicating ingestion of solid food (personal observations on MNHN collections).

A question arises now regarding the precise timing of weaning in *Alcidedorbignya* and whether it could be reflected in its dental ontogeny. First, it is worth noting that, in extant ungulates weaning is progressive since a milk-only period at the very beginning of life (stages 1 and 2) is followed by a mixed feeding period, during which the offspring feeds on both maternal milk and solid food. This is the weaning period, at the end of which the juvenile acquires nutritional independence (Langer 2008). In *Muntiacus reevesi* weaning occurs around eight weeks (Yahner 1978) and in *Dama dama* approximately by 11 weeks (Gauthier & Barrette 1985; Pélabon *et al.* 1998). A that age, in both species, the M1/m1 are just starting to erupt (Chapman *et al.* 1985; Brown & Chapman 1991), as in stage 2 of *Alcidedorbignya*. However, as mentioned by Yahner (1978), *Muntiacus* starts to graze at three weeks, i.e., entering the mixed-feeding period of Langer (2008). These observations concord with those of Smith (1991) on primates who states that "primates tend to nurse their offspring [...] until the beginning of emergence of the permanent dentition (commencing with M/l)" (see also Smith [1992] and Kelley & Smith [2003]). Therefore, if one follows observations on the recent cervids mentioned

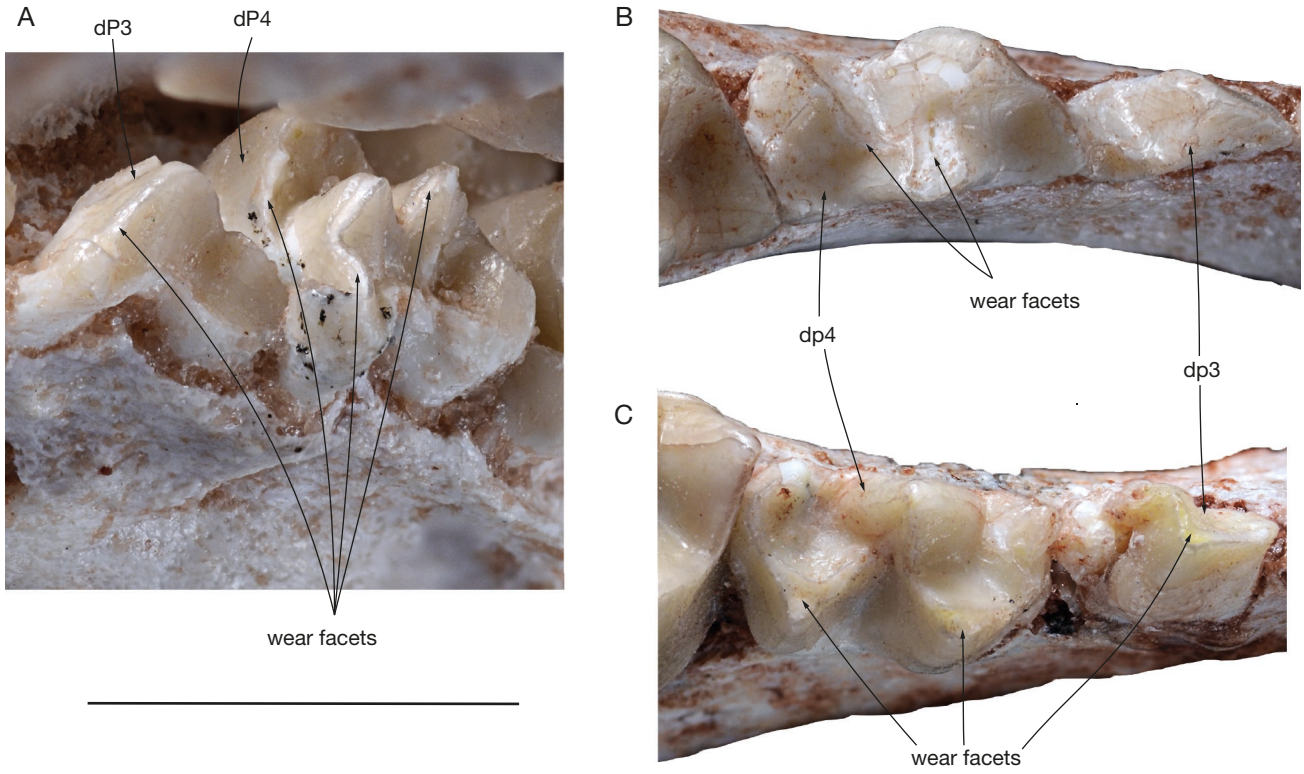

FIG. 44. — Wear facets on deciduous premolars of *Alcidedorbignya inopinata* indicating solid food ingestion: **A**, right dP4 of MHNC 8416 (stage 3); **B**, left dp4 of MHNC 8279 (stage 3+); **C**, right dp4 of MHNC 8298 (stage 3+). Scale bar: 5 mm.

above, in *Alcidedorbignya,* the mixed-feeding period (i.e., the beginning of the weaning period) should start during stage 2 and the juveniles should be weaned at the end of our stage 2+, in which M1/m1 are almost fully erupted. However, this is contradicted by the absence of wear facets not only on the erupting M1/m1 but also on the deciduous premolars of the specimens of *Alcidedorbignya* referred to these stages, which is an indication that solid food was not (or very little) ingested and that stage 2 and 2+ correspond to milk-only period (although probably the end of it). Therefore, it seems that weaning in *Alcidedorbignya* is delayed as compared to that observed in *Muntiacus* and *Dama*.

Stage 3 and stage 3+ correspond to the end of IDAS 1. In stage 3, M1 are only almost fully erupted since the metacingulum and postcingulum are still covered by the maxilla (MHNC 8416), but M2 and m2 are still in crypt (no M1 is known for stage 3+). Stage 3+ is slightly more advanced than stage 3 since in the latter dP1 is barely below the alveolar border and dp1 is still clearly below the border. In stage 3+ approximately one third of the crown of dp1 is above the alveolar border (no dP1 is known for this stage). No wear facet, even very weak is observed on the first molars of specimens of stages 3/3+. Therefore, if one follows Anders *et al.* (2011), weaning should occur after stage 3/3+. Because they have the adequate dental apparatus to do so, we hypothesize that stage 3/3+ juvenile *Alcidedorbignya* probably started to develop mixed feeding, ingesting more solid food than maternal milk. This is corroborated by the fact that distinct wear facets are present on the deciduous premolars, being more developed in stage 3+ than in stage 3. Facets are observed on the preparacrista of dP4 and on the protocristid of dp4 of MHNC 8416 (stage 3) and on most of the cristids and cuspids of dp4 of MHNC 8279 and 8298 (stage 3+) (Fig. 44). The presence of strong wear facets on deciduous premolars is regarded as resulting at least partly from mastication by solid food ingestion (i.e., abrasion), rather than resulting exclusively from tooth against tooth contact by occlusion (i.e., attrition). Therefore, this stage clearly corresponds to the mixed feeding period of Langer (2008), in which the offspring is still suckling but also ingest solid food. According to this author, they enter the transition or weaning period. If individuals of stage 3 and 3+ were still substantially suckling (they have no wear facets on M1/m1) then, weaning in *Alcidedorbignya* would have occurred later, as compared to dental eruption, than in *Muntiacus* and *Dama,* in which it occurs before full eruption of M1/m1 (i.e., at stage 2/2+). Interestingly, in cervids, when M1/m1 are just starting to erupt, the deciduous premolars feature heavy wear, whereas, in the case of *Alcidedorbignya*, at this stage (stage 2), no facet is observed on the deciduous premolars. Therefore, the lesser wear gradient between deciduous premolars and M1/m1 in *Alcidedorbignya* may indicate that maternal care may be more extended relative to dental eruption as compared to *Muntiacus* and *Dama*.

Stage 4 differs from stage 3/3+ in the presence of weak wear facets on M1/m1 (MHNC 8286, 8417, and 13857). A small facet is observed on the preparacrista, the paraconule and part of the paracingulum of MHNC 13857 and 13960, on the postcingulid and on the posterior edge of protocristid

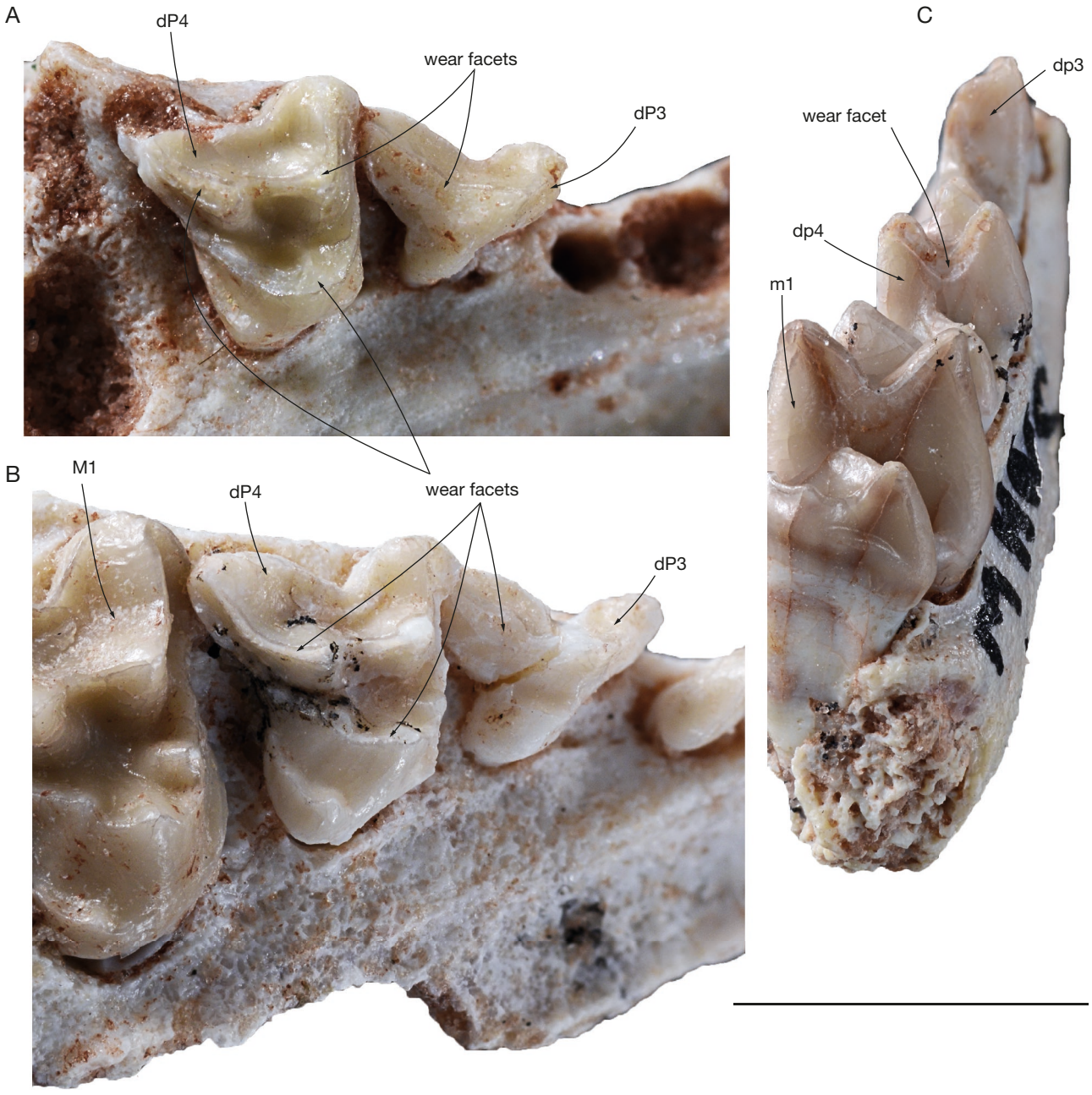

Fig. 45. — Wear facets on deciduous premolars of *Alcidedorbignya inopinata* indicating solid food ingestion: **A**, right dP3-4 of MHNC 13961 (stage 4); **B**, right dP3-4 of MHNC 13957 (stage 4); **C**, right dp4 of MHNC 8417 (stage 4). Scale bar: 5 mm.

on MHNC 8286, at the apex of the hypoconid and on the posterior edge of the protocristid of MHNC 8417, and at the posterior edge of the protocristid of MHNC 13964 (Fig. 34). On the deciduous premolars of stage 4 all crest, cusps, cristids, and cuspids feature distinct and large wear facets (Fig. 45). Therefore, following the definition of Anders *et al.* (2011), and because the M1/m1 of *Alcidedorbignya* are functional, weaning probably occurred at some time of the end of stage 3+ or beginning of stage 4 and it is highly probable that individuals of stage 4 and older were strict solid food feeders.

On stage 5 conspicuous M1/m1 wear facets are observed on the paraconule and paracingulum and on the apex of hypoconid and posterior edge of protocristid. M2/m2 are fully erupted but no wear facets are observed. M3 and m3 are well formed and present in crypt. Stage 6 is more advanced in dental eruption, since, M2 is fully erupted and bears wear facets, M3 is erupting and all other permanent teeth are functional. These two stages were fully weaned and, therefore, obviously strictly feeding on solid food.

To conclude, based on all this evidence, we hypothesize that stages 1 and 2 represent almost strictly suckling individuals, even if some mixed feeding might have started in stage 2 and 2+. Stage 3 and 3+ individuals probably represent mixed feeders, which have entered the transitional weaning period.

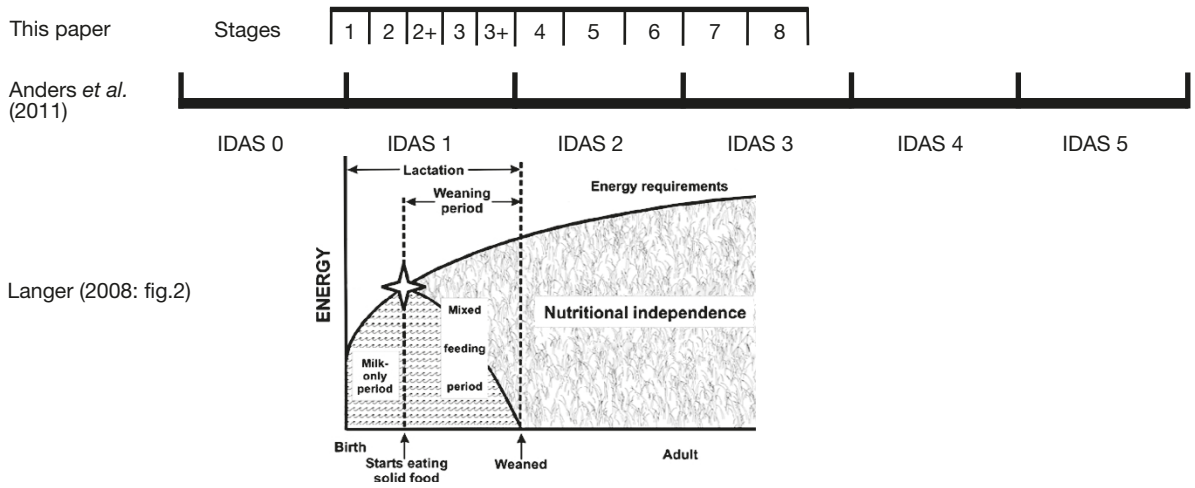

FIG. 46. — Correlation of the evolution of feeding and maternal investment in the juvenile eutherian mammals as illustrated by Langer (2008: fig. 2) with the dental stages (1 to 8) defined here and the IDAS of Anders *et al.* (2011).

Weaning would thus have occurred between stages 3+ and stage 4 and stages 4, 5 and 6 would include fully weaned individuals. Fig. 46 presents a juxtaposition of the distribution of our juvenile sample into the eight stages defined here, the IDAS of Anders *et al.* (2011), and the ontogeny of feeding and maternal investment in the juvenile eutherian mammals as exemplified by Langer (2008: fig. 2).

SEXUAL MATURITY VS DENTAL ERUPTION

After weaning another important life history event in development of juvenile mammals is the acquisition of sexual maturity. Of course, we have no direct indication concerning sexual maturity of *Alcidedorbignya* but a comparison with data from Reeve's muntjac may allow interesting approximation. Sexual maturity in this small cervid varies according to the gender. Females generally reach maturity around 7 to 8 months, but sexual maturity is delayed in males and is acquired between 9 and 14 months (Chapman & Harris 1997; Bottiau 2018). In *Muntiacus,* m2 starts to erupt at 8 months, is fully erupted at 11 months (Chapman *et al.* 1985). Therefore, females of *Muntiacus* are sexually mature when m2 starts to erupt (Chapman *et al.* 1985: pl. I, d), whereas sexual maturity occurs in males when m2 is fully erupted (Chapman *et al.* 1985: pl. I, e).

In the fallow deer (*Dama dama*), females become sexually mature at approximately 16 months and males are capable of breeding at the age of 18 months but do not generally breed until the age of 4-6 years because they are prevented from doing so by older, dominant males. (Shackleton 2019). In *Dama,* m2 starts to erupt at approximately 11 months and is fully erupted at 22 months (Chapman & Chapman 1970: fig. 2A; Brown & Chapman 1991: pl. 1, d and e). Therefore, sexual maturity occurs in *Dama dama* during eruption of m2, i.e., when m2 is half erupted (*c.* 16-18 months) but before its full eruption. Therefore, in both, *Muntiacus* and *Dama,* all individuals, males or females, are sexually mature when m2 is erupting or fully erupted.

Extrapolation of these observations in *Alcidedorbignya*, would indicate that sexual maturity could occur as early as at stage 4 and would be acquired at stage 5 in both sexes i.e., in a middle phase of IDAS 2. In *Muntiacus* and *Dama,* sexual maturity occurs slightly earlier in females than in males. In *Alcidedorbignya*, sexual dimorphism has been brought to light on the basis of the elevation of the maxilla and the size of the upper canine (Muizon *et al.* 2015). However, differentiation of sexual dimorphism is not possible on the fragmentary material available of stages 4 and 5 and, in any case, it would not probably be observable, even on complete skulls of sub-adult individuals because of possible allometry in the growth of the maxilla as related to skull size. Therefore, our sample does not provide indication on an eventual precocious sexual maturity in females as compared to males.

SKULL LENGTH AND SIZE VARIATION IN JUVENILES.

None of the three juvenile skulls of our sample are well-preserved enough to calculate proportions (cranial length/width) and provide indications on the actual size of the individual. However, some almost complete mandibles can give a reasonable approximation of the size of the individuals.

As can be noted on Table 2, the length of the mandible varies significantly within the same eruptional stage. In stage 1, the length of the dentary of MHNC 13859 is approximately 9% larger than that of MHNC 8373 (considering the length of the dentary, LCdSy). This size difference can be compared to that existing between MHNC 8372 (the inferred mother of MHNC 8373) and another adult female individual MHNC 8399 (cf. Muizon *et al.* 2015): MHNC 8399 is approximately 8% larger than MHNC 8372, which is very close to the size difference of the dentaries of the juvenile individual of stage 1. Therefore, the size variation observed between the juveniles of stage 1 is comparable to the individual size variation of the dentaries of adult females.

Another strong size difference (of the length of the dentary, LCdSy) is observed in our sample of stage 3+, between MHNC 8279 and 8298. In this case, the size difference is larger than that observed for stage 1. However, size variation of *Alcidedorbignya* is also depending upon sexual dimorphism,

TABLE 2. — Measurements of the mandible length in our sample of juvenile and adult *Alcidedorbignya*. Abbreviations: **LAgSy**, length from angular process to anterior end of dentary at symphysis; **LCdSy**, length from condylar process to anterior end of dentary at symphysis; **Hd4**, medial height of dentary at level of d4; **Hm1**, medial height of dentary at level of m1. Symbol: *, for MHNC 8416 indicates that measurement is biased because of some distortion of the ventral edge of the right dentary.

	L AgSy	LCdSy	Hd4	Hm1
Stage 1				
MHNC 8373 (R)	21.4	–	3.1	3.2
MHNC 8373 (L)	21.2	21.4	3.08	3.22
MHNC 13859	24	23.4	3.54	3.96
Stage 2				
MHNC 8423 (R)	23.5e	22.6e	3.77	4.84
MHNC 8423 (L)	–	21.5	4.26	5.08
Stage 2+				
MHNC 1213	–	27.4e	4.17	4.14
YPFB Pal 6352	23.6	22.5	4	4.6
Stage 3				
MHNC 8416 (R)	27.56	25.92	5*	5.6*
MHNC 8416 (L)	27.6	25.3	5.8	6.2
Stage 3+				
MHNC 8279	30.6	28.96	4.35	4.7
MHNC 8298	–	25.8	4.84	4.95
Adult females				
MHNC 8372 (R)	47.53	45.47	–	8.61
MHNC 8399 (R)	53.50	49.12	–	9.51
Adult male				
MHNC 13931	68.3	64.1	–	

TABLE 3. — Interindividual variation of skull length as compared to M1 labiolingual width in the two adult female skulls known of *Alcidedorbignya inopinata*.

	Skull length	Width M1
MHNC 8372	55.3	7.55
MHNC 8399	59.75	6.44
% size difference of MHNC 8399 as related to MHNC 8373	+ 8%	– 14%

as is observed on the adult male individual MHNC 13931 described by Muizon *et al.* (2015: 589-591). These authors calculated that the male skull MHNC 13931 was *c.* 20% larger than the female MHNC 8399 and 31% larger than the other female, MHNC 8372. Comparison based on LCdSy, indicates a size difference of respectively 38% and 41%. Therefore, the size difference observed between the specimens of our sample of Stage 3 could also be in part related to sexual dimorphism. Besides sexual dimorphism, a conspicuous interindividual variation is also observed in our cranial and dental sample as shown on fig. 7A of Muizon *et al.* (2015). Moreover, obvious interindividual variation of proportions results from comparison of the skull length to labiolingual width of M1 in the two well preserved female skulls described by Muizon *et al.* (2015) as underlined on Table 3. MHNC 8399, the skull of which is 8% longer than that of MHNC 8373, has 14% smaller M1s.

The comparison above indicates that the relative size of the juvenile specimens analysed here is not exclusively related to the dental eruption sequence, on which our stages are based.

TABLE 4. — Comparison of cranial measurements (in mm) in our sample of juveniles and adults of *Alcidedorbignya inopinata*. Abbreviations: **MO**, distance between the posterior edge of the external auditory meatus to the anterior edge of the orbit; **MC**, distance between the posterior edge of the external auditory meatus to the posterior edge of the choanae; **CS**, distance between the posterior edge of the choanae and the anterior edge of the Mx-Pmx suture anterior to the canine; **OS**, distance between the anterior edge of the orbit to the anterior edge of the Mx-Pmx suture anterior to the canine; **IS**, distance between the posterior edge of the infraorbital foramen to the anterior edge of the Mx-Pmx suture anterior to the canine.

	MO	MC	CS	OS	IS
Stage 2					
MHNC 8423	16.5	12.3	11.2	8.1	6.25
MHNC 13948	–	–	–	–	5.4e
MHNC 13949	–	–	–	–	6.4
Stage 3					
MHNC 8416	18.6	12.3	13.8	8.7	6.7
Stage 4					
MHNC 13857	–	–	–	–	8.28
MHNC 13861	–	–	–	–	7.54
Stage 5					
MHNC 13860	–	–	–	–	11.05
YPFB Pal 6363	–	–	–	–	8.9e
Adult females					
MHNC 8372 (R)	30.5	21.6	24.1	17.6	11.9
MHNC 8399 (R)	33e	23	25.8	18.2e	12.5
MHNC 8403	–	–	–	–	12.3e
Adult male					
MHNC 8400	–	–	–	–	14.5e
MHNC 8401	–	–	–	–	15.9e
MHNC 8405	–	–	–	–	13.2e
MHNC 13931	45.5	34.4e	32.9e	22.9	16.17

Sexual dimorphism and interindividual variation are also regarded as probable major factors of size difference in our juvenile sample.

Even if skull proportions cannot be calculated from our juvenile sample, some craniometric data can be obtained. Table 4 provides some measurements, which are analysed below.

Comparative analysis of these craniometric data with the dental ontogenetic stages and the proportion of erupted permanent cheek teeth (p3-m3 or P3-M3; following the same approach as Asher & Lehmann 2008) reveals further information on the craniodental ontogeny and growth dynamics in this species, although it was not possible to determine whether *Alcidedorbignya* had a delayed dental eruption of permanent cheek teeth relative to cranial growth (such as seen in many afrotherians; Asher & Lehmann 2008) or not (such as in many non-afrotherian mammals; Asher & Lehmann 2008; Asher & Olbricht 2009; Billet & Martin 2011). Although the lack of data on cranial proportions at intermediate stages of dental eruption (e.g., stages 6; see Table 4) prevented reaching conclusive results on this aspect, some observations can be made.

Our data show that juveniles prior to stage 4, with no more than 20% of permanent lower cheek teeth being fully erupted, were far from reaching the adult median length of the mandible (Fig. 47; Table 5). In addition, most juveniles pertaining to stages prior to stage 6, with no more than 40% of permanent upper cheek teeth being fully erupted, had a much shorter length of the anterior portion of their maxilla (IS measurement, Table 4) in comparison to adults (Fig. 47;

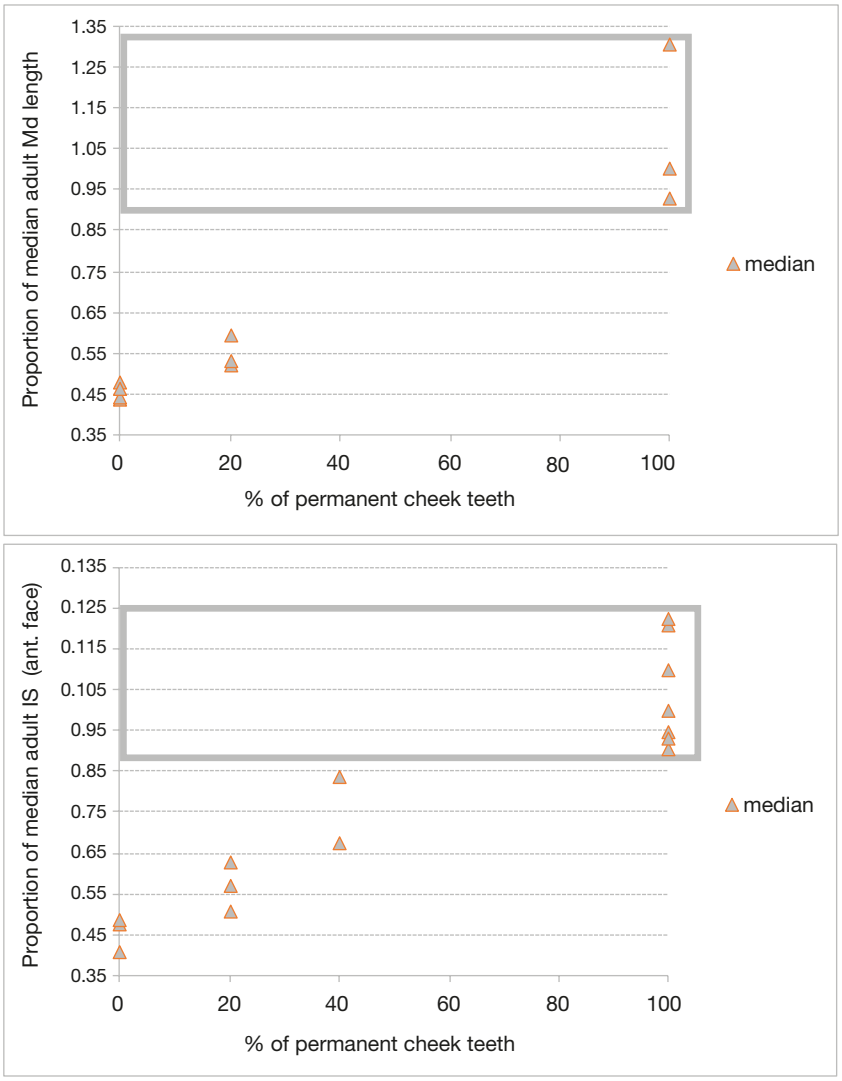

FIG. 47. — Proportion of adult craniomandibular measurements (y-axis, median adult value = 1.0) in relation to the proportion of erupted permanent cheek teeth (x-axis, all p3-m3 or P3-M3 erupted = 100). Areas within the grey rectangles represent the range of craniomandibular measurements in specimens with all permanent cheek teeth erupted. Data are based on Tables 5, 6 and 7.

TABLE 5. — Data on dental ontogenetic stages, erupted permanent cheek teeth and mandibular length (in mm) in *Alcidedorbignya inopinata*. Abbreviations: **LCdSy**, length from condylar process to anterior end of dentary at symphysis.

Specimens	Stage	Number of permanent cheek teeth (p3-m3)	% permanent erupted	Md length (LCdSy)	Specimen/ Adult mean	Specimen/ Adult median
MHNC 8373 (L)	1	0	0.00	21.4	0.40	0.44
MHNC 13859	1	0	0.00	23.4	0.44	0.48
MHNC 8423	2	0	0.00	21.5	0.41	0.44
YPFB Pal 6352	2+	0	0.00	22.5	0.43	0.46
MHNC 8416 (L)	3	1	20.00	25.3	0.48	0.52
MHNC 8279	3+	1	20.00	28.96	0.55	0.59
MHNC 8298	3+	1	20.00	25.8	0.49	0.53
MHNC 8372 (R)	adult	5	100.00	45.47	0.86	0.93
MHNC 8399 (R)	adult	5	100.00	49.12	0.93	1.00
MHNC 13931	adult	5	100.00	64.1	1.21	1.30
Mean adult	–	–	–	**52.90**	–	–
Median adult	–	–	–	**49.12**	–	–
Standard deviation adult	–	–	–	14.83	–	–
Coeff variation adult	–	–	–	28.03	–	–

TABLE 6. — Data on dental ontogenetic stages, erupted permanent cheek teeth and length of the anterior portion of the maxilla (in mm) in *Alcidedorbignya inopinata*. Abbreviations: **IS**, distance between the posterior edge of the infraorbital foramen to the anterior edge of the Mx-Pmx suture anterior to the canine.

Specimens	Stage	Number of permanent cheek teeth (P3-M3)	% permanent erupted	IS	Specimen/ Adult mean	Specimen/Adult median
MHNC 8423	2	0	0.00	6.25	0.45	0.47
MHNC 13948	2	0	0.00	5.4	0.39	0.41
MHNC 13949	2	0	0.00	6.4	0.46	0.48
MHNC 8416	3	1	20.00	6.7	0.49	0.51
MHNC 13857	4	1	20.00	8.28	0.60	0.63
MHNC 13861	4	1	20.00	7.54	0.55	0.57
MHNC 13860	5	2	40.00	11.05	0.80	0.84
YPFB Pal 6363	5	2	40.00	8.9	0.65	0.67
MHNC 8372 (R)	adult	5	100.00	11.9	0.86	0.90
MHNC 8399 (R)	adult	5	100.00	12.5	0.91	0.95
MHNC 8403	adult	5	100.00	12.3	0.89	0.93181818
MHNC 8400	adult	5	100.00	14.5	1.05	1.09848485
MHNC 8401	adult	5	100.00	15.9	1.15	1.20454545
MHNC 8405	adult	5	100.00	13.2	0.96	1
MHNC 13931	adult	5	100.00	16.17	1.17	1.225
Mean adult				13.78		
Median adult				13.20		
Standard deviation adult				1.75		
Coeff. variation adult				12.72		

TABLE 7. — Data on dental ontogenetic stages, erupted permanent cheek teeth and cranial measurements (in mm) in *Alcidedorbignya inopinata* (Fig. 47). Abbreviations: **MO**, distance between the posterior edge of the external auditory meatus to the anterior edge of the orbit; **CS**, distance between the posterior edge of the choanae and the anterior edge of the Mx-Pmx suture anterior to the canine.

Specimens	Stage	Number permanent cheek teeth (P2-M3)	% permanent erupted	MO (cranial length)	MO Juvenile specimen/ Adult mean	MO Juvenile specimen/ Adult median	CS (facial length)	CS Juvenile specimen/ Adult mean	CS Juvenile specimen/ Adult median
MHNC 8423	2	0	0.00	16.5	0.45	0.50	11.2	0.41	0.43
MHNC 8416	3	1	20.00	18.6	0.51	0.56	13.8	0.50	0.53
MHNC 8372	adult	5	100.00	30.5	0.84	0.92	24.1	0.87	0.93
MHNC 8399	adult	5	100.00	33	0.91	1.00	25.8	0.93	1.00
MHNC 13931	adult	5	100.00	45.5	1.25	1.38	32.9	1.19	1.28
Mean adult	–	–	–	**36.33**	–	–	**27.60**	–	–
Median adult	–	–	–	**33.00**	–	–	**25.80**	–	–
Standard deviation adult	–	–	–	8.04	–	–	4.67	–	–
Coeff variation adult	–	–	–	22.12	–	–	16.91	–	–

Table 6). One juvenile of stage 5, with 40% of permanent upper cheek teeth fully erupted (M1-2, Fig. 35), almost reached the lowest values found in adults (Fig. 47; Table 6). As already discussed above, sexual dimorphism (see Muizon *et al.* 2015: 408, 409) and further interindividual variation may cause some of the differences observed among individuals of a same stage but also among stages. It is therefore difficult to extract a clear signal from these data since sex determination is only tentative in adult specimens and impossible in juveniles.

Another aspect of their cranial growth may be less impacted by those issues. For both measurements on the upper and lower jaws (mandible length and length of the anterior portion of maxilla), juveniles with no erupted permanent cheek teeth (stages 1 and 2), exhibit a markedly reduced size in comparison to adults, being less than half of the adult median size (Fig. 47; Tables 5, 6). This is also true for other cranial measurements (see MO and CS in Table 7). Specimens at later stages 3 and 4, with 20% or less of their permanent cheek teeth fully erupted, remain very small as compared to adult median size for most measurements (<0.6 for the mandible length, Table 5; < 0.65 for the anterior portion of the maxilla, Table 6; Fig. 47). In other placentals documented for this trait, the size of individuals (mandible or palate length) with no erupted permanent cheek teeth (p3-m3 or P3-M3) is most often more than 0.5 that of the median adult size (Asher & Lehmann 2008: fig. 2 and appendix 2; Billet & Martin 2011; Kramarz & Bond 2013), with exceptions in the afrotherian tenrecoid *Tenrec ecaudatus* (Schreber, 1778) and the astrapothere *Astrapotherium magnum* (Owen, 1853). Of course, this might be influenced by differential sampling among species, since specimens with no erupted permanent cheek teeth may represent very different stages of early development. Therefore, this aspect would need further scrutiny with subdivision in various comparable stages of the category “no erupted permanent cheek teeth”, if possible.

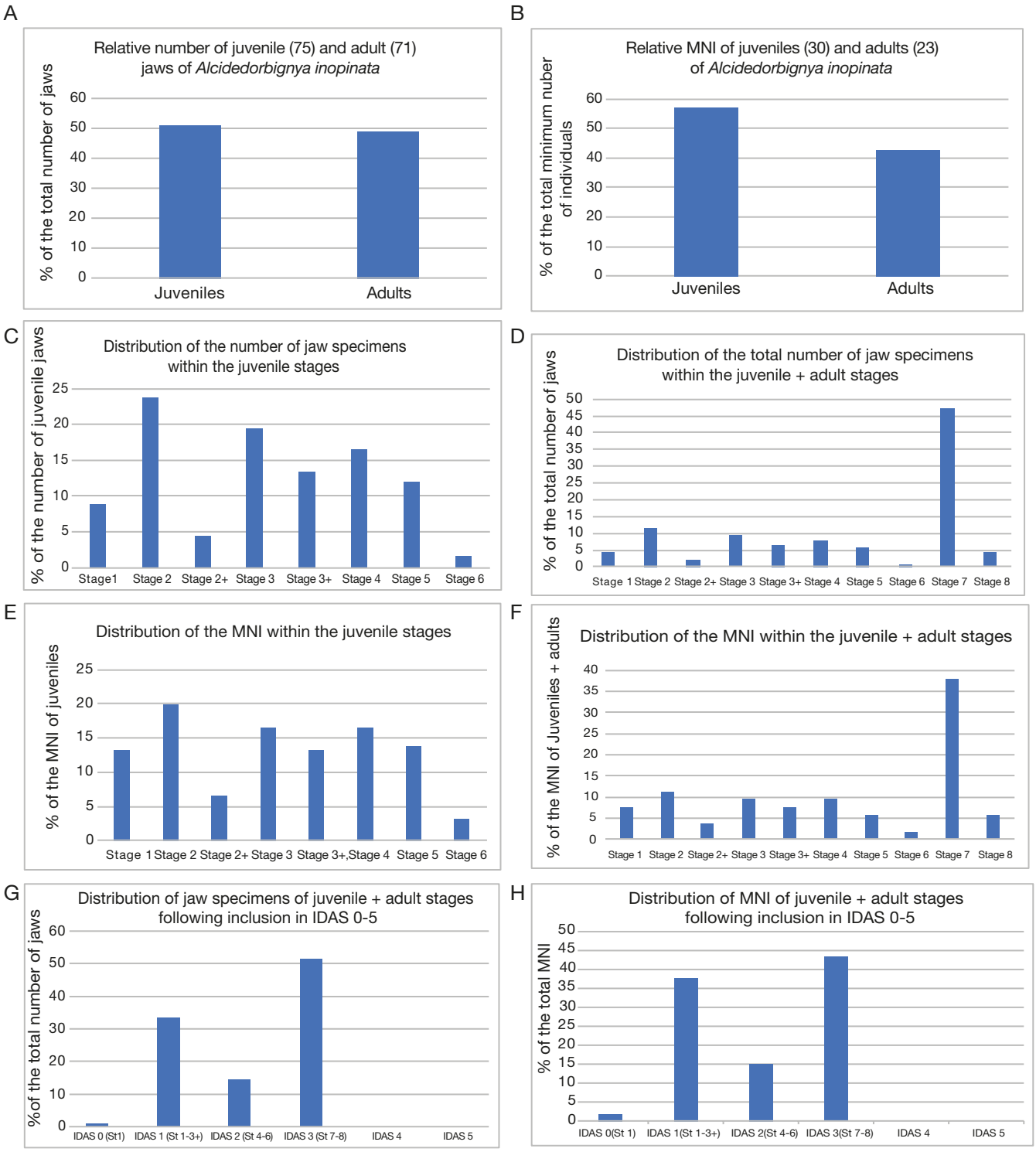

FIG. 48. — Histograms showing the relative proportions of adult and juvenile specimens of *Alcidedorbignya inopinata* and in the eight stages defined here: **A**, relative number of minimum number of individuals of adults and juveniles; **B**, relative number of adult and juvenile jaws; **C**, distribution of the number of jaw specimens within the juvenile stages; **D**, distribution of the number of jaw specimens within the adults and juveniles stages defined in text; **E**, distribution of the minimum number of individuals within the juvenile stages; **F**, distribution of minimum number of individuals within the adults and juveniles stages defined in text; **G**, distribution of jaw specimens of the adults and juveniles stages defined in text (stages 1-8) according to their inclusion in IDAS 0-5; **H**, distribution minimum number of individuals of the adults and juveniles stages defined in text (stages 1-8) according to their inclusion in IDAS 0-5.

Similarly, the size of individuals (mandible or palate length) with only few erupted cheek teeth (20% of their erupted permanent cheek teeth) is most often more than 0.6 that of the median adult size in other placentals documented, except for the afrotherian tenrecoid *Tenrec ecaudatus*, the astrapothere *Astrapotherium magnum* and the notoungulate *Nesodon*

TABLE 8. — comparison of the labial height of the dentary below m1 in adults and in juveniles just after eruption of that tooth (stages 3-5).

Specimen	Md lingual height below m1
Adults	
MHNC 8399	8.5
MHNC 8409	8.3
MHNC 8414	8.2
MHNC 8363	8.32
MHNC 8402	8.2
MHNC 8403	8.3
MHNC 8372	7.2
Mean	**8.14**
Juveniles (stages 3-5)	
MHNC 8416	4.9
MHNC 8398	4.82
MHNC 8279	4.39
MHNC 8286	4.50
MHNC 8417	5
MHNC 13969	4.2
MHNC 13858	5.58
YPFB Pal 6351	4.8
Mean	**4.77**
Juvenile mean/adult mean	0.586

TABLE 9. — Number of jaw specimens of juveniles (stages 1-6) and adults (stages 7-8) of *Alcidedorbignya inopinata* classified by categories of preserved elements.

	juveniles	adults
Skulls with mandibles	3	3
Associated maxillaries with mandibles	–	3
Maxillaries	29	32
Mandibles	43	33
Total per category	75	71
Total number of specimens	146	

imbricatus Owen, 1846 (Asher & Lehmann 2008: fig. 2 & appendix 2; Billet & Martin 2011; Kramarz & Bond 2013).

A comparison of the labial height of the dentary below m1 in adults of *Alcidedorbignya* and in juveniles just after eruption of that tooth (stage 3-5) also provides insights in this regard (see Gomes-Rodrigues *et al.* [2019: fig. 4]). The ratio of mandible height after eruption of m1/adult mandible height (Table 8) is 0.586, which further denotes a large difference in size between juveniles with freshly erupted m1 and adults in this species. This difference, which approaches that measured in the anthracothere *Lybicosaurus* Bonnarelli, 1947, is larger than in most documented artiodactyls (Gomes-Rodrigues *et al.* 2019: fig. 4). Interestingly, the result obtained for this measurement is roughly similar to that retrieved with the other mandibular and cranial measurements above for the stage with M1/m1 erupted (i.e., stages 3-5).

These comparisons suggest that *Alcidedorbignya* may be characterized by a reduced size of juveniles with no or few erupted permanent cheek teeth relative to adults, in comparison to modern placental species documented for these aspects. More comparative data on extant species are of course needed to test this possibility further since many groups are insufficiently documented in this regard. Further analyses of these traits in other well-documented extinct species, such as the larger pantodont *Coryphodon* (McGee & Turnbull 2010) is also necessary. The pattern found in the early Paleocene pantodont *Alcidedorbignya* in any case raises questions regarding the evolution of craniomandibular growth in mammals. Juveniles in stem mammals such as perinatal individuals of the Jurassic *Kayentatherium* Kermack, 1982 were very tiny in comparison to adults (Hoffman & Rowe 2018; see also Hopson 1971 for a series in the cynodont *Diademodon* Seeley, 1895). The rate and pattern of dental replacement drastically differ between stem mammals, early mammals and placental taxa and is thought to be correlated with patterns of cranial growth (Luo *et al.* 2004; O'Meara & Asher 2016), with indeterminate growth accompanying multiple and alternating dental replacements in stem mammals. Although this makes the craniodental patterns of growth hardly comparable across these groups, a markedly reduced size of juveniles, especially perinates, in comparison to adults may still represent the plesiomorphic pattern at the root of the mammalian clade as in stem mammals. This pattern was possibly retained, but to a much lower extent, in early placental taxa such as *Alcidedorbignya*. This remains however speculative and calls for further research in that direction.

MORTALITY PROFILE OF THE PANTODONT ASSEMBLAGE

In this section we will consider only the number of jaws and skulls, since isolated permanent teeth are not always easily referable to an adult or a juvenile individual. Our jaw sample of juvenile individuals (stages 1-6) is relatively large since it includes 75 specimens composed of 43 sub-complete or partial mandibles, 29 sub-complete or partial maxillaries, and three skulls with associated mandible. This juvenile jaw sample is slightly superior to that of our adult jaw sample (stage 7-8) which includes 71 specimens composed of 33 sub-complete or partial mandibles, 32 sub-complete or partial maxillaries, three specimens with associated sub-complete mandible and maxillary, and three sub-complete to partial skulls with associated mandible. (Table 9).

Therefore, juvenile jaws comprise 51% of our sample (Fig. 48A). Obviously, the number of specimens is probably an overestimation of the number of individuals. However, since this comparison considers relative values, it may represent a reasonable approximation, which shows that the juvenile members of the population of *Alcidedorbignya inopinata* preserved at Tiupampa were probably as numerous as the adults (or close). As a matter of fact, if one considers the minimum number of individuals (MNI) (i.e., 30 for juveniles and 23 for adults) the proportion is relatively similar although the number of juveniles (57%) is then slightly superior to that of adults (43%), (Table 10 and Fig. 48B).

Comparison of the distribution of specimens between stages requires to remove the eight juvenile jaws not complete enough to be referred to a given stage (Table 1). Table 11 provides the number of jaws and skulls referred to each stage. Therefore, 75 (total number) – 8 (undetermined stage) = 67 jaws and skull of juveniles will be considered.

TABLE 10. — Minimum number of individuals (MNI) per stages.

Stage	MNI
Juveniles	
Stage 1	4
Stage 2	6
Stage 2+	2
Stage 3	5
Stage 3+	4
Stage 4	5
Stage 5	3
Stage 6	1
Total MNI of juveniles	**30**
Adults	
Stage 7	20
Stage 8	3
Total MNI of adult + juveniles	**53**

TABLE 11. — Number of jaws and skulls of juvenile and adult individuals of *Alcidedorbignya inopinata* and proportion to the total number of specimens of identifiable juveniles and adults.

	Number of jaw + Skull specimens	% of the total number of identifiable juvenile jaws (67)	% of the total number of adults + identifiable juvenile jaws (138)
Stage 1	6	8.9	4.34
Stage 2	16	23.8	11.6
Stage 2+	3	4.4	2.17
Stage 3	13	19.4	9.4
Stage 3+	9	13.4	6.5
Stage 4	11	16.4	7.97
Stage 5	8	11.9	5.8
Stage 6	1	1.5	0.72
Unidentified juveniles jaws	8	–	–
Total juveniles jaws and skulls	75	–	–
Total identifiable juveniles jaws	**67**	–	–
Stage 7	65	–	47.1
Stage 8	6	–	4.34
Total adults + identifiable Juveniles jaws	**138**	–	–

Fig. 48C, D shows the distribution of the juvenile jaw specimens. Stage 2 (and 2+) and stage 3 (and 3+) are the most represented stages of juveniles. Furthermore, it is noteworthy that the juvenile specimens included in stages 1 to 3+ and which correspond to non-weaned individuals (45 specimens) represents 69% of our juvenile sample. Therefore, as compared to the whole jaw sample (adults + identifiable juveniles = 138 specimens) this category represents 31% of the sample that is still requiring maternal investment. The dependence of these juveniles, which were therefore more vulnerable, may explain the greater mortality of this category (non-weaned individuals, stages 1-3+). Distribution of MNI (minimum number of individuals) is presented on Fig. 38E, F and, noticably, this distribution is not significantly different from that of jaw specimens.

On Fig. 48G, H and Table 12, our stages 1 to 8 have been integrated in their corresponding IDAS (see above) and the distribution of the newly defined *Alcidedorbignya inopinata* IDAS are presented. Concerning stage 1, we have tentatively included in IDAS 0 the specimen MHNC 8373, which has been regarded as a possible near-term foetus. The remaining specimens of stage 1, which are slightly more advanced than the aforementioned specimen, have been included in IDAS 1. As mentioned above, according to our sample, IDAS 4 and 5 are lacking. In this case again, the distribution considering the minimum number of individuals is very similar to that considering the jaws number. Not surprisingly IDAS 3 is the most abundantly represented but to a lesser extent than in most populations considered by Anders *et al.* (2011: fig. 8). In this latter paper, one IDAS distribution (*Cainotherium huerzeleri* Heizmann, 1983) is ecologically biased (Anders *et al.* 2011: 329) and the distribution of IDAS of *Cainotherium* sp. features a representation of IDAS 3 identical to that of our sample. If one excludes the biased distribution of *Cainotherium huerzeleri,* our number of specimens included in IDAS 1 is far superior to that in the examples from Anders *et al.* (2011: fig. 8). Interestingly, the number of our specimens included in IDAS 2 is lesser than that in IDAS 1 especially because of the underrepresentation of the weaned subadults (see above; especially stage 6 with one specimen only), whereas the contrary is true in examples from Anders *et al.* (2011: fig. 8). This may be the result of some taphonomical bias, or may result from some ecological behaviour such as the departure (or exclusion) of the sexually mature subadult individuals from the community. This distribution may also indicate that our sample may include individuals resulting from several breeding seasons, if breeding of *Alcidedorbignya* was seasonal (see below). It could also indicate a greater vulnerability of the juveniles within stages 2 to 5 (as mentioned above concerning stages 1 to 3+) and that most of the individuals of stage 6 (sub-adults) had reached stage 7 (full adult) because they were more resistant to health problems, had more experience, and/or were more vigorous to resist predators and to avoid the dangers of life in a rainforest. Similarly, the total absence in our sample of individual referable to IDAS 4 and 5 is noteworthy. Given the number of specimens available, it probably does not represent a taphonomical bias. It is therefore possible that the absence of old individuals in the pantodont population of Tiupampa represents a specific selection. As for the subadults of stage 6, these individuals may have left (or have been excluded from) the community. Another alternative could be that the food ingested by *Alcidedorbignya inopinata* was soft enough to have a slow effect on tooth wear and that the longevity of that species was shorter than the time needed to reach full abrasion of molars as observed in IDAS 4 and 5.

To conclude, even if the number of specimens does not indicate the number of individuals, it suggests that

TABLE 12. — Number of specimens jaws and skulls of juvenile and adult individuals of *Alcidedorbignya inopinata* included in the IDAS of Anders *et al.* (2011).

Stage	1	2	2+	3	3+	4	5	6	7	8	Specimens in IDAS
IDAS 0	1										1
IDAS 1	5	16	3	13	9						46
IDAS 2						11	8	1			20
IDAS 3									65	6	71
IDAS 4											0
IDAS 5											0

juvenile individuals were very abundant and probably approached the number of adult individuals. This is confirmed by the estimations of the minimal number of individuals per stage and per IDAS, for which juveniles may even slightly outnumber the adults (Fig. 48A, E). Therefore, the *Alcidedorbignya* population of Tiupampa may represent that of a breeding season if the ecology of this species was characterised by reproductive seasonality. However, the fact that specimens of juveniles of almost all stages of dental eruption are present associated with adults specimens, could be an indication of limited seasonality with a reproduction not time-regulated over the year. Another alternative would be that our juvenile sample includes individuals from different breeding seasons. In this case, the mortality profile of our population could be biased as it would correspond to a pluriannual time span.

This hypothesis requires some comments on the taphonomy of the site called the "Quarry" (Marshall *et al.* 1995). These authors and others (Ladevèze *et al.* 2011) have suggested that the Quarry mammal fauna was the result of a catastrophic event such as a flood of the river on the banks of which the fauna was living. The occurrence at the Quarry of abundant complete skeletons of small and fragile vertebrates (frogs, lizards, snakes, new-born crocodiles) added to the discovery of a crocodile nest (including at least a dozen eggs), complete to partial (in some cases intermingled) metatherian skeletons (at least 20 of *Pucadelphys* Marshall & Muizon, 1988, six of *Andinodelphys* Marshall & Muizon, 1988, three of *Mizquedelphys* Marshall & Muizon, 1988) and two pantodont skeletons (one partial of juvenile and one complete adult) strongly suggests that this fauna has not suffered any transportation and that it has been trapped by a sudden event like a catastrophic flood. In particular the intermingled skeletons of metatherians could indicate that they were surprised in their burrows. In contrast, the great amount of isolated pantodont jaws suggests that these individuals probably died and were disarticulated before the event and that their disarticulated remains have suffered the catastrophic event, being trapped in the same sediment as the living metatherians and pantodonts. Most of the remains for *Alcidedorbignya* are indeed fragmentary jaws, isolated teeth, and a moderate number of isolated postcranial elements (Muizon & Marshall 1992, 2015). The latter count among the earliest skeletal elements to be transported by fluvial currents (Voorhies, 1969),. Cranial and mandibular remnants rather count as lag elements, which resist transport for a much longer time. Therefore, the anatomical composition of the total sample of fossils found of *Alcidedorbignya* at the Quarry suggests that these do not represent victims of a catastrophic event, in contrast to marsupials, but are rather lagged elements belonging to individuals that probably did not die at the same time. This could agree with the mortality profile of the pantodont assemblage at this locality, which may not reflect the typical age profile of a pantodont population and thus not result from a catastrophic event. In ungulates, the expected profile in a catastrophic event would show successively older age classes containing progressively fewer individuals (Klein & Cruz-Uribe 1983). Although it is uncertain whether the structure of pantodont populations was comparable to that of ungulates, such a pattern was not observed for *Alcidedorbignya* (Fig. 48).

Both the anatomical composition and mortality profile thus suggest that the remains of the pantodont individuals preserved at Tiupampa may be slightly diachronic, although they were probably buried all at once by the same catastrophic flooding event that trapped metatherian, pantodont, reptile and frog skeletons at the Quarry. The rather fresh look of bones for the preserved pantodont specimens, with a low amount of cracks and flaking of surface bone, indicates reduced weathering, probably less than one year under the then tropical climate at Tiupampa (see Behrensmeyer & Miller 2012: fig. 5.3, for a comparison under a tropical, climate). Therefore, the diachronism within the pantodont assemblage is probably rather limited.

Be that as it may, such a great amount of *Alcidedorbignya* specimens (juveniles being as numerous as the adults) in the Quarry fauna indicates that this site may have been at or near a breeding place for this taxon. Interestingly, *Alcidedorbignya* is the only mammal taxon at Tiupampa for which so many juvenile specimens (as compared to adults) have been found. Concerning metatherians, only four sub-adult specimens (one isolated mandible and three skulls and associated mandibles) of *Pucadelphys* (out of 35 complete or partial skulls and skeletons) (Ladevèze *et al.* 2011), and only one jaw of a juvenile kollpaniine "condylarth" (*Molinodus*) and a few isolated deciduous teeth of other "condylarths" are known (Muizon & Cifelli 2000; Muizon *et al.* 2019). Therefore, at Tiupampa, the ratio of juvenile to adult specimens in mammals other than *Alcidedorbignya* is drastically smaller. An overrepresentation of young individuals may match with a profile of mortality, called attritional, where vulnerable age categories are more represented (Klein & Cruz-Uribe 1983). However, the underrepresentation of old individuals (stage 8 poorly represented; IDAS 4-5 absent) does not match with this profile. This reinforces the hypothesis that the Quarry was at or near a breeding site for the Tiupampa pantodont, whether or not our sample represents individuals of the same breeding season or of different breeding season or of a non-seasonal reproductive behaviour.

CONCLUSION

The Tiupampa mammal fauna includes more than 25 species of metatherians and eutherians (Muizon *et al.* 2015, Muizon & Ladevèze 2020). Some of them are abundantly represented, such as the metatherians *Pucadelphys*, *Mizquedelphys*, and *Andinodelphys* and the eutherians *Alcidedorbignya* and kollpaniine "condylarths". However, *Alcidedorbignya* is the only taxon known from very abundant mandibular and cranial remains of juvenile specimens, which are roughly as abundant as the adult specimens, which suggests that the Quarry at Tiupampa was at or near a breeding site for this early pantodont. The abundance of juveniles enabled us to describe in detail the dental ontogeny in this pantodont species. The numerous juvenile and adult dental remains are attributed to eight different stages and provide new information on the eruption sequence, the sequence of cusp mineralisation and the cranial growth in this species and on the mortality profile of this assemblage at Tiupampa. Based on comparative data in extant placentals, possible timings for weaning and sexual maturity relative to the sequence of dental eruption are proposed for this species. Altogether, this offers an unprecedented amount of craniodental ontogenetic data in a Paleocene placental mammal, which thus paves the way towards a better understanding of development and growth patterns in the early history of placentals. The main findings and hypotheses are summarized below.

Our sample of juvenile fossil remains in *Alcidedorbignya* includes 75 specimens of skulls and jaws and 30 isolated teeth, to which must be added several tenths of uncatalogued isolated deciduous teeth in the collections of the Cochabamba Museum (Bolivia). This sample can be distributed into six ontogenetic stages from perinatal individuals (stage 1) to sub adults (stage 6). This very complete set has allowed reconstruction of the eruption sequence (excluding incisors) of *Alcidedorbignya inopinata*, as follows:

Uppers: dC-dP2-4 (probably erupted at birth, order unknown), M1, dP1, M2, I3, C, P4, P2-3, M3.

Lowers: di1-3-dc-dp3-4, dp2 (probably erupted at birth, order unknown), m1, dp1, m2, i3, c, p2, p4, p3, m3.

As in the later diverging pantodont *Coryphodon* (McGee & Turnbull 2010), the M3/m3 of *Alcidedorbignya* erupt last. This condition is likely an apomorphic character, which evolved several times in different extinct and extant eutherians: for example, in cetartiodactyls (Gomes-Rodrigues *et al.* 2019), primates (Monson & Hlusko 2018a), and perissodactyls (Domingo *et al.* 2018 and references therein).

Eight stages of dental eruption have been defined, which correspond to IDAS 0 to 3 of Anders *et al.* (2011). Stages 1 to 2+ are strict to almost strict suckling individuals since no conspicuous wear facets are observed on the deciduous cheek teeth, which indicates that little or no solid food was ingested. Distinct wear facets are present on deciduous cheek teeth of stages 3 and 3+, which indicates that mixed feeding had started. At stage 4, the first wear facets are observed on the M1/m1, indicating that weaning probably occurred at late stage 3+ or early stage 4 (IDAS 2 of Anders *et al.* 2011).

The study of the tooth germs contained within crypts by computed microtomography indicates that on lower cheek teeth the trigonid mineralises before the talonid and on the former the order of mineralisation is protoconid, metaconid and paraconid. On the upper cheek teeth, the paracone mineralises first. The early mineralisation of these labial cusps on cheek teeth is similar to what is known in many placentals and viewed as a widespread pattern (Butler 1956 and literature therein; Hershkovitz 1971; Jernvall 1995).

Comparative analysis of craniometric data with the dental ontogenetic stages and the proportion of erupted permanent cheek teeth revealed that juvenile individuals of *Alcidedorbignya* with no more than 20% of erupted permanent cheek teeth (p3-m3 or P3-M3) showed a markedly small size relative to adults when compared to most other documented placental species. Although more comparative data are needed, this suggests that this Paleocene placental species may have partly retained a plesiomorphic pattern, in which juveniles are much smaller than adults, as seen for instance, but with a much greater magnitude, in stem mammals (Hoffman & Rowe 2018).

The mortality profile of the *Alcidedorbignya* assemblage at Tiupampa indicates that, among the juvenile specimens, the great majority of remains are unweaned juvenile individuals (stages 1 to 3+) corresponding mostly to IDAS 1. An overrepresentation of young individuals may match with an attritional profile of mortality, where vulnerable age categories are more represented (Klein & Cruz-Uribe 1983), but the underrepresentation of old individuals is not congruent with it. Overall, the observed profile may suggest that in the early Paleocene, Tiupampa was a breeding area for this early pantodont.

Furthermore, the mortality profile of *Alcidedorbignya* is in fact largely bimodal when categorised with IDAS stages (overrepresentation of IDAS 1 and 3). In particular, old individuals featuring very worn teeth (i.e. IDAS 4 and 5 of Anders *et al.* 2011) are absent in our *Alcidedorbignya* sample at Tiupampa. As discussed above, given our relatively large sample, this absence is probably not related to a taphonomic bias, but rather concerns some ethological behaviour, for which we have no interpretation other than speculations, or an overall wear of cheek teeth during the life of pantodont individuals that never or rarely erase completely the internal enamel profile (wear stages of IDAS 4 and 5 never reached).

Finally, both the anatomical composition (mostly jaws and isolated teeth) and the mortality profile of the assemblage at Tiupampa suggest that the mostly disarticulated pantodont remains are slightly diachronic. They therefore do not match a catastrophic mortality profile. This marks a clear difference to the numerous complete marsupial skeletons, the two pantodont skeletons, and the non-mammalian tetrapods, which were trapped in situ at the Quarry (e.g., Ladevèze *et al.* 2011), although both the latter and the

disarticulated pantodont remains (which correspond to individuals, that may have died slightly before the event) were probably buried all at once by the same catastrophic flooding event eventually.

Acknowledgements
The locality of Tiupampa was discovered in 1982 during a field expedition funded by National Geographic Society (grant N°2467/82). The specimens described here have been collected during field expeditions funded by the National Geographic Society (grants 6296/98, 7109/01, 9394/13); Funds for fieldwork were also provided by the Muséum national d'Histoire naturelle (Paris, France), in 2006 and 2012. Fossil collecting was carried out under the auspices of research agreements between the Museo de Historia Natural Alcide d'Orbigny of Cochabamba (Bolivia) and the Muséum national d'Histoire naturelle (France). All the specimens collected are the property of the MHNC and were provided on loan to the MNHN for curation and publication. Field expeditions have benefited of logistical support from the IRD (Institut de Recherche pour le Développement) in Bolivia. We thank our Bolivian colleague Ricardo Céspedes-Paz, for his collaboration and logistic support during all the field seasons. Special thanks are due to Céline Bens, Aurélie Verguin, and Joséphine Lesur (MNHN), who provided access to MNHN specimens under their care. Warm thanks are due to Robert Asher and Thomas Martin, whose careful reviews allowed significant improvement of the manuscript. CT scanning of the specimens MHNC 8279, 8298, 8373, 8416, 13859 was performed by Miguel García at the AST-RX technical platform of scientific access to RX tomography (UMS 2700 "Acquisition et Analyse de Données pour l'Histoire naturelle", CNRS-MNHN, Paris). Data processing was undertaken by Florent Goussard and Nathalie Poulet at the 3D imaging facilities Lab of the UMR 7207 CR2P (MNHN CNRS SU). CT scanning of the specimens MHNC 1213, 8417, 8423, 13948, 13949, 13857, 13861, 13858 was performed by Renaud Lebrun using the micro-CT facilities of the MRI platform member of the national infrastructure France-BioImaging supported by the French National Research Agency (ANR-10-INBS-04, "Investments for the future"), and of the Labex CEMEB (ANR-10-LABX-0004) and NUMEV (ANR-10-LABX-0020). Photographs are by Philippe Loubry and Lilian Cazes.

REFERENCES

Anders U., Koenigswald W. von, Ruf I. & Smith H. 2011. — Generalized individual dental age stages for fossil and extant placental mammals. *Paläontologische Zeischrift* 85: 321-339. https://doi.org/10.1007/s12542-011-0098-9

Asher R. J., Gunnell G. F., Seiffert E. R., Pattinson D., Tabuce R., Hautier L. & Sallam H. M. 2017. — Dental eruption and growth in Hyracoidea (Mammalia, Afrotheria). *Journal of vertebrate Paleontology* 37: e1317638. https://doi.org/10.1080/02724634.2017.1317638

Asher R. J. & Lehmann T. 2008. — Dental eruption in afrotherian mammals. *BMC Biology* 6: 1-11. https://doi.org/10.1186/1741-7007-6-14

Asher R. J. & Olbricht G. 2009. — Dental ontogeny in *Macroscelides proboscideus* (Afrotheria and *Erinaceus europeus* (Lipotyphla). *Journal of Mammalian Evolution* 16: 99-115. https://doi.org/10.1007/s10914-009-9105-2

Azorit C., Analla M., Carrasco R., Calvo J. A. & Muñoz-Cobo J. 2002. — Teeth eruption pattern in red deer (*Cervus elaphus hispanicus*) in southern Spain. *Anales de Biología* 24: 107-114.

Beck R. M. D., Voss R. S. & Jansa S. A. 2022. — Craniodental morphology and Phylogeny of marsupials. *Bulletin of the American Museum of Natural History* 457: 1-350. http://hdl.handle.net/2246/7298

Behrensmeyer A. K. & Miller J. H. 2012. — Building links between ecology and paleontology using taphonomic studies of recent vertebrate communities, *in* Louys J. (ed.), *Paleontology in Ecology and Conservation*. Springer Earth System Sciences, Berlin, Heidelberg: 69-91. https://doi.org/10.1007/978-3-642-25038-5_5

Billet G. & Martin T. 2011. — No evidence for an afrotherian-like delayed dental eruption in South American notoungulates. *Naturwissenschaften* 98: 509-517. https://doi.org/10.1007/s00114-011-0795-y

Bottiau 2018. — Le cerf muntjac (*muntiacus reevesi*) : *Écologie, biologie, dynamique des populations et étude de son potentiel invasif.* Thèse pour le doctorat vétérinaire, École nationale vétérinaire d'Alfort: 1-135.

Brown W. A. B. & Chapman N. G. 1991. — Age assessment of fallow deer (*Dama dama*): from a scoring scheme based on radiographs of developing permanent molariform teeth. *Journal of Zoology* 224: 367-379. https://doi.org/10.1111/j.1469-7998.1991.tb06031.x

Butler P. M. 1956. — The ontogeny of molar pattern. *Biological Reviews* 31: 30-69. https://doi.org/10.1111/j.1469-185X.1956.tb01551.x

Chaplin R. E. & White R. W. G. 1969. — The use of tooth eruption and wear, body weight and antler characteristics in the age estimation of male wild and park Fallow deer (*Dama dama*). *Journal of Zoology* 157: 125-132. https://doi.org/10.1111/j.1469-7998.1969.tb01692.x

Chapman D. I. & Chapman N. G. 1970. — Development of the teeth and mandible of the fallow deer. *Acta Theriologica* 15: 111-131.

Chapman N. G. & Harris S. 1997. — Evidence that the seasonal antler cycle of adult Reeves' muntjac (*Muntiacus reevesi*) is not associated with reproductive quiescence. *Journal of Reproductive Fertility* 92: 361-369. https://doi.org/10.1530/jrf.0.0920361

Chapman D. I., Chapman N. G. & Colles C. M. 1985. — Tooth eruption in Reeves' muntjac (*Muntiacus reevesi*) and its use as a method of age estimation (Mammalia: Cervidae). *Journal of Zoology*, London 205: 205-221. https://doi.org/10.1111/j.1469-7998.1985.tb03529.x

Coccioni R., Bancalà G., Catanzarit B., Fornaciari E., Frontalini F., Giusberti L., Jovane L., Luciani V., Savian J., & Sprovieri M. 2012. — An integrated stratigraphic record of the Palaeocene–lower Eocene at Gubbio (Italy): new insights into the early Palaeogene hyperthermals and carbon isotope excursions. *Terra Nova* 24: 380-386. https://doi.org/10.1111/j.1365-3121.2012.01076.x

Cohen K. M., Finney S.C., Gibbard P. L., & Fan J. 2013 [updated]. — The ICS International Chronostratigraphic Chart. *Episodes* 36: 199-204.

Decombeix A.-L., Escapa I. H., De Franceschi D. & Béthoux O. 2021. — Reinvestigation of the type specimen of Ginkophyllum grassetiiv Saporta 1875 using Reflectance Transforming Imaging. *Review of Palaeobotany and Palynology* 295: 104526. https://doi.org/10.1016/j.revpalbo.2021.104526Get

Domingo M. S., Cantero E., García-Real I., Chamorro-Sancho M. J., Martin-Perea D. M., Alberdi M. T. & Morales J. 2018. — First radiological study of a complete dental ontogeny sequence of an extinct equid: implications for Equidae life history and taphonomy. *Scientific Reports* 8, 8507: 1-11. https://doi.org/10.1038/s41598-018-26817-3

DRION P. V., HANZEN C., WIRTH D., BECKERS J. F., LEBOEUF B., ROPSTAD E., BALLIGAND M., BAUVIR E., GABRIEL A. & COLLIN B. 2003. — Physiologie de la reproduction et endocrinologie chez les cervidés : une revue. *Annales de Médecine vétérinaire* 147: 191-313.

GARDNER A. L. 1971. — Postpartum oestrus in a red brocket deer, *Mazama Americana* from Peru *Journal of mammalogy* 52: 623-624. https://doi.org/10.2307/1378604

GAUTHIER D. & BARRETTE C. 1985. — Suckling and weaning in captive white-tailed and fallow deer. *Behaviour* 94: 128-149. https://doi.org/10.1163/156853985X00307

GHEERBRANT E., PEIGNÉ S. & THOMAS H. 2007. — Première description du squelette d'un hyracoïde paléogène : *Saghatherium antiquum* de l'Oligocène inférieur de Jebel al Hasawnah, Libye. *Paleontographica* Abteilung A 279: 93-145. https://doi.org/10.1127/pala/279/2007/93

GINGERICH P. D., UL-HAQ M., KOENIGSWALD W. VON, SANDERS W. J., SMITH B. H. & ZALMOUT I. S. 2009. — New protocetid whale from the middle Eocene of Pakistan: Birth on land, precocial development, and sexual dimorphism. *PLoS ONE* 4(2): e4366. https://doi.org/10.1371/journal.pone.0004366

GODDARD J. 1970. — Age criteria and vital statistics of a black rhinoceros population. *East Africa Wildlife Journal* 8: 105-121. https://doi.org/10.1111/j.1365-2028.1970.tb00834.x

GODFREY L. R., SAMONDS K. E., WRIGHT P. C. & KING S. J. 2005. — Schultz's unruly rule: dental developmental sequences and schedules in small-bodied, folivorous lemurs. *Folia Primatologica* 76: 77-99. https://doi.org/10.1159/000083615

GOMES-RODRIGUES H. G., HERREL A. & BILLET G. 2017. — Ontogenetic and life history trait changes associated with convergent ecological specializations in extinct ungulate mammals. *Proceedings of the National Academy of Sciences*, 114: 1069-1074. https://doi.org/10.1073/pnas.1614029114

GOMES-RODRIGUES E., LIHOREAU F., ORLIAC M., THEWISSEN J. G. M. & BOISSERIE J.-R. 2019. — Unexpected evolutionary patterns of dental ontogenetic traits in cetartiodactyl mammals *Proceeding of the Royal Society B:* 286 20182417. https://doi.org/10.1098/rspb.2018.2417

GOMES-RODRIGUES H., TABUCE R., ASHER R. J. & HAUTIER L. 2020. — Developmental origins and homologies of the hyracoid dentition. *Evolution and Development*. 22: 323-335. https://doi.org/10.1111/ede.12337

HALL-MARTIN A. J. 1976. — Dentition and age determination of the giraffe *Giraffa Camelopardalis*. *Journal of Zoology* 180: 263-289. https://doi.org/10.1111/j.1469-7998.1976.tb04678.x

HERSHKOVITZ P. 1971. — Basic crown patterns and cusp homologies of mammalian teeth, *in* DAHLBERG A. A. (ed.), *Dental Morphology and Evolution*. University of Chicago Press, Chicago: 95-150.

HOFFMAN E. A. & ROWE T. B. 2018. — Jurassic stem-mammal perinates and the origin of mammalian reproduction and growth. *Nature* 561: 104-108. https://doi.org/10.1038/s41586-018-0441-3

HOPSON J. A. 1971. — Postcanine replacement in the gomphodont cynodont *Diademodon*, *in* KERMACK D. M. & KERMACK K. A. (eds), *Early Mammals*. Academic Press, London: 1-21.

JÄGER K. R. G., CIFELLI R. L. & MARTIN T. 2021. — Tooth eruption in the Early Cretaceous British mammal *Triconodon* and description of a new species. *Papers in Palaeontology* 7: 1065-1080. https://doi.org/10.1002/spp2.1329

JERNVALL J. 1995. — Mammalian molar cusp pattern: developmental mechanisms of diversity. *Acta Zoologica Fennica* 198:1-61.

JOUVE S., MUIZON C. DE, CÉSPEDES-PAZ R., SOSSA-SORRUCO V. & KNOLL S. 2020. — The longirostrine crocodyliforms from Bolivia and their evolution through the Cretaceous-Palaeogene boundary. *Zoological Journal of the Linnean Society* 20: 1-35-000. https://doi.org/10.1093/zoolinnean/zlaa081

KELLEY J. & SMITH T. M. 2003. — Age at first molar emergence in early Miocene *Afropithecus turkanensis* and life-history evolution in the Hominoidea. *Journal of Human Evolution* 44: 307-329. https://doi.org/10.1016/S0047-2484(03)00005-8

KINDAHL M. E. 1957. — Some observations on the development of the tooth in *Elephantulus myurus jamesoni*. *Arkiv for Zoologi* 11: 21-29.

KLEIN R. G. & CRUZ-URIBE K. 1983. — The computation of ungulate age (mortality) profiles from dental crown heights. *Paleobiology* 9: 70 – 78. https://doi.org/10.1017/S0094837300007399

KRAMARZ A. & BOND M. 2013. — On the status of *Isolophodon* Roth, 1903 (Mammalia, Astrapotheria) and other little-known Paleogene astrapotheres from central Patagonia. *Geobios* 46: 203-211. https://doi.org/10.1016/j.geobios.2012.10.015

LADEVÈZE S., MUIZON C. DE, BECK R, GERMAIN D. & CÉSPEDES-PAZ R. 2011. — Earliest evidence of mammalian social behaviour in the basal Tertiary of Bolivia. *Nature* 474: 83-86. https://doi.org/10.1038/nature09987

LANGER P. 2008. — The phases of maternal investment in eutherian mammals. *Zoology* 111: 148-162. https://doi.org/10.1016/j.zool.2007.06.007

LOWE V. P. W. 1967. — Teeth as indicators of age with special reference to red deer (*Cervus elaphus*) of known age from Rhum. *Journal of Zoology*, London 152: 137-153. https://doi.org/10.1111/j.1469-7998.1967.tb01881.x

LUCAS S. G. & SCHOCH R. M. 1990. — Ontogenetic studies of early Cenozoic *Coryphodon* (Mammalia, Pantodonta). *Journal of Paleontology* 64: 831-841. https://doi.org/10.1017/S0022336000019028

LUCKETT W. P. 1993. — An ontogenetic assessment of dental homologies in therian mammals, *in* SZALAY F. S., NOVACEK M. J. & MCKENNA M. C. (eds), *Mammal Phylogeny*. Vol. 1: *Mesozoic Differentiation, Multituberculates, Monotremes Early Therians and Marsupials.* Springer-Verlag, New York: 182-204. https://doi.org/10.1007/978-1-4613-9249-1_13

LUO Z.-X., KIELAN-JAWOROWSKA Z. & CIFELLI R. L. 2004. — *Bulletin of the Carnegie Museum of Natural History* 36: 159-175. https://doi.org/dng546

MAO F. Y., ZHENG X. T., WANG X. L., WAND Y. Q., BI S. D. & MENG, J. 2019. — Evidence of diphyodonty and heterochrony for dental development in euharamiyidan mammals from Jurassic Yanliao Biota. *Vertebrata PalAsiatica* 57: 51-76. https://doi.org/10.19615/j.cnki.1000-3118.180803

MARSHALL L. G., MUIZON C. DE & SIGOGNEAU-RUSSELL D. 1995. — Part I: The locality of Tiupampa: age, taphonomy and mammalian fauna, *in* MUIZON C. DE (ed.), *Pucadelphys andinus* (Marsupialia, Mammalia) from the Early Paleocene of Bolivia. Muséum national d'Histoire naturelle, Paris: 11-20 (Mémoires du Muséum national d'Histoire naturelle ; 165).

MARTIN T. 1997. — Tooth replacement in Late Jurassic Dryolestidae (Eupantotheria, Mammalia). *Journal of Mammalian Evolution* 4: 1-18. https://doi.org/10.1023/A:1027300726126

MCGEE E. M. & TURNBULL W. D. 2010. — A Paleopopulation of *Coryphodon lobatus* (Mammalia: Pantodonta) from Deardorff Hill *Coryphodon* Quarry, Piceance Creek Basin, Colorado. *Fieldiana Geology* 52:1-12. 2010. https://doi.org/10.3158/0096-2651-52.1.1

MCKAY C. J., WELBOURN-GREEN C., SEIFERT E. R., SALLAM H., LI J., KAKARALA S. E., BENNET N. C. & ASHER R. J. 2022. — Dental development and first premolar homology in placental mammals. *Vertebrate Zoology* 72: 201-208. https://doi.org/10.3897/vz.72.e78234

MILLER F. L. 1972. — Eruption and attrition of mandibular teeth in barren-ground caribou. *The Journal of Wildlife Management* 36: 606-612.

MONSON T. A. & HLUSKO L. J. 2018a. — Breaking the rules: phylogeny, not life history, explains dental eruption sequence in primates. *American Journal of Physical Anthropology* 167 (2): 217-233. https://doi.org/10.1002/ajpa.23618

MONSON T. A. & HLUSKO L. J. 2018b. — The evolution of dental eruption sequence in artiodactyls. *Journal of Mammalian Evolution* 25: 15-26. https://doi.org/10.1007/s10914-016-9362-9

MUIZON C. DE & CIFELLI R. L. 2000. — The "condylarths" (archaic Ungulata, Mammalia) from the early Palaeocene of Tiupampa (Bolivia): implications on the origin of the South American ungulates. *Geodiversitas* 22: 47-150.

MUIZON C. DE & LADEVÈZE S. 2020. — Cranial anatomy of *Andinodelphys cochabambensis*, a stem metatherian from the early Palaeocene of Bolivia. *Geodiversitas* 42 (30): 597-739. https://doi.org/10.5252/geodiversitas2020v42a30. http://geodiversitas.com/42/30

MUIZON C. DE & MARSHALL L. G. 1992. — *Alcidedorbignya inopinata* (Mammalia: Pantodonta) from the early Paleocene of Bolivia: phylogenetic and paleobiogeographic implications. *Journal of Paleontology* 66: 499-520. https://doi.org/10.1017/S002233600003403X

MUIZON C. DE, LADEVÈZE S. & CESPEDES R. (in press). — The beginning of the age of therian mammals in South America: Tiupampa, a transition between Northern and Southern worlds in the basal Paleocene, *in* Rosenberger A. & Tejedor M. (eds), *Origins and Evolution of Cenozoic South American Mammals*. Springer Verlag, New York.

MUIZON C. DE, BILLET G., ARGOT C., LADEVÈZE S. & GOUSSARD F. 2015. — *Alcidedorbignya inopinata,* a basal pantodont (Eutheria, Mammalia) from the early Palaeocene of Bolivia: anatomy, phylogeny, and palaeobiology. *Geodiversitas* 37 (4): 397-634. https://doi.org/10.5252/g2015n4a1

MUIZON C. DE, BILLET G. & LADEVÈZE S. 2019. — New remains of kollpaniine "condylartyhs" (Panameriungulata) from the early Palaeocene of Bolivia shed light on hypocone origins and molar proportions among ungulate-like placentals. *Geodiversitas* 41 (25): 841-874. https://doi.org/10.5252/geodiversitas2019v41a25. http://geodiversitas.com/41/25

O'MEARA R. N. & ASHER R. J. 2016. — The evolution of growth patterns in mammalian versus nonmammalian cynodonts. *Paleobiology* 42: 439-464. https://doi.org/10.1017/pab.2015.51

PÉLABON C., YOCCOZ N. G., ROPPERT-COUDERT Y., CARON M. & PEREIRA V. 1998. — Suckling and allosuckling in captive fallow deer (*Dama dam*a, Cervidae). *Ethology* 104: 75-86. https://doi.org/10.1111/j.1439-0310.1998.tb00031.x

QUINBY D. C. & GAB J. E. 1957. — Mandibular dentition as an age Indicator in Rocky Mountain elk. *The Journal of Wildlife Management* 21: 435-451. https://doi.org/10.2307/3796676

SCHULTZ J. A., BHULLAR B. A. S. & LUO Z. X. 2019. — Re-examination of the Jurassic Mammaliaform *Docodon victor* by Computed Tomography and Occlusal Functional Analysis. *Journal of Mammalian Evolution* 26: 9-38. https://doi.org/10.1007/s10914-017-9418-5

SEVERINGHAUS C. W. 1949. — Tooth development and wear as criteria of age in white-tailed deer. *The Journal of Wildlife Management* 13: 195-216. https://doi.org/10.2307/3796089

SHACKLETON D. 2019. — *Dama dama* Linnaeus, European Fallow deer, Fallow deer, family: Cervidae, *in* KLINKENBERG B. (ed.), E-Fauna BC: Electronic Atlas of the Fauna of British Columbia [efauna.bc.ca]. Lab for Advanced Spatial Analysis, Department of Geography, University of British Columbia, Vancouver. Downloaded from http://linnet.geog.ubc.ca/efauna/Atlas/Atlas.aspx?sciname=Dama%20dama (accessed: 2021-01-12).

SINGER R. & BONÉ E. L. 1960. — Modern giraffes and the fossil giraffids of Africa. *Annals of the South African Museum* 45: 375-548.

SLAUGHTER B. H., PINE R. H. & PINE N. E. 1974. — Eruption of cheek teeth in insectivora and Carnivora. *Journal of Mammalogy* 55: 115-125. https://doi.org/10.2307/1379261

SMITH B. H. 1991. — Age of weaning approximates emergence of the first permanent molar in nonhuman primates. *American Journal of Physical Anthropology* 34:163-164.

SMITH B. H. 1992. — Life history and the evolution of human maturity. *Evolutionary Anthropology* 1: 134-142. https://doi.org/10.1002/evan.1360010406

SMITH B. H. 2000. — 'Schultze's rule' and the evolution of tooth emergence and replacement patterns in primates and ungulates, *in* TEAFORD M. F., SMITH M. M. & FERGUSON M. W. J. (eds), *Development, Function and Evolution of Teeth*. Cambridge University Press, Cambridge: 212-227.

SPRAIN C. J., RENNE P. R., WILSON G. P. & CLEMENS W. A. 2015. — High-resolution chronostratigraphy of the terrestrial Cretaceous-Paleogene transition and recovery interval in the Hell Creek region, Montana. *Geological Society of America Bulletin* 127 (3-4): 393-409. https://doi.org/10.1130/B31076.1

UHEN M. D. 2000. — Replacement of deciduous first premolars and dental eruption in archaeocete whales. *Journal of Mammalogy* 81: 123-133. https://doi.org/bbtd82

VAN NIEVELT A. F. H. & SMITH K. K. 2005. — To replace or not to replace: the significance of reduced functional tooth replacement in marsupials and placental mammals. *Paleobiology* 31: 324-346. https://doi.org/cjw3jn

VEITSCHEGGER K. & SÁNCHEZ-VILLAGRA M. R. 2016. — Tooth eruption sequences in cervids and the effect of morphology, life history, and phylogeny. *Journal Mammalian Evolution* 23: 251-263. https://doi.org/10.1007/ s10914-015-9315-8

VOORHIES M. R. 1969. — Taphonomy and population dynamics of an early Pliocene vertebrate fauna, Knox County, Nebraska. *University of Wyoming, Special Contributions to Geology, Special Papers* 1: 1-69. https://doi.org/10.2113/gsrocky.8.special_paper_1.1

WEST R. M. 1971. — Deciduous dentition of the Early Tertiary Phenacodontidae (Condylarthra, Mammalia). *American Museum Novitates* 2461: 1-37. http://hdl.handle.net/2246/2669

WEST R. M. 1972. — Upper deciduous dentition of the Oligocene insectivore *Leptictis* (= *Ictops*) *acutidens*. *Annals of the Carnegie Museum of Natural History* 44: 25-32. https://www.biodiversitylibrary.org/page/54241062

WEST R. M. 1979. — Paleontology and geology of the Bridger Formation, Southern Green River Basin, Southwestern Wyoming. Part 3. Notes on *Hyopsodus*. *Contributions in Biology and Geology* 25: 1-52.

WILLIAMS R. C. & EVANS H. E. 1978. — Prenatal dental development in the dog, Canis familiaris: chronology of tooth germ formation and calcification of deciduous teeth. *Anatomia Histologia Embryologia* 7: 152-163. https://doi.org/10.1111/j.1439-0264.1978.tb00665.x

WILLIAMSON T. E. & LUCAS S. G. 1992. — *Meniscotherium* (Mammalia, "Condylarthra") from the Paleocene-Eocene of North America. *Bulletin of the New Mexico Museum of Natural History* 1: 1-75.

YAHNER R. H. 1978. — Some features of mother-young relationships in Reeve's Muntjac (*Muntiacus reevesi*). *Applied Animal Ethology* 4: 379-388. https://doi.org/10.1016/0304-3762(78)90009-3

ZIMICZ A. N., FERÁNDEZ M., BOND M., CHORNOGUBSKY L., ARNAL M., CÁRDENAS M. & FERNICOLA J. C. 2020. — *Archaeogaia macachaae* gen. et sp. nov., one of the oldest Notoungulata Roth, 1903 from the early-middle Paleocene Mealla Formation (Central Andes, Argentina) with insights into the Paleocene-Eocene south American biochronology. *Journal of South American Earth Sciences*: 102772. https://doi.org/10.1016/j.jsames.2020.102772

Submitted on 25 January 2022;
accepted on 20 April 2022;
published on 1 December 2022.